AD NUMBER

ADB003843

LIMITATION CHANGES

TO:

Approved for public release; distribution is unlimited.

FROM:

Distribution authorized to U.S. Gov't. agencies only; Test and Evaluation; 16 DEC 1974. Other requests shall be referred to Army Missile Command, Attn: AMSMI-RK, Redstone Arsenal, AL 35809.

AUTHORITY

USAMC ltr, 14 Aug 1975

RK-CR-75-27

FLUORINE GENERATOR

R. B. Leining, D. T. Sauer, H. L. Young, and E. D. Casseday

HERCULES INCORPORATED
ALLEGANY BALLISTICS LABORATORY
CUMBERLAND, MARYLAND

FINAL REPORT

2 APRIL 1975

PREPARED FOR
U. S. ARMY MISSILE RESEARCH DEVELOPMENT
AND ENGINEERING LABORATORY
U. S. ARMY MISSILE COMMAND
REDSTONE ARSENAL, ALABAMA

Copy No._____

AO263-115-01-028

DISPOSITION INSTRUCTIONS

DESTROY THIS REPORT WHEN IT IS NO LONGER NEEDED. DO NOT RETURN IT TO THE ORIGINATOR.

DISCLAIMER

THE FINDINGS IN THIS REPORT ARE NOT TO BE CONSTRUED AS AN OFFICIAL DEPARTMENT OF THE ARMY POSITION UNLESS SO DESIGNATED BY OTHER AUTHORIZED DOCUMENTS.

TRADE NAMES

USE OF TRADE NAMES OR MANUFACTURERS IN THIS REPORT DOES NOT CONSTITUTE AN OFFICIAL INDORSEMENT OR APPROVAL OF THE USE OF SUCH COMMERCIAL HARDWARE OR SOFTWARE.

UNCLASSIFIED

SECURITY CLASSIFICATION OF THIS PAGE (When Data Entered)

REPORT DOCUMENTATION PAGE		READ INSTRUCTIONS BEFORE COMPLETING FORM
1. REPORT NUMBER RK-CR-75-27	2. GOVT ACCESSION NO.	3. RECIPIENT'S CATALOG NUMBER
4. TITLE (and Subtitle) Fluorine Generator		5. TYPE OF REPORT & PERIOD COVERED Final Feb 2 through June 30, 1974
		6. PERFORMING ORG. REPORT NUMBER
7. AUTHOR(s) R. B. Leining, D. T. Sauer, H. L. Young, E. D. Casseday		8. CONTRACT OR GRANT NUMBER(s) DAAH01-73-C-1074
9. PERFORMING ORGANIZATION NAME AND ADDRESS Hercules Incorporated, P. O. Box 98 Bacchus Works Magna, Utah 84044		10. PROGRAM ELEMENT, PROJECT, TASK AREA & WORK UNIT NUMBERS
11. CONTROLLING OFFICE NAME AND ADDRESS Commander U.S. Army Missile Command Attn.: AMSMI-RK Redstone Arsenal, ALA 35809		12. REPORT DATE 2 April 1975 13. NUMBER OF PAGES 92
14. MONITORING AGENCY NAME & ADDRESS(if different from Controlling Office)		15. SECURITY CLASS. (of this report) UNCLASSIFIED 15a. DECLASSIFICATION/DOWNGRADING SCHEDULE

16. DISTRIBUTION STATEMENT (of this Report)

Distribution limited to U.S. Government agencies only; Test and Evaluation (16 Dec. 1974). Other requests for this document must be referred to Commander, U.S. Army Missile Command, Attn: AMSMI-RK, Redstone Arsenal, ALA 35809

17. DISTRIBUTION STATEMENT (of the abstract entered in Block 20, if different from Report)

18. SUPPLEMENTARY NOTES

19. KEY WORDS (Continue on reverse side if necessary and identify by block number)

Gas generator, fluorine, $N_2F_4 \cdot AsF_5$, NF_4AsF_6, HF laser, combustion sensitivity, DF laser, boron, boron carbide, pressed grain, oxidizer, hydrolysis, nozzle cooling, atomic fluorine.

20. ABSTRACT (Continue on reverse side if necessary and identify by block number)

The energetic salts NF_4AsF_6 and $N_2F_4 \cdot AsF_5$ were used in the preparation of fluorine generator grains. Based on thermochemical calculations, blends of these salts with a fuel and fluorocarbon binder were formulated and pressed into solid grains. Stability, compatibility, and sensitivity data were gathered. Solid grains were successfully combusted. Mechanical properties were demonstrated from inert specimen data. Precombustor concepts and insulation materials were evaluated for application to HF/DF laser systems.

DD FORM 1 JAN 73 1473 EDITION OF 1 NOV 65 IS OBSOLETE

UNCLASSIFIED

SECURITY CLASSIFICATION OF THIS PAGE (When Data Entered)

PREFACE

This report is the final technical report covering the effort conducted at the Bacchus Works of Hercules Incorporated, Magna, Utah, under ABL Mill Order 65849 in accordance with contract DAAH-01-73-C-1074, U. S. Army Missile Research, Development and Engineering Laboratory, Redstone Arsenal, Alabama. The effort was conducted under the technical cognizance of Dr. O. E. Ayers, AMSMI/RKL.

Report RK-CR-75-24, titled "Smokeless Motor Technology for Air Defense Application," covers a smokeless propellant effort conducted under the same contract at Hercules/Allegany Ballistics Laboratory.

Principal investigator was Mr. R. B. Leining, supported by Dr. D. T. Sauer, Dr. H. L. Young, and Mr. E. D. Casseday.

In addition to the authors, technical support was provided by G. M. Daurelle, Dr. K. B. Isom, and J. A. Kohlbeck, C. E. Ebeling, and T. D. McComas.

TABLE OF CONTENTS

LIST OF FIGURES

LIST OF TABLES

SUMMARY

The purpose of this program was to develop a solid fuel generator for the DF chemical laser. The solid fuel should be suitable for feasibility demonstration in a state-of-the-art DF chemical laser apparatus. A source of fluorine was developed for the DF chemical laser. The solid formulation consisted of an energetic complex fluorine salt, a perfluorocarbon binder, and the fuel additive, boron. The solid was predicted to furnish atomic fluorine at the specified temperatures, after heat loss and dilution by helium gas at between 2 and 4 moles per 100 gm solid. The net atomic fluorine supplied in gm per 100 gm solid will be 6 if the readily available salt $N_2F_4 \cdot AsF_5$ is used, or 12 if an advanced perfluoroammonium (NF_4^+) salt is used. The combustion products are predicted to remain gaseous.

The salt $N_2F_4 \cdot AsF_5$ was synthesized in the laboratory. The salt NF_4 AsF_6 was available from another program. The salt NF_4BF_4 was excluded from this study. A sample of a compatible insulation material was supplied by TRW Systems Group.

Powdered formulations were pressed into solid specimens of 1.2 gm each at a density of 2.5 gm/cc. The specimens were combusted in a small window bomb at nitrogen pressures of 500 and 1000 psig. Good combustion required the fuel additive boron. A particle size was found at which the boron additive was consumed close to the burning surface. A typical burn rate at 1000 psi was 0.25 in./sec. It is predicted that the minimum pressure for stable combustion will be between 500 and 1000 psi. At 1000 psi, a thermocouple indicated a temperature of at least 1370° C (1643° K) before burning out.

A precombustor concept was designed for combustion testing of solid fuel grains of 100 gm or more at 1000 psi.

The effect of binder content on mechanical properties was found by compression testing of pressed formulations with inert salt. At 10 weight percent Teflon FEP (13 vol percent), the maximum compressive stress was 4000 psi, the strain at maximum stress was 3 percent, and the average modulus was 2×10^5 psi.

Pressed specimens with 10 weight percent FEP binder were degraded visibly but non-violently by humidity. Weight increased. Arsenic fluorides were not detected in the vapor phase. Better encapsulation is desirable. The salt and the formulations should be processed in a dry inert atmosphere.

The salt and the formulations in powdered form were considered to be explosive on the basis of sensitivity to impact. Sensitivity of formulations to friction depended on the concentration of boron particles of submicron size. Elimination of submicron particles from crystalline boron by wet-sieving and settling made the powdered formulation much less sensitive to friction. Numerous energetic specimens were pressed in stainless steel dies at up to 17,000 psi without incident.

Samples of energetic salts, powdered binders, and energetic formulations were shipped.

A. INTRODUCTION

The purpose of this effort is to develop a solid fuel for the DF chemical laser and to deliver samples. The emphasis is on a solid source of atomic fluorine. This source must deliver free fluorine with sufficient energy to maintain the monatomic state after the heat loss and dilution typical of a state-of-the-art chemical laser apparatus. The temperatures after dilution have been specified as 1800° K in the plenum at 150 to 300 psia, and 250 to 400° K in the cavity at 5 to 20 Torr.(1)

In a typical laser apparatus (Figure 1), the precombusted gases lose energy by convection and radiation to the walls. Furthermore, they are diluted with an inert gas of high specific heat ratio prior to nozzle expansion. The solid fluorine source must be sufficiently energetic to keep the unbound fluorine in monatomic form after heat loss and dilution. Therefore, a formulation effort must consider these factors simultaneously with the fluorine stoichiometry. For a state-of-the-art laser apparatus of unspecified size, heat loss was assumed as 50 percent of the heat precombustion, with most of the loss occurring in the array of slit nozzles. The actual loss will be a function of laser nozzle dimensions and gas flow rate.

Thermochemical calculations were made to screen formulations in terms of atomic fluorine concentration in the plenum chamber after assumed heat loss and dilution.

Energy release in combustion can be increased by adding a solid fuel ingredient. The fuel should form a noncondensable gas and should obtain a maximum energy release per atom of fluorine consumed. The standard heats of formation of BF_3 and CF_4, from JANNAF tables,(2) restated as average energy released per gram atom of fluorine consumed, are 90 kcal and 55 kcal, respectively. Therefore, elemental boron is a more energetic fuel additive than carbon. Boron carbide and boron nitride may have advantages of cost, purity, and availability compared to the element boron, although less energetic. Thermochemical calculations were made to compare elemental boron with the carbide and nitride as fuel additives.

The temperature specification of 1800° K was corrected by estimates of heat loss and dilution in order to arrive at the adiabatic combustion temperature required of the solid fuel formulation. The adiabatic combustion temperature was related to trial formulations by chemical equilibrium computations, assuming the solid ingredients to be pure.

The solid formulation is subject to constraints. Exhaust products capable of interfering with DF lasing, such as HF, H_2O, and CO_2, are to be avoided. The gas should be optically smokeless at the wavelength of the laser. The gas should not foul the slit nozzles of the laser apparatus, which are typically a few thousandths of an inch wide and are constrained to low surface temperature by the corrosiveness of the gas. The binder was constrained to at least 10 percent by weight, arbitrarily, pending tests of mechanical properties. Within these constraints, the net free fluorine was to be maximized.

Toxicity and amenability of exhaust to waste treatment are obviously important considerations for the long term. For the work period covered by this report, however, the emphasis was on demonstration of feasibility rather than a final formulation. Consequently, toxicity was not a formulation constraint.

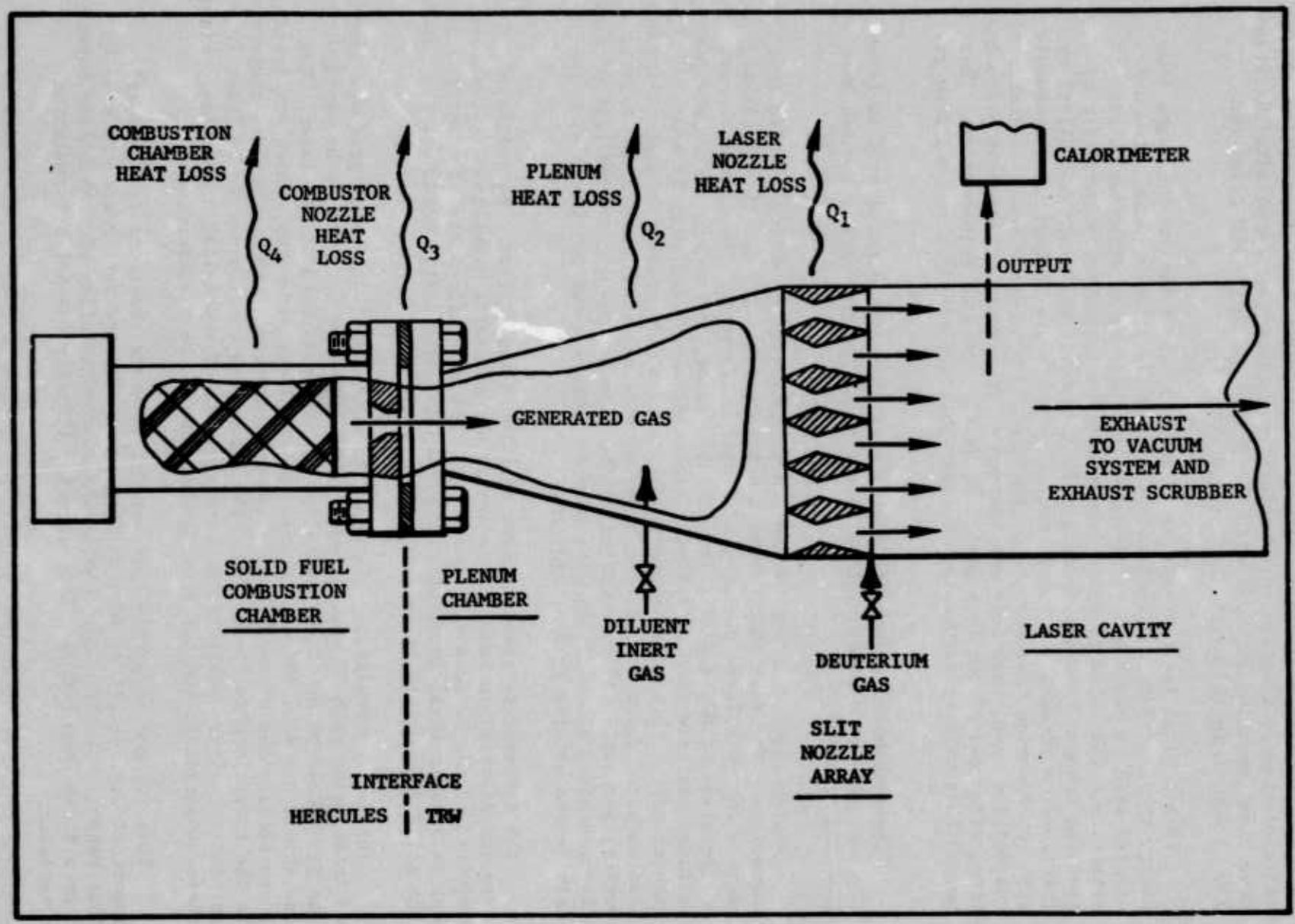

Figure 1. Laser Demonstration Concept

The solid formulation consists of a complex perfluoronitrogen or interhalogen salt, a perfluorocarbon polymeric binder, and a potentially smokeless fuel additive, such as finely powdered boron. The salts $N_2F_4 \cdot AsF_5$ and $KClF_4$ are easily made,[3,4] and, hence, are considered state-of-the art ingredients. The fluorocarbon binders, TFE and FEP, are commercially available in powdered form. However, the salts NF_4 BF_4 and NF_4 AsF_6[5,6,7,8] and the binder polyperfluorobutadiene (PPFB)[9] are difficult to make; hence are considered advanced ingredients.

Specimens of the salt NF_4 AsF_6 mixed with a solid fluorocarbon had been burned in powdered form at low pressure.[10]

Specimens of the salt $N_2F_4 \cdot AsF_5$ with FEP and boron (up to 250 micron) were pressed into a solid pellet of density 2.6 gm/cc and combusted under nitrogen pressure in tests supported by Hercules IR&D funding. The specimens were consumed partially at 300 psig and completely at 1000 psig. High-speed color motion pictures showed dull orange particles being ejected. These were believed to be large particles of boron whose combustion was incomplete. Boron of a smaller particle size was recommended.[11]

In a typical solid propellant gas generator, analogous to the solid fuel precombustor, the chamber interior surfaces are protected by ablative insulation. The insulation is typically a synthetic rubber, with added resins and mineral fillers. In the present application, such materials will consume fluorine and produce HF (which is a laser de-activator), smoke, and debris. A compatible insulator is needed that is free of hydrogen, consumes a minimum of fluorine, discharges no particulates, and whose structure offers good ablative properties. The subtask of identifying a compatible perfluoroinsulation polymer was assigned to TRW Systems Group.

The problems of formulation, heat loss, materials properties, and combustion testing require iterative solution. To develop a solid fuel amenable for demonstration firings, a design concept of the precombustor and its sonic orifice was needed. This need became more acute when early combustion tests showed combustion of the solid fuel to be more efficient at 1000 psi than at 500 or 300 psi. The preliminary design of a precombustor, to hold 100 gm of the baseline solid fuel, was assigned as a subtask to Allegany Ballistics Laboratory (ABL). The final report of this effort is included in Appendix A.

A solid fuel development program was established at Bacchus under Mill Order 65849 from Allegany Ballistics Laboratory (ABL) contract DAAH01-73-C-1074. The program comprised seven tasks:

(1) Thermochemical calculations

(2) Preparation and compatibility of fluorine compounds

2.1 Compatible insulation material (TRW)

(3) Combustion and mechanical properties of formulations

(4) Stability and sensitivity tests

(5) Chemical process data

(6) Delivery of samples

(7) Reporting.

The effective dates were 2 February through 30 June 1974. Four monthly progress reports were submitted. Progress during June is included in the final report. This is the final report of development of a solid fuel for a chemical laser under ABL M. O. 65849.

B. DISCUSSION

1. Task 1, Thermochemical Calculations

Thermochemical computations were made in support of the formulation effort for the following systems of ingredients:

(a) Salt $N_2F_4 \cdot AsF_5$ with TFE, boron

(b) Salt NF_4AsF_6 with TFE, boron

(c) Substituting boron carbide (B_4C) or nitride (BN) for elemental boron

(d) Substituting binder PPFB for TFE

(e) Salt $KClF_4$ with TFE, boron

(f) Dilution of the above with helium.

The goal was to maximize atomic fluorine after losses and within constraints. Further objectives were to identify major products of combustion and product recombination versus temperature, to evaluate product condensation as a possible source of smoke, and to verify simplifying assumptions for use in manual calculations.

a. Basis

Gas composition and properties were predicted at chemical equilibrium by means of a free-energy specific impulse program, Bacchus No. 65005.[12] Trivial products were omitted. Equilibria were allowed to shift as follows in systems containing arsenic:

$$\sum_{1}^{4} CF_x + \sum_{1}^{4} (4 - x)F = CF_4$$

$$AsF_3 + 2F = AsF_5$$

$$F + F = F_2$$

The significant product, arsenic trifluoride (AsF_3), was available in the computer product list as a gas only. The possibility of its condensation is treated in a separate paragraph of this report. The heat loss was estimated as half the heat of solid fuel combustion. This amounted to a loss of 47 kcal per 100 gm solid fuel for the baseline formulation. The loss was assigned to 1 gm of the $-(C_2F_4)-$ fluorocarbon binder as a large, additional negative heat of formation. The baseline solid fuel composition was as follows (wt percent):

Salt $N_2F_4 \cdot AsF_5$	85
Fluorocarbon $-(C_2F_4)-$	11
Boron, crystalline	4
	100

Each ingredient was assumed to be pure. Some thermochemical properties are given in Appendix B.

For the heat of formation of the complex salt, an estimated value of -332.9 kcal/gm mole was used. The inert diluent helium was added in the following ratios (gram moles He per 100 gm solid fuel): 0, 1, 2, 4, 8. The work of injecting the helium was neglected in the energy balance by introducing this gas at a temperature of 298° K.

After dilution and attaining equilibrium in the stagnant plenum chamber, the gas composition was frozen, and no further heat loss was allowed. Although heat loss is known to occur in a practical laser nozzle, it is convenient when using program 65005 to assign all heat losses to the plenum chamber and assume that the subsequent nozzle expansion is isentropic. Two alternate expansions were considered for the arsenic systems:

	Plenum		Cavity	
	Psi	Atm	Torr	Atm
1)	66	4.5	4.5	0.006
2)	12.5	0.85	3.0	0.004

Of the over-all expansion, only a portion actually occurs within a state-of-the-art laser nozzle. The rest occurs externally after the introduction of the cavity fuel, deuterium, complicated by a plume-mixing process. In these computations, the cavity fuel and mixing process were neglected. A single isentropic expansion was assumed from plenum pressure to cavity pressure.

In systems where the energetic salt was $KClF_4$, the major products were assumed to be BF_3, CF_4, KF gas, ClF, and F. Minor products were CF fragments, gas dimer $(KF)_2$, Cl, Cl_2, KCl gas, and F_2. Condensed phases of KF and KCl were omitted because program No. 65005 changes phase according to temperature only. Instead, condensation was predicted manually by comparing partial pressure with vapor pressure, as had been done previously for AsF_3. The condensation of potassium fluoride, KF, appeared to exclude this salt from further consideration. For a full evaluation of the condensation problem, equilibrium was considered at the following precombustor pressures:

(1) 0.85 and 4.5 atmospheres, corresponding to the precombustors of existing Cl II and Cl V lasers

(2) 10.2 and 20.4 specified in the advanced solid fuel precombustor[1]

(3) 68.0 corresponding to solid fuel combustion tests.

Two terms useful for rapid screening of solid fluorine sources were the FOMOX ratio and the net fluorine.

The FOMOX ratio was defined as the ratio of fluorine oxidizer available to fluorine oxidizer consumed by the fuel elements. It is analogous to the OMOX ratio, which is used with solid propellants, to compare the total oxygen with the fuel elements aluminum and carbon. In the FOMOX ratio, the fuel elements have coefficients based on their expected fluorides instead of oxides. A value less than unity indicates deficiency as a solid source of fluorine. The extent that the value exceeds unity is a direct measure of fluorine excess. Where the energetic salt contains arsenic,

$$FOMOX = F/(3As + 3B + 4C)$$

When the salt $KClF_4$ is used, K and Cl are considered as fuel elements, and the ratio is defined from the major products as follows:

$$FOMOX = F/(3B + 4C + Cl + K)$$

The net fluorine was defined as the fluorine remaining after formation of the major products. It was expressed as gm atom or gm per 100 gm of solid formulation.

After confirmation of the major products, these terms were used to eliminate many candidate formulations on the basis of elemental composition from simple manual calculations.

b. Formulations of $N_2F_4 \cdot AsF_5$, TFE, and Boron

Formulations of the salt $N_2F_4 \cdot AsF_5$ with polytetrafluoroethylene (TFE) binder and boron feed additive were evaluated in Tables I and II. The temperatures of Table I are adiabatic, allowing CF_4 to dissociate. All the temperatures of Table II have been lowered to 2200°K or below by the assumed heat loss, and dilution with helium lowers temperatures further.

At temperatures of about 2700° K and below, all the carbon appears as CF_4. Thus, CF_4 is confirmed as a major product, and any fluorine obtained by dissociation of CF_4 is unlikely to remain available.

In Table I, the formulation 80-16-4, at a FOMOX ratio of unity, obtained atomic fluorine by CF_4 dissociation and was therefore rejected. The baseline formulation 85-11-4, at a FOMOX ratio of 1.10, obtained 0.3 gm atom or 6 gm of net fluorine after forming CF_4 and was, therefore, retained for further evaluation.

The arsenic appears as the major product AsF_3, except where temperature is lowered by reformulation for more excess fluorine (Table I), or by heat loss and dilution accompanied by severe fluorine loss. (See Table II.) Loss of atomic fluorine on cooling occurs by formation of AsF_5 rather than molecular F_2. (See Table II and Figures 2 and 3.) The loss begins at about 1800° K. At 1500° K, half the net fluorine is lost. At 1250° K, the atomic fluorine is negligible.

The baseline formulation can meet the specified cavity temperature after 50 percent heat loss and dilution by 2 to 4 gm moles helium per 100 gm of solid formulation. (See Table II.) Atomic fluorine is 3 to 5 gm per 100 gm solid fuel, depending on the dilution.

Calculations were made to determine if gaseous AsF_3 would condense during nozzle expansion. Condensation to liquid droplets or solid particles might introduce smoke in the laser cavity. Isentropic expansion of the gas mixture could lower the static temperature to the normal boiling point of pure AsF_3, which is 63° C (336° K) and possibly even to the normal melting point, which is -8.5° C (264.5° K).[13] The range of pressures considered from the throat to the cavity was 0.45 atm to 0.004 atm. Dilution by the other exhaust species and by helium, of course, reduces the partial pressure of the AsF_3. Assumptions were ideal gases, frozen composition, constant specific heat ratio, steady state, and no further heat loss beyond the assumed 47 kcal per 100 gm solid fuel. Figure 4 shows that the partial pressure of AsF_3 will remain 1000 times smaller than its vapor pressure. Therefore, AsF_3 should neither condense nor freeze in bulk during laser operation.

TABLE I

GAS PROPERTIES VERSUS FORMULATION

Temperature, Adiabatic (^{o} K)*	Pressure (psia)	Atomic Fluorine g atom/100 grams		$\frac{CF_4}{C}$-	$\frac{AsF_3}{A_2}$-	FOMOX	Formulation, g/100g			
		Total	Net				Salt $N_2F_4 \cdot AsF_5$	Teflon	Boron	Desig.
3484	1000	0.324	0.018	0.465	0.97	1.001	80	16	4	D
	50	0.433	0.016	0.316	0.975	1.001				
3470	1000	0.4608	0.32	0.630	0.98	1.105	85	11	4	C
	50	0.563	0.32	0.415	0.98	1.105				
2733	1000	0.471	0.47	1.00	0.996	1.17	80	18	2	
2304	1000	0.779	0.779	1.00	0.949	1.36	90	7	3	A
2071	1000	0.670	0.670	1.00	0.88	1.31	85	13	2	B

*CF_4 allowed to dissociate to CF fragments and F

TABLE II

TEMPERATURE AND CONCENTRATION AT EQUILIBRIUM VS HELIUM DILUTION

Helium Diluent	Plenum Chamber[a]													Cavity[b]			
	Pressure		Temp	Gas Moles		Specific	Atomic Fluorine Concentration				CF_4	AsF_3	1/2 F_2	Pressure		Temp	Specific
g Mole 100 g Solid	Psia	Atm	°K	per 100 g Mix	per 100 g Solid	Heat Ratio γ = Cp/Cv	g Atom 100 g Mix	Mole %	Grams 100 g Mix	Grams 100 g Solid	C	As	F_1	Torr	Atm	°K	Heat Ratio γ = Cp/Cv
0	66	4.5	2190	1.52	1.52	1.15	0.311	20.4	5.91	5.91	1.00	1.0	8.6×10^{-4}	4.56	0.006	937	1.16
1.0	66	4.5	1860	2.42	2.52	1.22	0.295	12.2	5.60	5.82	1.00	0.995	2.6×10^{-3}	4.56	0.006	532	1.27
2.0	66	4.5	1666	3.24	3.50	1.27	0.259	8.0	4.92	5.32	1.00	0.96	6.1×10^{-3}	4.56	0.006	357	1.45
4.0	66	4.5	1493	4.64	5.38	1.335	0.1435	3.1	2.73	3.17	1.00	0.775	9.4×10^{-3}	4.56	0.006	255[c]	1.42[d]
8.0	66	4.5	1250	6.99	9.21	1.42	0.0106	0.15	0.20	0.26	1.00	0.519	6.6×10^{-3}	4.5	0.006	160[c]	--
1.0	12.5	0.85	1854	2.43	2.62	1.22	0.30	12.4	5.71	5.94	1.00	1.0		3.04	0.004	685	1.245
2.0	12.5	0.85	1625	3.26	3.50	1.27	0.285	8.75	5.41	5.81	1.00	0.996		3.04	0.004	486	1.34
4.0[e]	12.5	0.85	1440	4.65	5.40	1.335	0.15	3.2	2.85	3.31	--	0.775		3.04	0.004	375	--

[a] Assumed heat loss 47 kcal/100 g solid fuel

[b] Isentropic expansion from plenum at frozen composition

[c] Calculated by hand using estimated mean specific heat ratio

[d] At 298° K

[e] Extrapolated

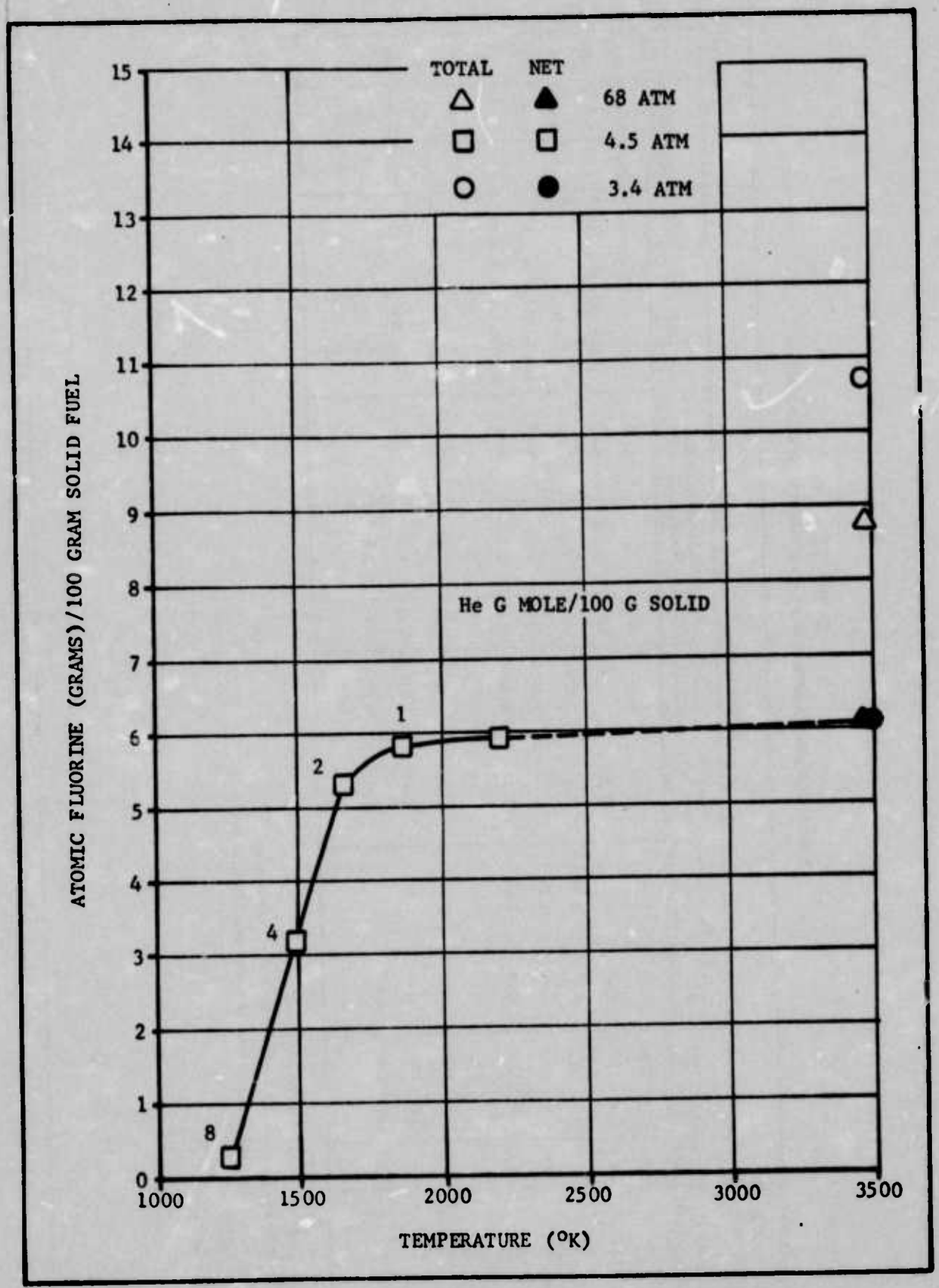

Figure 2. Atomic Fluorine vs Temperature

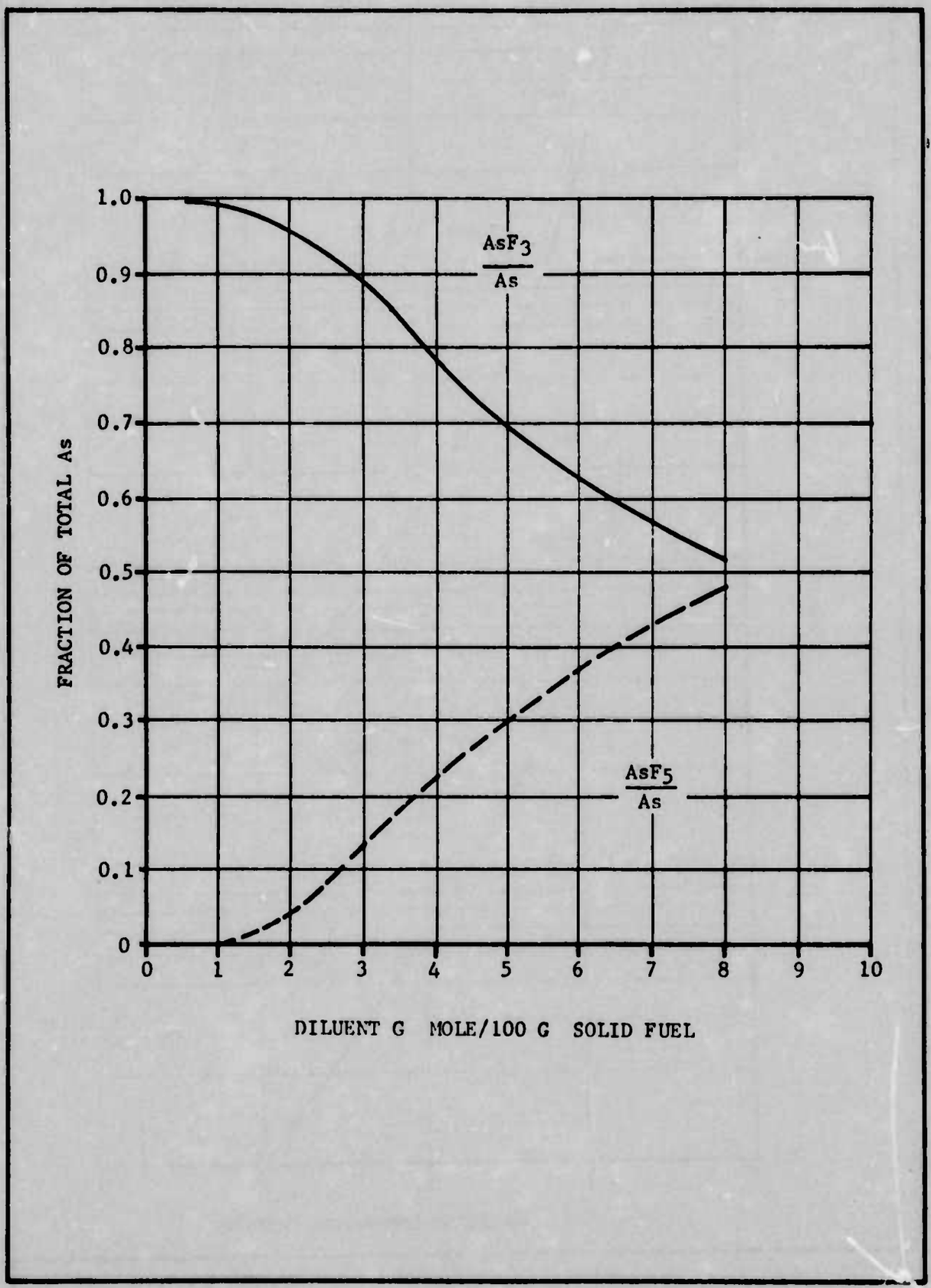

Figure 3. Shifting of Arsenic Fluorides with Helium Dilution

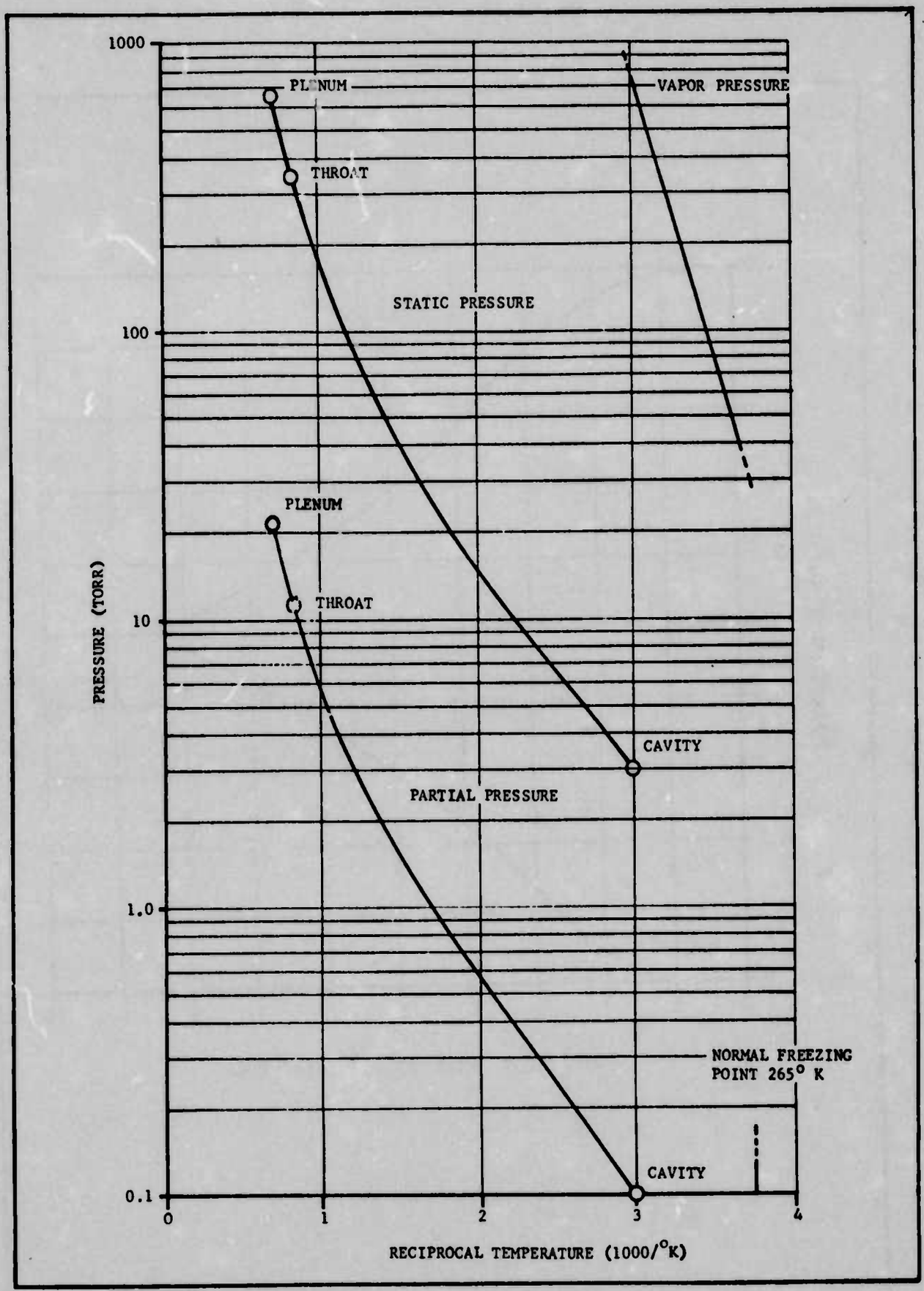

Figure 4. Partial Pressure of AsF_3 vs Vapor Pressure During Nozzle Expansion

During the start-up sequence of a solid-fueled laser, helium alone will flow. Expansion to 0.004 atm, if isentropic, will cool helium from 298° K to 35° K. Heat exchange between the helium and the nozzle walls may precool them sufficiently to condense and freeze some AsF_3 during subsequent gas generator ignition. If this should occur, however, any such condensate will likely sublime after the ignition transient is completed.

In conclusion, thermochemical calculations show that the formulation 85 percent $N_2F_4 \cdot AsF_5$, 11 percent TFE, and 4 percent boron can furnish atomic fluorine at the specified temperatures. Further optimization of the formulation depends on the pressure ratio and the heat loss of a specific laser apparatus.

c. Advanced Ingredients NF_4AsF_6 and PPFB

Thermochemical predictions were made to evaluate the advanced salt NF_4AsF_6 and the advanced perfluorocarbon binder PPFB in solid formulations. Use of NF_4AsF_6 in place of $N_2F_4 \cdot AsF_5$ increases the free fluorine at approximately equal adiabatic combustion temperature. Use of the binder PPFB in place of Teflon TFE allows using more binder and less boron to achieve a given temperature and amount of atomic fluorine. Some boron addition is still needed to achieve an adiabatic combustion temperature of about 3500° K. (See Table III.)

d. Boron Carbide and Nitride

Thermochemical calculations show that boron carbide is theoretically a substitute for elemental boron, gram-for-gram, at slight loss of free fluorine. This loss can be compensated by decreasing the amount of $-(C_2F_4)-$ fluorocarbon and increasing the amount of salt by 1 gm each per 100 gm solid fuel. (See Table IV.) The net cost savings depends on the production cost of the energetic salt, which will be a function of scale presently unknown. (For the effect of boron carbide on sensitivity and burning rate, refer to paragraphs 3c, "Combustion Tests", and 4a, "Sensitivity to Impact and Friction".)

Boron nitride, BN, represents a possible fixed nitrogen ingredient within a solid fuel grain. The nitrogen contribution is 0.02 gm mole N_2 per gm BN added. For instance, adding 10 gm of BN to the baseline formulation (C of Table IV) would increase the specific heat ratio from 1.160 to 1.173, if gas properties were otherwise constant. (See Figure 5.) The nitride BN is also a form of boron available in high purity at low cost.

TABLE III

GAS PROPERTIES PREDICTED AT 1000 PSI WITH ADVANCED INGREDIENTS

Ingredients Complex Salt	Binder	Formulation, gm/100 gm Salt	Binder	Boron	Temperature Adiabatic °K (a)	$\frac{CF_4}{C}$	$\frac{AsF_3}{As}$	Atomic Fluorine g. atom/100 gm Total (a)	Net (b)	g/100 gm Net	FOMOX	Gas Moles 100 gm (a)
$N_2F_4 \cdot AsF_5$	PPFB	87	10	3	3430	0.753	1.0	0.555	0.456	8.66	1.164	1.716
		83	15	2	3386	0.785	1.0	0.469	0.338	6.4	1.114	1.631
$NF_4^+AsF_6^-$	PPFB	83	15	2	3383	0.865	1.0	0.678	0.600	11.4	1.206	1.682
$NF_4^+AsF_6^-$	Teflon TFE	86	10	4	3446	0.394	1.0	0.711	0.647	12.3	1.229	1.745
$N_2F_4 \cdot AsF_5$	PPFB	80	20	0	2825	1.0	1.0	0.514	0.512	9.73	1.182	1.594
$NF_4^+AsF_6^-$	PPFB	80	20	0	2600(c)	1.0	1.0	0.774	0.774	14.7	1.273	1.697
$N_2F_4 \cdot AsF_5$	Teflon TFE	85	11	4	3470	0.630	0.98	0.461	0.32	6.08	1.105	1.67
$N_2F_4 \cdot AsF_5$	Teflon TFE	86	10	4	3455	0.675	0.98	0.491	0.38	7.22	1.13	1.69

(a) CF_4 allowed to dissociate to CF fragments and F

(b) Basis all C as CF_4

(c) Hand estimation

TABLE IV

BORON ELEMENTAL VS CARBIDE AND NITRIDE

Desig	Formulation g/100 g					Temp Adiabatic °K	Pressure (psia)	Atomic Fluorine g atom/100 grams		FOMOX	$\frac{CF_4}{C}$	$\frac{AsF_3}{As}$	$\frac{N_2}{100\ g}$ g mole	Gas Moles per 100 g		Specific Heat Ratio (1000° K) a
	Salt $N_2F_4AsF_5$	Teflon	Boron	Boron Carbide	Boron Nitride			Total	Net					Chamber	a	
C	85	11	4	-	-	3470 3020 2190b	1000 50 50	0.461 0.563 0.31	0.32 0.32 0.31	1.105	0.630 0.415 1.00	0.98 0.98 1.00	0.31	1.67 1.77 1.52	1.52	1.16
	85	11	-	4	-	3365 2936 b,c	1000 50 50	0.384 0.480	0.263 0.269	1.09	0.76 0.606	0.985 0.99	0.31	1.59 1.68	1.46	1.15
	86	10	4	-	-	3455 3016 b,c	1000 50 50	0.491 0.590	0.380 0.382	1.13	0.675 0.445	0.98 0.98	0.31	1.69	1.57	1.17
	86	10	-	4	-	3352 b,c	1000 50 50	0.414	0.32 0.32	1.11	0.80	1.0	0.31	1.60	1.51	1.16
	85	9	-	-	6	2015 1726 b,c	1000 50 50	0.496 0.648	0.496 0.648	1.33	1.00 1.00	0.649 0.825	0.43	1.70 1.83	1.72[d] 1.83[d]	1.18[d] 1.20[d]
	80	12	-	-	8	2948 2755	1000 50	0.3075 0.350	0.304 0.306	1.11	0.988 0.89	0.998 0.995	0.45	1.62 1.66	1.61	1.17

[a] Basis all C in CF_4, all As in AsF_3, no F_2.

[b] Heat loss 47 kcal/100 grams assumed.

[c] Computation did not converge.

[d] Basis like "a" but actual AsF_5 used.

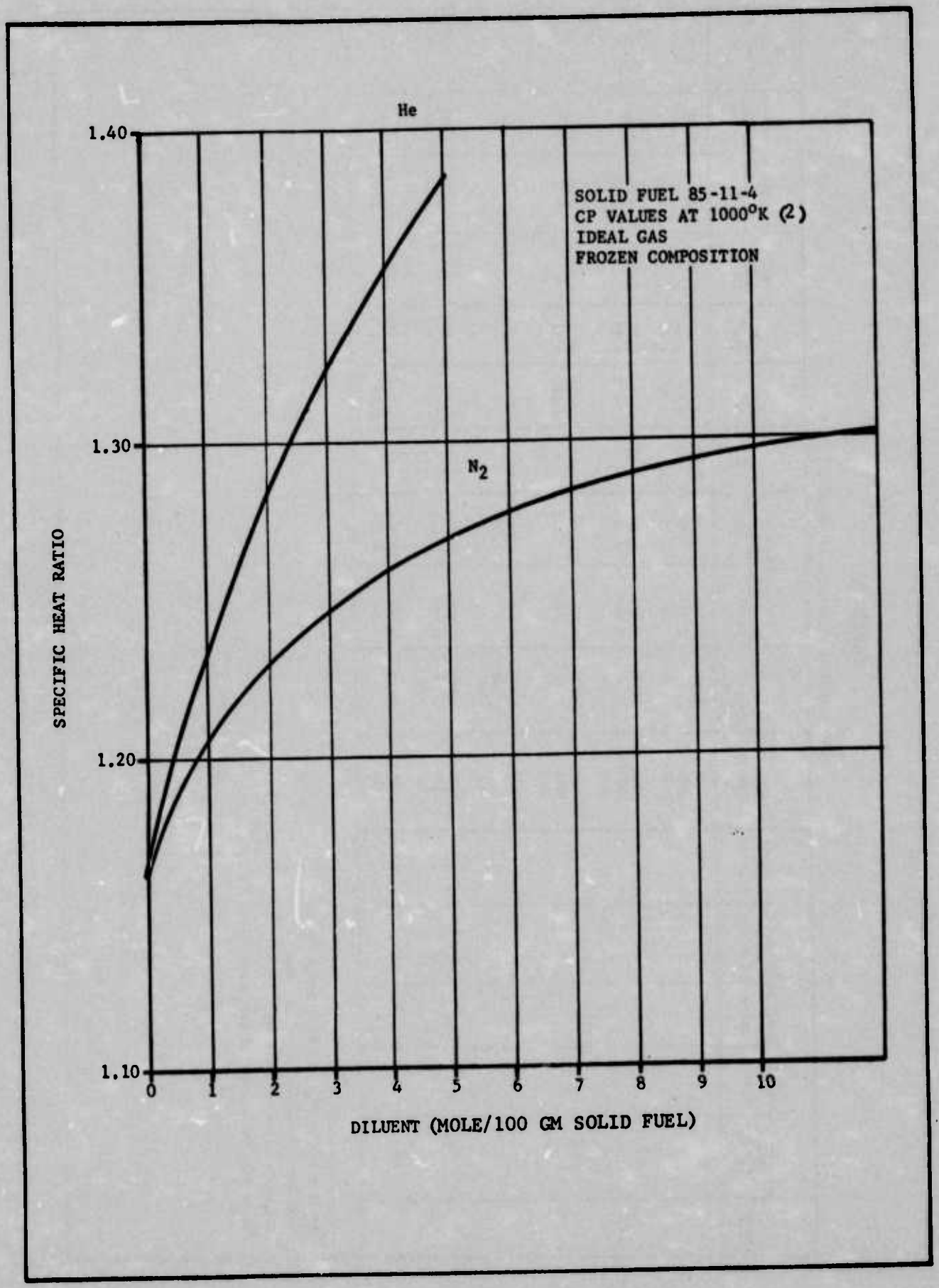

Figure 5. Specific Heat Ratio vs Dilution

Substituting boron nitride in place of elemental boron or boron carbide on a gram-for-gram basis lowers adiabatic flame temperature severely. Boron nitride contains 44 percent boron by weight. Substitution on the basis of boron content is shown in Table IV. Use of the nitride increases the specific heat ratio from 1.16 to 1.20 in one formulation (85-9-6) that at 2000° K is probably too cool to support heat loss and dilution. In a more energetic nitride formulation (80-12-8), the specific heat ratio is equal to that obtained with elemental boron or with the carbide. (See Table IV.)

e. Formulations of $KClF_4$, TFE, and Boron

Thermochemical calculations were made to formulate a solid fuel from the interhalogen salt $KClF_4$. The other ingredients were a perfluorocarbon binder, either Teflon TFE or polyperfluorobutadiene, PPFB, and a fuel additive, elemental boron. Each ingredient was assumed to be pure.

The total atomic fluorine, ·F, from equilibrium adiabatic combustion (Table V) included a contribution when dissociation of the major product chlorine monofluoride, ClF. When the formulation was changed to increase temperature at the expense of free fluorine, this dissociation was encouraged, as shown by the ratio ClF/Cl in Table VI. When a given formulation was cooled by heat loss and dilution, the ClF was reformed, and most of the atomic fluorine was lost, as shown by comparing the ratio ClF/Cl with the atomic fluorine in Table VI.

The molecular fluorine, F_2, was negligible; less than 0.01 gm moles/100 gm solid even after heat loss and dilution at temperatures down to 1300° K. Below 1300° K, F_2 grew significant at the expense of atomic F. The relative concentrations depended on pressure. (See Table VI.) Comparison of Table VI with Table II and Figures 2 and 3 shows that the net fluorine remains atomic at lower temperatures when arsenic is absent than when arsenic is present.

The potassium fluoride, KF, was divided evenly between monomeric KF and the dimer $(KF)_2$ at adiabatic combustion temperature. A trend toward more of the dimer, as temperature was lowered by heat loss and dilution, was fictitious because condensation will occur instead.

The condensation of potassium fluoride, KF, vapor is a possible source of smoke. In order to predict condensation, the partial pressure of KF was compared with its vapor pressure. Partial pressure was calculated assuming ideal gas, Dalton's law, and frozen composition during isentropic expansion in the laser nozzle. The mole fraction, KF, was calculated by including the dimer of KF as the equivalent KF. Vapor pressure data at subatmospheric pressure[13] were extrapolated to higher pressures. Comparisons appear in Tables V and VI.

TABLE V

GAS PROPERTIES OF FORMULATIONS WITH $KClF_4$

Formulation gm/100 gm				Temp	Pressure		Atomic Fluorine						Molecular Fluorine	Chlorine Monofluoride ClF	Condensable Gas KF						Gas moles	
							Total	N_2							gm	Mole	Partial Pressure		Vapor Pressure		per 100 gm (a)	
Salt	TFE	FPFB	Boron	Adiabatic	psia	atm	gm atom	gm atom	gm	FOMOX	CF_4	ClF/Cl	F_2 gm mol	gm mol	mole	fraction	atm	Torr	atm	Torr		
				°K			100gm	100gm (a)	100gm (a)	(a)			100 gm	100 gm	100 gm							
88	10	--	2.0	1853	1000	68	0.200	0.215	4.08	1.085	1.0	0.965	0.018	0.563	0.58	0.328	22.3				1.548	1.768
				1727	150	10.2	0.231				1.0	0.946	0.0075	0.553		0.326	3.3				1.602	
				1565	12.5	0.85	0.256				1.0	0.920	0.0025	0.538		0.322	0.274	208			1.669	
87.5	10	--	2.5	2147	1000	68	0.210	0.069	1.32	1.026	1.0	0.75	0.004	0.435	0.58	0.331	22.5	17100	(9.0)	(b)	1.615	1.663
				1966	150	10.2	0.244				1.0	0.70	0.002	0.405		0.326	3.3	2530	(3.5)	(b)	1.687	
				1758	12.5	0.85	0.284				1.0	0.63	7×10^{-4}	0.367		0.320	0.27	207	0.92	700	1.767	
89	--	10	1.0	1800	1000	68	0.233	0.258	5.47	1.118	1.0	0.98									1.553	1.809
				1679	150	10.2	0.273				1.0	0.975	0.015	0.576	0.59						1.607	
				1526	12.5	0.85	0.302				1.0	0.96									1.671	
88.5	--	10	1.5	2115	1000	68	0.240	0.143	2.71	1.055	1.0	0.815									1.619	1.704
				1938	150	10.2	0.275				1.0	0.765	0.003	0.451	0.59						1.690	
				1733	12.5	0.85	0.314				1.0	0.710									1.769	
90	7.5		2.5	1831	150	10.2	0.264	0.202	3.85	1.081	1.0	0.88	0.0015	0.313	0.60						1.627	1.779
89.5	7.5	--	3.0	2049	150	10.2	0.289	0.057	1.09	1.022	1.0	0.615	0.0017	0.364	0.59						1.764	1.673
91	--	7.5	1.5	1654	150	10.2	0.299	0.330	6.27	1.140	1.0	0.985	0.020	0.594	0.60						1.639	1.863
90.5	--	7.5	2.0	1923	150	10.2	0.298	0.185	3.51	1.074	1.0	0.80	0.0035	0.432	0.60						1.723	1.757
90	--	7.5	2.5	2132	150	10.2	0.328	0.040	0.75	1.015	1.0	0.52	0.0015	0.313	0.60						1.809	1.779
92	5	--	3	1922	150	10.2	0.304	0.19	3.62	1.220	1.0	0.80	0.0036	0.491	0.61						1.754	2.001
91.5	5	--	3.5	2130	150	10.2	0.335	0.045	0.86	1.017	1.0	0.53	0.0015	0.322	0.61						1.642	1.684

(a) Based on major products. No condensation.

(b) Extrapolated)

TABLE VI

GAS PROPERTIES AFTER HEAT LOSS AND DILUTION

Helium gm mole/ 100 gm solid	Pressure psia	Pressure atm	Temp T °K	Gas moles per 100 gm mix	Gas moles per 100 gm solid	Specific Ht Ratio γ = Cp/Cv @ T°K x1000°K		Atomic Fluorine gm atm 100 gm mix	Atomic Fluorine gm atm 100 gm solid	Molecular Fluorine gm atm 100 gm mix	Molecular Fluorine gm atm 100 gm solid	Molecular Fluorine gm mol 100gm mix	Molecular Fluorine gm 100gm solid	CF_4 C	ClF Cl	Chlorine mono fluoride gm mol 100 gm mix	Chlorine mono fluoride gm mol 100 gm solid	Condensable Gas KF gm mol 100gm mix	Condensable Gas KF mole fraction	Vapor Pressure partial pressure atm	Vapor Pressure partial pressure Torr	Vapor Pressure atm	Vapor Pressure Torr
0	300	20.4	1700	1.468	1.468	1.16	1.202 (a)	0.103	0.103	1.96	1.96	0.004	0.152	1.0	0.93	0.539	0.539	0.58	0.344	7.04	5340	0.60	460
	150	10.2	1660	1.484	1.484	1.17		0.1103	0.1103	2.10	2.10	0.003	0.114	1.0	0.92	0.534	0.534		0.343	3.5	2660	0.44	335
	66	4.5	1610	1.504	1.504	1.17		0.1178	0.1176	2.24	2.24	0.002	0.076	1.0	0.91	0.528	0.528		0.343	1.54	1170	0.29	220
	12.5	0.85	1515	1.544	1.544	1.175		0.1309	0.1305	2.48	2.48	0.001	0.038	1.0	0.89	0.517	0.517		0.341	0.29	220	0.12	93.4
1	300	20.4	1525	2.328	2.42	1.23	1.273	0.0717	0.0745	1.36	1.415	0.0047	0.18	1.0	0.975	0.544	0.565	0.56	0.218	4.45	3400	1.135	101
	150	10.2	1500	2.340	2.43	1.23		0.0775	0.0805	1.47	1.53	0.0034	0.13	1.0	0.97	0.541	0.562		0.218	2.22	1700	0.11	81
	66	4.5	1465	2.356	2.45	1.235		0.0837	0.087	1.59	1.65	0.0023	0.0875	1.0	0.96	0.536	0.557		0.218	0.98	745	0.075	57
	12.5	0.85	1395	2.391	2.49	1.24		0.0943	0.0986	1.80	1.87	0.0011	0.042	1.0	0.945	0.528	0.549		0.217	0.18	140	0.035	27
2	300	20.4	1375	3.139	3.27	1.28	1.326	0.0524	0.0565	0.995	1.075	0.0075	0.285	1.0	0.99	0.534	0.577	0.54	0.159	3.25	2470	0.028	21
	150	10.2	1360	3.148	3.28	1.28		0.0580	0.0623	1.10	1.19	0.0054	0.205	1.0	0.99	0.533	0.576		0.159	1.62	1230	0.023	18
	66	4.5	1340	3.159	3.29	1.29		0.0635	0.0685	1.205	1.30	0.0035	0.133	1.0	0.99	0.532	0.575		0.159	0.72	544	0.018	14
	12.5	0.85	1295	3.186	3.31	1.29		0.0724	0.0781	1.375	1.485	0.0014	0.053	1.0	0.98	0.527	0.570		0.158	0.135	102	0.010	8
3	300	20.4	1250	3.896	4.37		1.366	0.037	0.041	0.703	0.708	0.013	0.53	1.0	0.995	0.52	0.58	0.52	0.125	2.55	1940		
	150	10.2	1240	3.903	4.37			0.043	0.048	0.817	0.912	0.010	0.42							1.28	975		
	66	4.5	1230	3.91	4.38			0.050	0.056	0.950	1.06	0.007	0.30							0.56	425		
	12.5	0.85	1200	3.93	4.40			0.059	0.066	1.12	1.25	0.003	0.11							0.11	84		
4	300	20.4	1150	4.618	5.35		1.398	0.024	0.028	0.45	0.53	0.018	0.80	1.0	1.0	0.50	0.58	0.50	0.103	2.10	1600		
	150	10.2	1145	4.623	5.35			0.029	0.034	0.55	0.65	0.015	0.65							1.05	800		
	66	4.5	1140	4.629	5.36			0.036	0.042	0.68	0.80	0.011	0.49							0.46	350		
	12.5	0.85	1120	4.643	5.38			0.050	0.058	0.95	1.10	0.005	0.23							0.09	67		

The formulation 87.5 percent salt, 10 percent TFE, and 2.5 percent boron was evaluated in Table VI and Figure 6. The partial pressure of KF versus adiabatic combustion temperature lay on a straight line that crossed the vapor pressure line when the total pressure in the precombustor was 150 psia (10.2 atm). At this pressure and above, condensation of KF is likely. However, because the two lines are almost parallel, their exact intersection is sensitive to error in the extrapolation of vapor pressure. In the equilibrium precombustor after heat loss, temperatures were typically 1300 to 1700° K. (See Table VI.) With or without dilution by helium, the partial pressure of KF was far greater than the vapor pressure. (See Table VI and Figure 6.) Therefore, condensation should occur in bulk, creating smoke.

The other formulations considered in Table V have approximately equal KF concentrations, total pressure, and temperatures. Therefore, the partial pressure of KF will exceed the vapor pressure for the other formulations also when combusted at a total pressure of 150 psia or more. Along the present formulation approach, significantly higher adiabatic combustion temperatures are not available while maintaining free fluorine. (See Table V.)

Isentropic expansion from an equilibrium precombustor at a pressure of 150 psia or more was not calculated because the KF will condense in bulk prior to expansion and, by the assumption of frozen composition, will remain condensed.

Figure 6 shows the partial pressure of KF during frozen isentropic expansion from an equilibrium precombustor at 66 psia. After 50 percent heat loss, with or without dilution, the partial pressure of KF exceeded the vapor pressure initially and throughout the expansion.

In an idealized case where both heat loss and dilution were assumed absent, the partial pressure was initially less than the vapor pressure, became equal to the vapor pressure at the nozzle throat, and exceeded the vapor pressure thereafter. (See Figure 6.) The assumption of frozen composition needs to be re-examined.

The specified final temperature of between 250 and 400° K, after expansion to 5 Torr, is achievable by dilution with helium at 2 to 4 gm moles He per 100 gm solid. However, the cooling effect of adding this much He to the equilibrium precombustor will be KF condensation (Figure 6), which causes smoke.

f. Other Formulations

The thermodynamic advantage of excluding arsenic from advanced solid formulations is shown in Figure 7.[14] Molecular fluorine, F_2, dissociates at lower temperaturs than does arsenic pentafluoride, AsF_5. From JANNAF tables[2] and Appendix B, the standard heats of dissociation are found as follows:

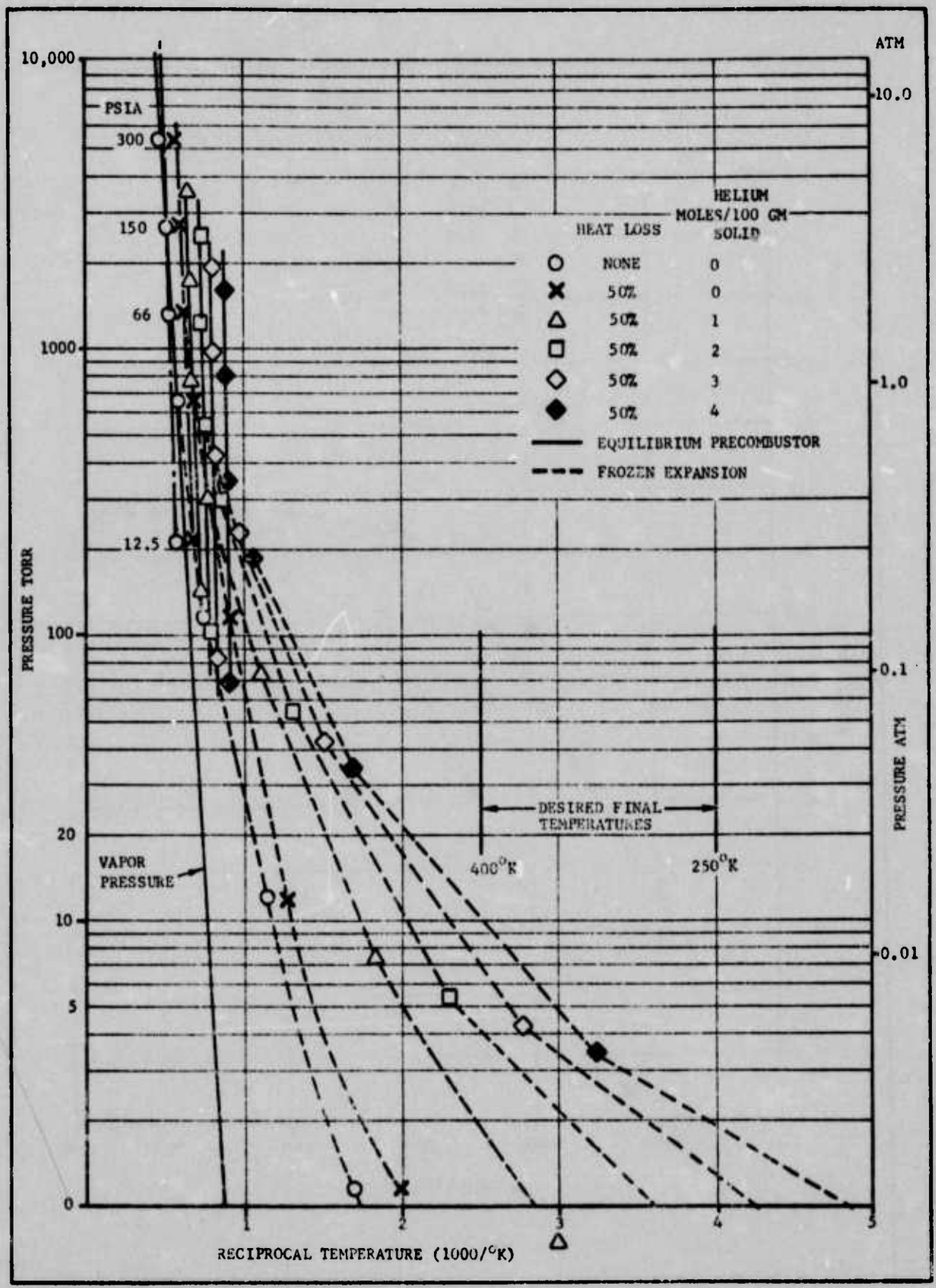

Figure 6. KF Partial Pressure vs Vapor Pressure

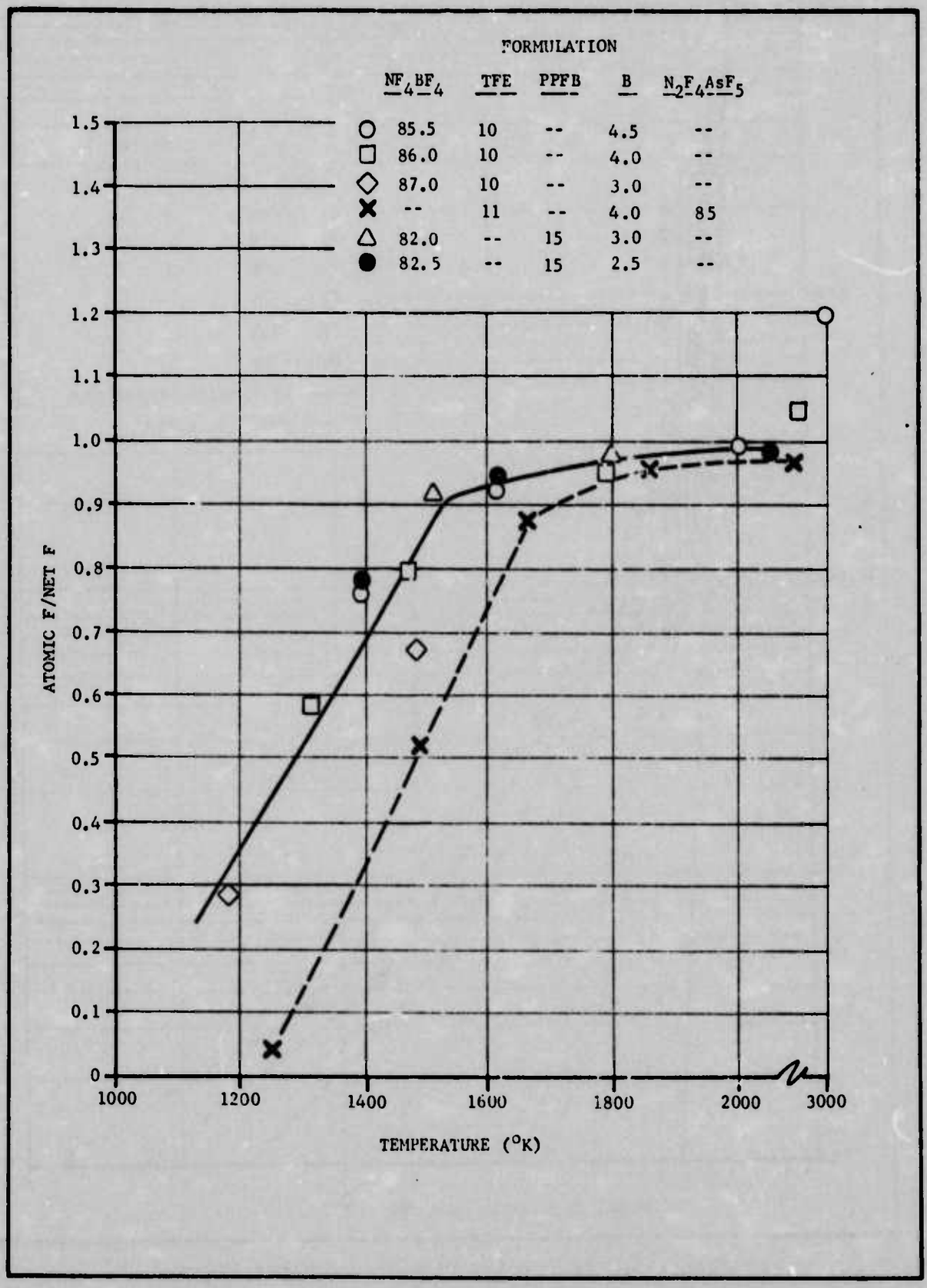

Figure 7. Dissociation of Fluorine at 4.5 Atmospheres

$$1/2\ F_2 \rightleftarrows F \quad \Delta H^\circ_{298} = +\ 18.86 \text{ kcal/gm atom F}$$

$$1/2\ AsF_5 \rightleftarrows 1/2\ AsF_3 + F \quad \Delta H^\circ_{298} = +\ 54.9 \text{ kcal/gm atom F}$$

2. Task 2, Preparation and Compatibility of Fluorine-Containing Compounds

a. Energetic Salts

The energetic salt, $N_2F_4 \cdot AsF_5$, was synthesized from gaseous tetrafluorohydrazine (N_2F_4) and arsenic pentafluoride (AsF_5). Typically, the ingredients were combined at liquid nitrogen temperatures and allowed to react at -78° C for 12 hours. The reactor was then slowly warmed to room temperature and excess reagents removed by evacuation.(3) Commercially available 75-125 ml stainless steel Hoke reactors were used in the preparation of 10 gram batches. Approximately 90 grams of salt were synthesized during this program. The N_2F_4 was produced in the Bacchus pilot plant at a purity of at least 97 mole percent. Unspecified purity arsenic pentafluoride was procured from Ozark-Mahoning, Tulsa, Oklahoma.

The salt was analyzed for metallic impurities by hydrolysis, followed by X-ray fluorescence spectroscopy. These metals, which are potential sources of smoke in laser systems, are formed by corrosion of the reactor and total < 0.5 percent by weight.

The salt is formed in a condensed phase and is obtained as a hard cake. The cake is pulverized to remove the solid from the reactor. The caking also entraps gaseous reactants; hence, evacuation of the pulverized product was necessary to remove such unreacted gases. The solid, $N_2F_4 \cdot AsF_5$, was ground with an agate mortar and pestle and screened through a -60 mesh (250μ) sieve prior to use. The grinding and sieving were performed under inert atmosphere in a nitrogen filled glove box. All equipment used in processing the energetic salt was degreased with Freon 113 and dried at 100° C prior to use.

The interhalogen salt, $KClF_4$, was not synthesized since thermochemical calculations predicted condensation of KF in bulk which would result in probable smoke problems in laser systems. (See paragraph 1e.)

b. Material Compatibility

The energetic salt, $N_2F_4 \cdot AsF_5$, was tested for compatibility with the materials listed in Table VII. Compatibilities at room temperature were demonstrated by mixing the materials at room temperature in a nitrogen atmosphere. Fisher-Johns compatibilities were tested by addition of the materials to a metal planchet which was then heated with a Fisher-Johns melting point apparatus. Any observed change in physical appearance of the salt was noted as evidence of reaction.

TABLE VII

MATERIAL COMPATIBILITY WITH $N_2F_4 \cdot AsF_5$

	Room Temperature	Fisher-Johns
Carbon	no reaction	stable to 150° C
Teflon	no reaction	no reaction to 150° C
Boron	no reaction	boron particles soften slightly at 140° C
Teflon/Boron	no reaction	boron particles soften slightly at 140° C
Hydraulic fluid	smokes	--
Halocarbon oil	slight gassing observed by microscopy	--
Iron filings	no reaction	no reaction
Polyethylene powder	no reaction	--
Vacuum oil (hydrocarbon)	flashes	--
Teflon/boron/polyethylene	no reaction	mixture turns brown and fumes at 70-80° C
Polyperfluorobutadiene	no reaction	no reaction to 120° C

As indicated in the data, hydrocarbon based materials decrease the thermal stability of the energetic salt and energetic salt blends. Sensitivity measurements of energetic blends with polyethylene added also indicated greater sensitivity to both impact and friction. Because of the increased hazards involved in using hydrocarbon based materials, all materials and apparatus that contacts energetic salts will be made of inert materials.

Compatibility testing with NF_4AsF_6 indicates that its compatibilities parallel the $N_2F_4 \cdot AsF_5$ salt quite closely. Both salts react instantaneously with water and ignite alcohol and acetone. The compatibility of NF_4^+ based salts with fluorocarbons has been studied.[10] These tests indicate that most of these materials do not react with NF_4^+ salts.

c. Task 2.1, Compatible Insulation Material

Compatible insulation materials are currently being evaluated to minimize heat losses in DF laser systems. TRW systems was assigned the task for investigation of compatible high char insulation materials. An important result of their prior studies was the development of a crosslinking reaction suitable for application to polyphenylquinoxaline (PPQ) resin. This crosslinking eliminated the thermal plasticity normally observed above 600° C. The TRW crosslinked PPA (CPPQ) resin was found to be a promising high char yielding resin and appears compatible with energetic salts in initial tests. Key properties are outlined in Table VIII.

TABLE VIII

SUMMARY OF FILM PROPERTY RESULTS
ON CROSSLINKED PPQ SYSTEM

Test	Property
Tensile Strength/Elongation (1)	17.5 Psi/17% (2)
Color	Very Dark Amber
Initial Thermo-oxidative Stability (3)	510° C (950° F)

(1) Conditions employed: 0.2 in./min crosshead speed; specimen dimensions: Thickness 0.005 in., width 0.50 in.

(2) Average of five specimens

(3) TGA conditions: 3° C/min scan rate and 100 ml/min air flow

Film samples of this product demonstrated that at 900° C the char yield was approximately 95 percent. At 1800° C, the char yield was 65 percent. These test results indicate that the polymer CPPQ merits consideration as a potential high char yielding insulation material in laser systems.

3. Task 3, Combustion and Mechanical Properties of Selected Formulations

Combustion specimens were blended and pressed from an energetic salt, fluorocarbon binder, and a boron fuel additive. The ingredients were characterized before use.

a. Ingredients

1) Salts

The energetic salts included $N_2F_4 \cdot AsF_5$, synthesized in Task 2, and NF_4AsF_6. The salt NF_4AsF_6 was prepared by Stanford Research Institute (SRI) under Hercules IR&D funding prior to issuance of the ABL Mill Order No. 65849. It was made by thermal activation and pressure in a Monel reactor.

The supplier estimated NF_4AsF_6 purity at 90 percent by weight, based on hydrolysis of NF_4^+ to NF_3. Copper and nickel impurities were detected qualitatively by chemical spot test. No other impurities were detected by infrared analyses. Therefore, the supplier believed the major impurities were copper and nickel hexafluoroarsenates, introduced by corrosion of the Monel reactor during synthesis. The normal sublimation points of the fluorides of copper and nickel are 950-1100 and 1000° C, respectively.[13] Such metallic impurities are potential sources of smoke. If the salt NF_4AsF_6 represents about 85 percent of the solid formulation by weight, then the consequent addition of metallic impurities will be 1.2 percent by weight of the solid formulation.

2) Fluorocarbon Binder

Teflon FEP was obtained as a submicron powder and Teflon TFE as an 8-10μ powder from Liquid Nitrogen Corp. Prior to use, both were dried by heating at 100° C.

Polyperfluorobutadiene (PPFB) was prepared by SRI under IR&D funding from TRW Systems Group in 1973. The molecular weight was reported by the supplier to be 8500 as measured by intrinsic viscosity. The coarse powder was dried by evacuation at room temperature.

3) Boron Fuel Additives

Initial combustion tests used elemental crystalline boron, supplied by Alfa-Ventron at up to 250μ, which was then sieved in the laboratory through -325 mesh (45μ).

A survey was made of commercially available types and particle sizes of boron, boron carbide, and boron nitride. (See Tables IX and X.) At equal nominal purities, the carbide, the nitride, and amporphous boron were less expensive than crystalline boron. Thermochemical calculations had shown the carbide to be equivalent to elemental boron, but had eliminated the nitride. (See paragraph 1d.) Formulations with amorphous boron were eliminated by their extreme sensitivity to friction in previous tests.(11)

Boron and boron carbide samples were received from two vendors, Atlantic Equipment Engineers (AEE) and U. S. Borax Research.

The samples were analyzed at Bacchus for trace metals, semi-quantitatively, by X-ray fluorescence spectroscopy. Metallic impurities are of interest as potential sources of smoke, because their normal boiling or sublimation points are in the range 1000 to 2500° C (1300-2800° K).[13] The major metallic impurities are aluminum, up to 0.8 percent, and iron, up to 0.6 percent. Total of all metals was 0.6 to 1.6 percent. (See Table XI.) If the boron additive represents up to 4 percent of a solid fuel formulation, then the consequent addition of metallic impurities will be 0.024 to 0.064 percent of the total solid formulation.

The particle sizes of boron and boron carbide were determined by photomicrograph and by Coulter counter. Photomicrographs of samples of boron and boron carbide are shown in Figures 8 thru 16. Table XII shows measurements of particle size distribution by Coulter counter. In all the samples, particle sizes of less than 0.8μ are not measured by the Coulter counter. In view of this fact, the weight-average diameters of Table XII may appear larger than actually contained in the samples. It should be noted that the boron carbide samples do not appear to be the submicron and 1-5μ sizes that were ordered and indicated on the vendor's label. The distribution of particle sizes instead resembles that of the -325 mesh boron.

Submicron and oversize (> 325 mesh) particles were effectively removed from commercially available -325 mesh crystalline boron by wet sieving and settling procedures.

Figure 10 is a photomicrograph showing a sample of crystalline boron, nominally -325 mesh, as received from the vendor, U. S. Borax Research. Figure 14 shows similar material after further wet sieving(16) and settling in the laboratory. The submicron particles removed are shown in Figure 16. Figure 15 shows the oversize boron particles that were removed.

TABLE IX

BORON CARBIDE AND NITRIDE: PURITY, PARTICLE SIZE, AND COST

Material	Purity %		Particle Size			February 1974 Cost $/lb		Potential Supplier
			Mesh			Qty		
	Min	Typical	Min	Max	Microns	1 lb	Other	
Boron Carbide (B_4C)		99.7			1-5	23.40		Atlantic Equipment Engineers
		99.7			< 1	27.75		
		99+			10-50	85		Atomergic Chemicals Co.
		99+			?	60		
		95-99.5		-60		7.50		Kawecki-Berylco Industries Inc
		95-99.5			-20	12.50		
Boron Nitride (BN)		99.7			0.3-0.7	34.		Atlantic Equipment Engineers
		99.7			< 1	27.75		

TABLE X

BORON: PURITY, PARTICLE SIZE, AND COST

Material	State	Purity, %		Impurities, %							Particle Size			Feb 1974 Cost, $/lb		Potential Supplier
											Mesh					
		Min	Typical	Mg	Fe	Si	O	C	N	Basis	Min	Max	Microns	Qty 1 lb	Other	
Boron, elemental	Cryst	99.5	--									-325	(-44)	115.	--	Atlantic Equipment Engineers
		99											10-50	250	--	Atomergic Chemicals
		--	99.	0.02[a]	0.2	0.01	0.18	0.05	0.01	Typ		-325	(-44)	175.	--	Atomergic Chemicals
		--	98.5	0.3[a]	0.5	0.08	0.2	0.5	0.01	Max			1-30	150.	--	Atomergic Chemicals
		99.5	--										< 1	115.	--	Atlantic Equipment Engineers
		--	97	0.2	0.2	0.2	0.2	0.2	0.2	Max		-325	(-44)	100.	--	U.S. Borax Research[f]
		--	94.68		0.2	0.27	0.27	3.54	0.19	Typ		-100		--	72.50[b]	Shieldalloy Corp, from H.C. Starck, of Germany[f]
		97.5	--	0.05	1.0	0.15	0.3	0.3	0.05	Max		-325	(-44)	--	82.00[b]	
Boron, elemental	Amorph	--	99.995									60			c	Atomergic Chemicals
		--	99										0.5-1.5			U.S. Borax Research
			95-97	1.0-2.5[a]	0.15	0.10	2.0	0.5	0.5	Typ			0.5-2.0	125.		Atomergic Chemicals
			95-97	0.8	0.15	0.1	2.1		0.5	Typ			0.7-3.0[d]	30.[d]		Shieldalloy/Starck[f]
			95										0.5-1.5	35.		U.S. Borax Research
			94-96										1.	32.		Kawecki Berylco Industries, Inc
			92-95										2-3	23.00		Atlantic Equipment
			92-95										< 1	27.		Atlantic Equipment
			90-92	5.	0.3		4.		4.	Typ[e]			0.7-3.0	25.		Shieldalloy/Starck[f]
			90-92										≤ 1	30.		Kerr-McGee Chemical

[a] Metals other than iron.

[b] In quantities of 10 pounds.

[c] Quantity 100 grams @ $18 per gram.

[d] Minimum order $50.00.

[e] Also 4% hydrogen, other heavy metals 0.3%.

[f] Foreign manufacture

TABLE XI

TRACE METALS ANALYSIS OF BORON AND BORON CARBIDE

Material	Vendor	State	Particle Size Specified		Purity Specified	Trace Metals (Analysis No. 76797)													(Total)
			Mesh	Microns		Fe	Mn	Co	Ni	Cu	Pb	K	Ca	Ti	Al	Si	Zr	Zn	
Boron	Atlantic Equipment Engineers	Cryst.	-325	(-44)	99.5	.50	.20	.02	.02	< .01	.05	T	.05	.05	.20	.10	< .01	< .01	1.22
Boron	Atlantic Equipment Engineers	Cryst.	--	< 1	99.5	.04	.20	.02	.01	< .01	.01	.10	.02	< .01	.10	.10	--	< .01	0.63
Boron	U.S. Borax Research	Cryst.	-325	(-44)	97	.60	.10	--	.04	< .01	< .01	T	.10	.05	.20	.10	--	< .01	1.2?
Boron Carbide	AEE	Cryst.	--	< 1	99.7	.20	.02	--	< .01	< .01	.05	.02	.04	.20	.80	.20	--	--	1.5?
Boron Carbide	AEE	Cryst.	--	1 to 5	99.7	.15	.02	--	< .01	< .01	--	.02	.03	.30	.80	.30	--	--	1.64
Boron	U.S. Borax	Cryst.	*	*	--	0.50	.1	.02	.02	.05	T	T	.05	--	T	T	T	T	0.74

T = trace

* -325 mesh U. S. Borax boron treated to remove oversize and submicron particles

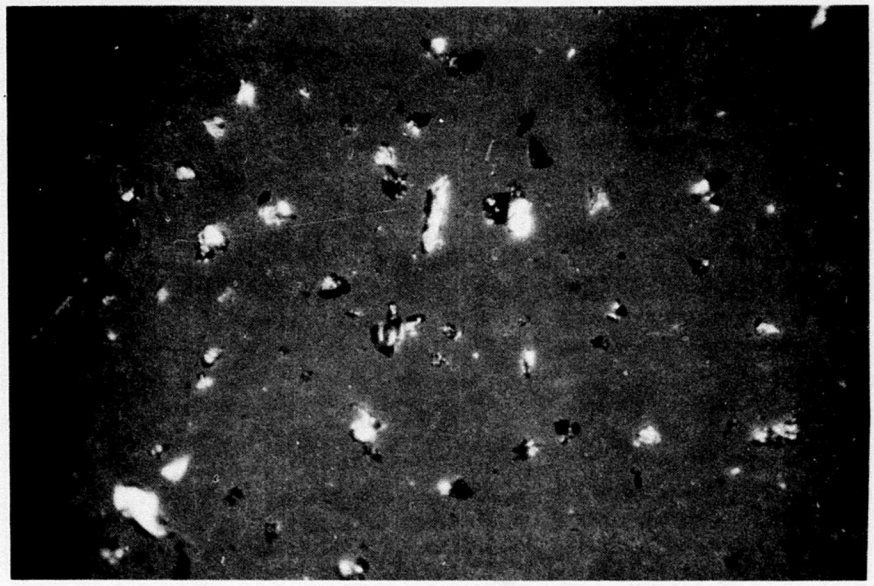

Figure 8. 715μ x 473μ
-325 mesh crystalline boron
Alfa/Ventron, 138x

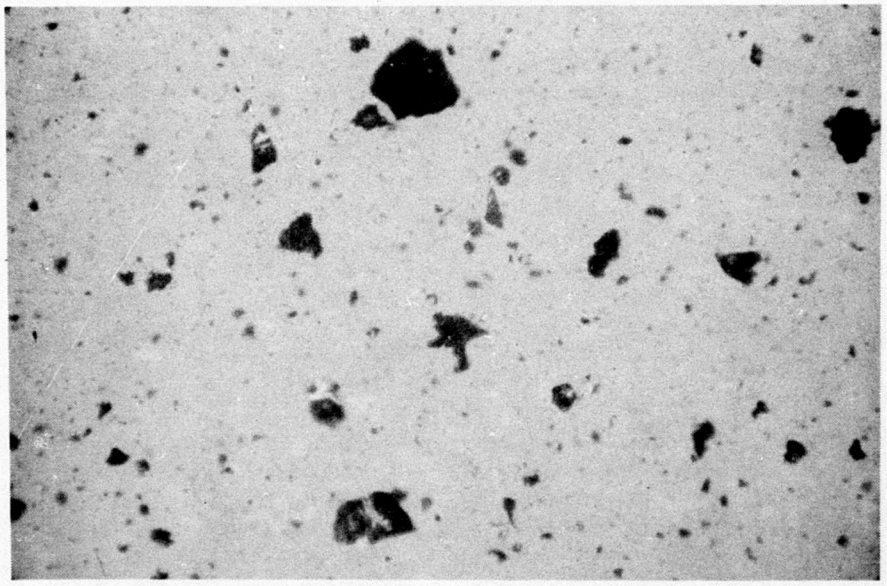

Figure 9. 715μ x 473μ
-325 mesh crystalline boron
AEE, 138x

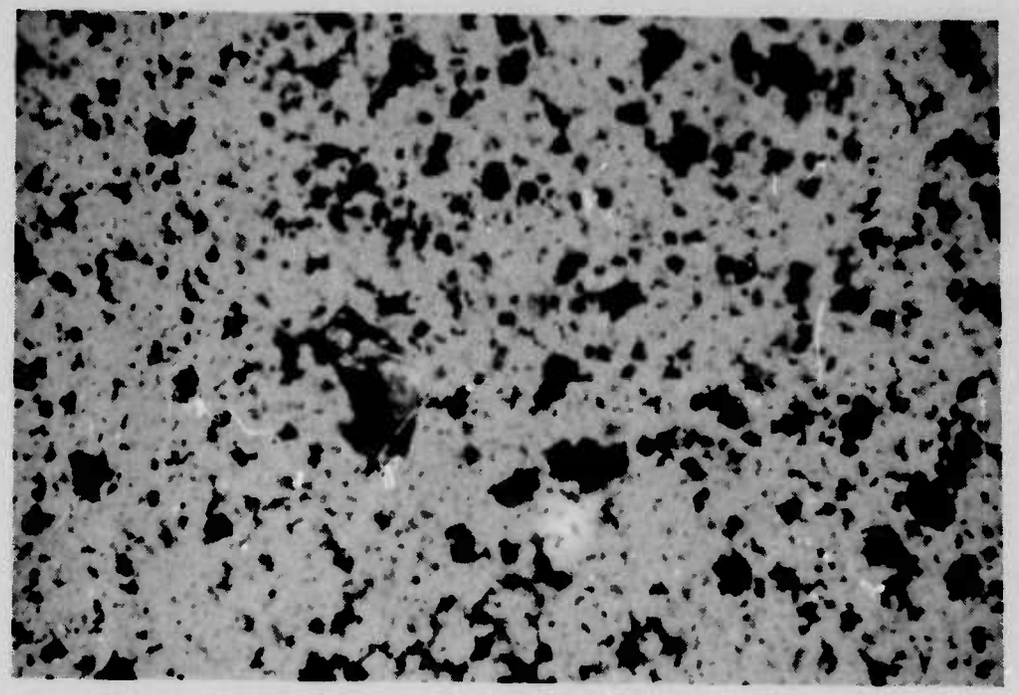

Figure 10. 715μ x 473μ
-325 mesh crystalline boron
U. S. Borax, 138x

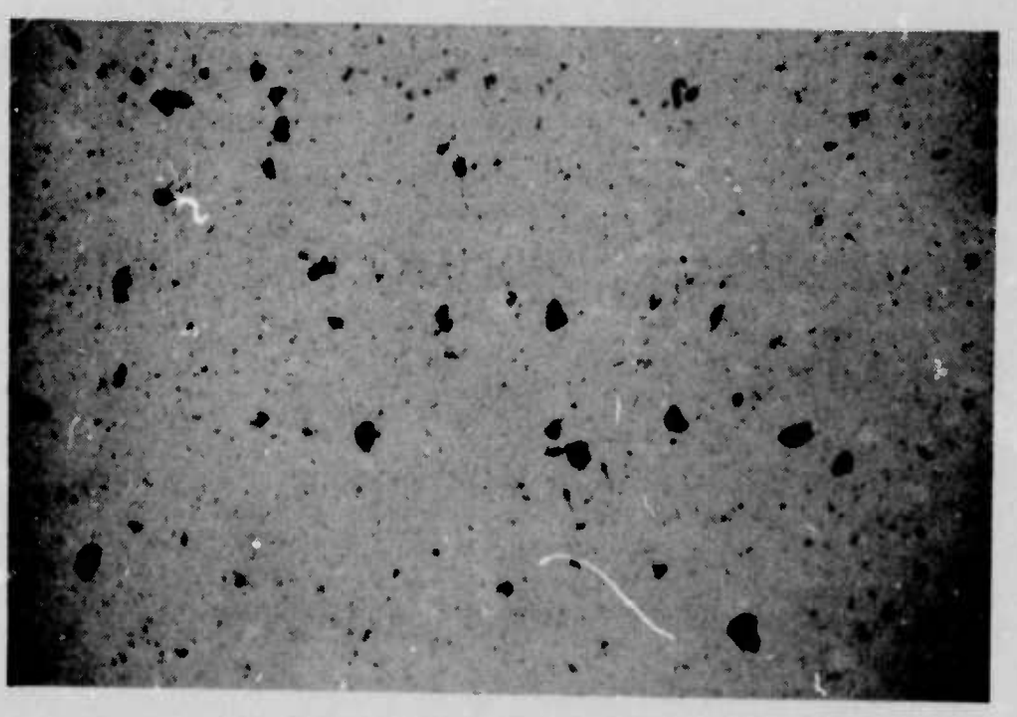

Figure 11. 715μ x 473μ
submicron crystalline boron
AEE, 138x

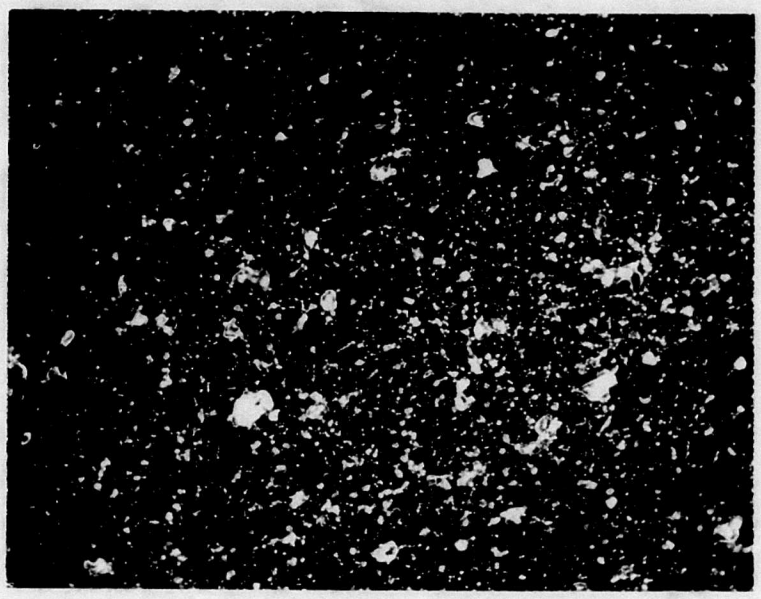

795μ x 620μ
Figure 12. Submicron boron carbide (138x)

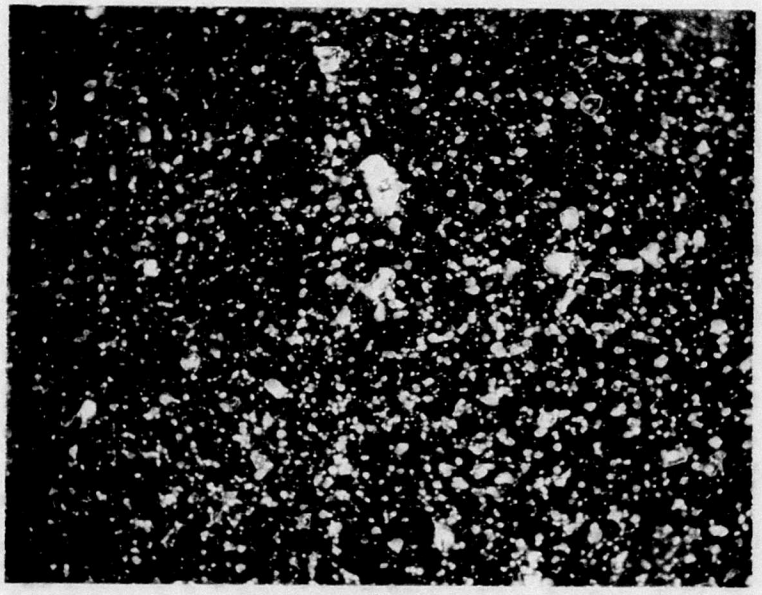

795μ x 620μ
Figure 13. 1-5 micron boron carbide (138x)

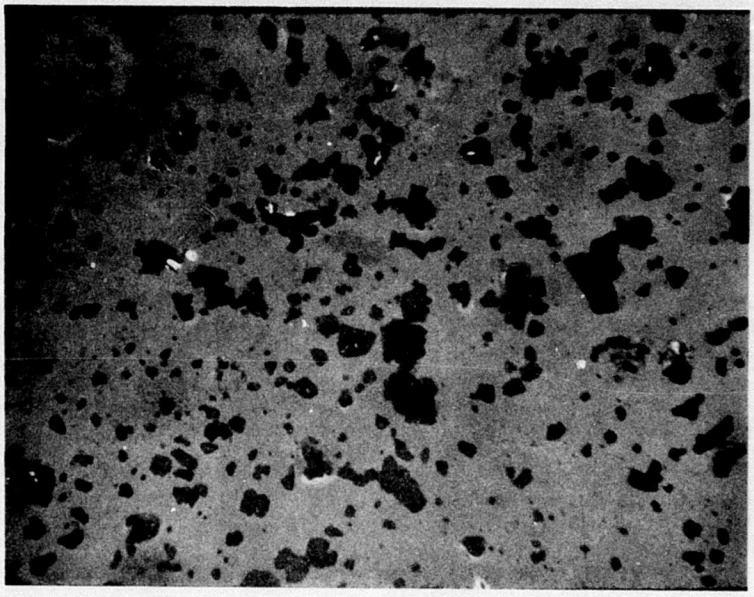

715μ x 473μ
Figure 14. Boron after wet sieving & settling (138x)

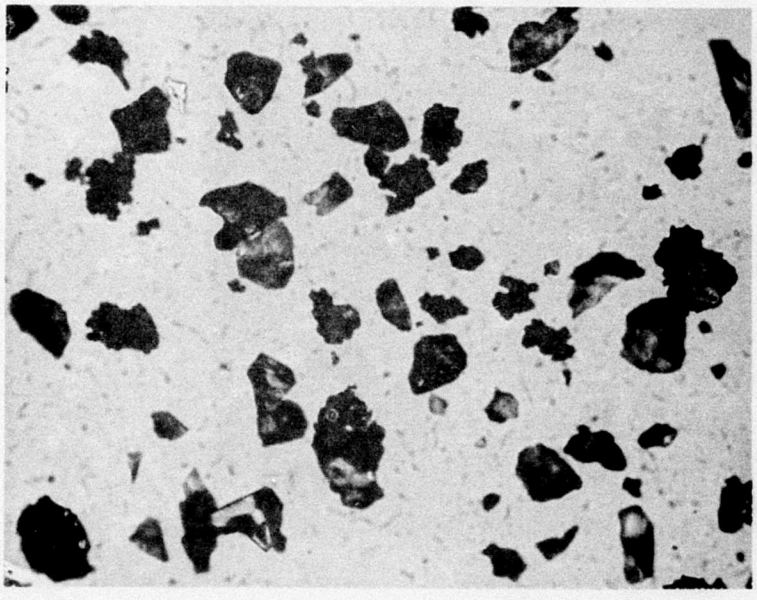

795μ x 620μ
Figure 15. Oversized boron particles removed (138x)

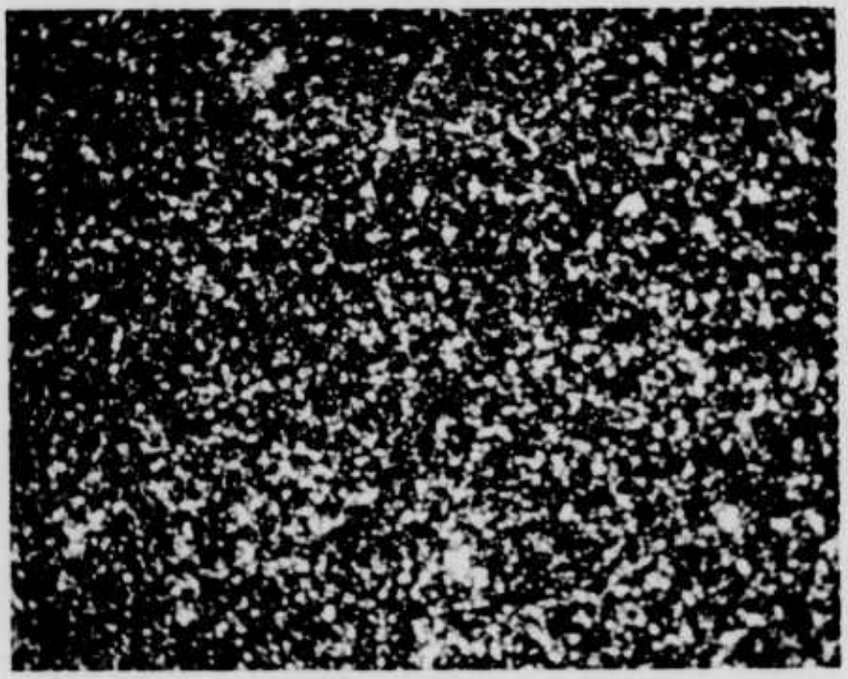

795μ x 620μ

Figure 16. Submicron particles removed (138x)

TABLE XII

BORON AND BORON CARBIDE PARTICLE SIZE DISTRIBUTION

Material	Particle Size Ordered & Labeled	Vendor	Measured Diameter (Microns) WAD	WMD	D (10)	D (90)	Comments
Boron	-325 mesh	AEE	15.57	13.015	5.110	28.423	63% ranges from 7.74 to 24.57μ
Boron	submicron	AEE	3.60	2.774	1.163	6.820	60% ranges from 1.64 to 5.2μ
Boron	-325 mesh	U. S. Borax	17.44	13.836	5.379	29.923	62% ranges from 7.74 to 24.57μ
Boron Carbide	submicron	AEE	12.06	11.204	3.101	22.136	61% ranges from 7.74 to 24.57μ
Boron Carbide	1-5μ	AEE	15.62	13.276	4.662	26.245	62% ranges from 7.74 to 24.57μ

WAD = weighted average diameter
WMD = weighted mean diameter
D (10) = diameter below which 10% of the weight occurs
D (90) = diameter below which 90% of the weight occurs

Boron corresponding to Figure 14 was used in the final combustion tests.

b. Combustion Specimens

Combustion specimens were pressed in the form of discs, each 0.500 in. diameter by about 0.18 in. high, and weighing about 1.2 gm. The ingredients were blended and pressed in a dry nitrogen atmosphere glove box. The die set was a Beckman No. 5020, modified externally to allow remote disassembly. The hydraulic press was an "Enerpac" Model RC104, with a capacity of 10 tons. For safety, the conventional hydraulic oil was replaced with a halogenated oil, Halocarbon Products Corp, type 18-CS-100.

The three combustion specimens of Table XII were pressed at a calculated die pressure of 6840 psi to an average density of 2.50 gm/cc. The specimens of Table XIII were pressed at a calculated die pressure of 17,000 psi for 15 minutes. All pressing was at room temperature.

c. Combustion Tests

Combustion samples were tested in a small window bomb. The hot gases reacted with the acrylic windows, which had to be replaced after each test. Later, gas windows were used with which no reaction was observed. The bomb was pressurized with nitrogen to the nominal test pressure, typically 500 or 1000 psig. The thin disc, mounted vertically, was ignited at the top edge by means of a nichrome wire. The specimen burned along the moving upper edge only; the flame never spread over the flat surface of the disc. When the binder was submicron FEP, the burning edge regressed at a rate uniform enough to be measured. Color motion pictures were taken at film speeds of 1000 or 2000 frames per sec; timing marks were superimposed by a neon bulb at 120 cycles/sec.

The samples of Table XIV, containing -325 mesh boron, burned at a rate of 0.27 in./sec at 1000 psig and 0.19 in./sec at 500 psig. Comparison suggests that the rate was proportional to the square root of pressure. In both cases, ignition was relatively smokeless. Combustion resembled that of a good CMDB propellant. Incandescent particles were brilliant blue-white, small, and distributed uniformly within the flame. This was in contrast to previous combustion with 250 boron in which particles were dull orange, large, and ejected erratically.[11] When the third sample was combusted at 500 psi, occasional agglomerates of Teflon binder burned slowly and loitered on the surface.

TABLE XIII

DENSITY OF SOLID FUEL SPECIMENS

Formulation (wt %)	Weight (gm)	Volume (cc)	Density (g/cc)	Die Pressure (psi)
85% $N_2F_4 \cdot AsF_5$/11% Teflon FEP/4% Boron[a]	1.2664	0.5038	2.514	6,840
85% $N_2F_4 \cdot AsF_5$/11% Teflon FEP/4% Boron[a]	1.1818	0.4757	2.486	6,840
85% $N_2F_4 \cdot AsF_5$/11% Teflon FEP/4% Boron[a]	1.2001	0.4801	2.500	6,840
90% NaCl/10% Teflon FEP	1.0738	0.5467	1.964	22,800
100% Teflon FEP	0.4582	0.2431	1.885	22,800
100% Teflon TFE	0.9790	0.4799	2.040	22,800

[a]Crystalline boron -325 mesh (<45 microns)

TABLE XIV

BURNING RATE VS BORON FUEL

Fuel				Formulation, wt %			Combustion Pressure	Burn Rate
Boron Type	Original Particle Size	Vendor	Re-Sieved?	Salt $N_2F_4AsF_5$	Binder FEP	Fuel	psig N_2	in./sec
Elemental Crystalline	-325 mesh	U.S. Borax Research	Yes See text.	85	11	4	1000	0.265
							500	0.076
Elemental Crystalline	-325 mesh	U.S. Borax Research	No	85	11	4	1000	0.260
							500	0.132
Carbide	-325 mesh	Atlantic Equipment Engineers	No	86	10	4	1000	0.24
							500	0.078

Combustion testing was conducted on blends of 85 percent $N_2F_4 \cdot AsF_5$, 11 percent Teflon, 4 percent boron. The boron was resized from -325 mesh, U. S. Borax crystalline boron. Combustion of this formulation proved quite satisfactory. The boron particles appeared to be consumed nearer the burning surface than in tests that had used -325 mesh boron, as received. The lowering of burn rate at 500 psi is believed due to removing submicron boron particles. Rate data at intermediate pressures are needed to establish the rate versus pressure slope.

Boron carbide (B_4C) was evaluated as a fuel by direct comparison with crystalline boron in blends with $N_2F_4 \cdot AsF_5$ and Teflon FEP. The formulations being compared were adjusted to equal theoretical exhaust properties.(3) The fuel particle sizes were nominally equal, -325 mesh, and used as received from the vendor. The size distributions were approximately equal, although the carbide was slightly finer than the elemental boron. (See Table XII.) Qualitatively, the B_4C did not burn as well as the elemental boron blends. As B_4C burned, glowing particles were noted streaming away from the burning surface and out of the field of view, indicating incomplete fuel combustion. Comparative burn rates indicate that the carbide burns more slowly than the element, especially at the lower pressure. (See Table XIV.)

The carbide might be a useful modifier of burning rate in the future, if the particle size were reduced.

Combustion tests were made on mixtures of energetic salts with the experimental binder polyperfluorobutadiene (PPFB). The form was a coarse powder. Used as received, without further size reduction, it was blended with energetic salts and pressed without curing.

Samples comprised of 80 percent NF_4AsF_6 and 20 percent PPFB burned very quickly along an irregular front, appearing to burn or melt in depth. Combustion was very smoky and left a heavy carbon residue. Thermochemical calculations had indicated that a flame temperature of 2600° K should be attained. In a fluorine-rich environment, carbon should not remain unreacted at this temperature. This formulation apparently did not yield the calculated temperature.

The binder, PPFB, was tested further in a blend of 87 percent $N_2F_4 \cdot AsF_5$, 10 percent PPFB, and 3 percent boron. This formulation burned well without any visible smoke or residual carbon. This test indicates that direct substitution of uncured PPFB for Teflon FEP in an energetic grain is feasible. No evaluation of comparative burn rates is possible at this time since the PPFB blend contained large shards of polymer, which caused irregular surface regression.

An attempt was made to measure the temperature of a burning grain comprised of 86 percent NF_4AsF_6/10 percent Teflon FEP/4 percent boron. A chromel-alumel thermocouple, placed near the grain, was used to record the temperature of the burning specimen. A temperature of at least 1370° C (1643° K) was attained before the thermocouple leads were destroyed by the hot corrosive gases. Thermochemical calculations predicted a flame temperature of 3400° K for this formulation.

d. Mechanical Property Tests

Mechanical properties data were needed to evaluate the minimum binder content of 10 weight percent assumed arbitrarily during thermochemical calculations and combustion tests.

The combustion specimens, in the form of thin discs, were brittle during handling. Specimens of powdered FEP or TFE when pressed without filler had the consistency of soap and lacked the cohesion of normal FEP or TFE sheet stock. Inert specimens of Teflon FEP, filled with table salt, resisted penetration but shattered under a hammer blow. After these preliminary observations, conventional tensile testing of dogbone specimens was rejected in favor of compression testing and temperature cycling. Because brittle failure was expected, the properties of most interest were resistance to temperature cycling and strain capability.

One inert specimen 0.5 in. diameter x 0.5 in. thick, was temperature cycled three times between -196° C and +110° C. No damage was visible when cycling was conducted over a 3 hour period.

For testing of mechanical properties, 24 inert specimens were prepared. These specimens were cylinders 0.5 in. diameter x 0.5-0.6 in. long. They contained dry table salt screened through a 60 mesh (-250μ sieve), and Teflon FEP as a submicron powder. They were pressed at a calculated die pressure of 17,000 psi for 15 min at room temperature. The inert salt was justified for reasons of safety, operator acceptance, and expediting the tests. The boron fuel was omitted for greater inertness and to avoid abrasion. Some tests need to be repeated with an energetic salt and boron to represent the full particle wetting and packing problem.

Compression tests were performed on an Instron Model 1115 testing machine in accordance with ASTM D695. The pen of the chart recorder was capable of rising to full scale in 1 second.

The mechanical loading problem to be simulated was the ignition transient of a solid-fueled gas generator in which the pressure might rise to 1000 psi during 1/10 or 1/2 sec. Choosing appropriate speeds of crosshead and chart required a preliminary test to determine the modulus and the strain at failure.

Three specimens of table salt and FEP, 90 percent and 10 percent by weight respectively, were tested at a crosshead speed of 0.01 in./min, and ambient pressure at room temperature. The modulus of 1.75 x 10^{-5} psi was determined from the linear portions of the stress-strain curves. (See Figure 17.) Stress and strain were calculated from the dimensions of the specimen before test. This simplification was justified by the small strain observed at maximum stress which was 3 percent. (See Table XV.)

Calculations indicated that ignition would be simulated by a crosshead speed of 1.0 in./min, and that the specimen containing 10 percent binder should fail in about 1.0 sec. At a time to failure of 1 sec, the lag of the recorder pen would distort the chart record. To expedite the tests, the existing recorder and a crosshead speed of 0.1 in./min were used. Results of tests conducted at 0.1 in./min with varying binder levels are summarized in Table XV. Strain capabilities are somewhat improved at increased binder levels, but do not represent a vast improvement over lower binder level formulations.

The mode of failure at 0.01 in./min (1.7%/min) and 0.1 in./min (17%/min) was spalling. The mode of failure at 1.0 in./min (175%/min) was total shattering of the specimens. The compressive stress at failure was four times the pressure expected at ignition. Therefore, the solid grain is likely to withstand ignition.

Because strain capabilities differ little over the range of binder levels tested, the formulations might be adjusted with lower binder levels (higher F· yields) without significant loss of strain capability. However, the compression tests and temperature cycles should be repeated using the energetic salt and the boron fuel additive at their final particle sizes.

4. Task 4, Sensitivity and Stability of Energetic Formulations

a. Sensitivity to Impact and Friction

Friction and impact sensitivities were measured on a number of energetic salt blends as indicated in Table XVI. These tests indicate the hazards when processing the ingredients in powdered form. The results of these tests were expressed as threshold initiation levels (TIL) representing 10 consecutive no-fires at the level cited, after firing at the previous greater height or greater force. When samples are compared, the sample whose initiation requires the greater impact height, or the greater friction force at the given velocity, is considered to be the less sensitive and, therefore, the safer to process.

The neat energetic salts, $N_2F_4 \cdot AsF_5$ and NF_4AsF_6 were screened through a -60 mesh (250μ) sieve prior to sensitivity testing. Although neither sample was sensitive to friction (> 1000 lbf @ 8 ft/sec), both were impact sensitive.

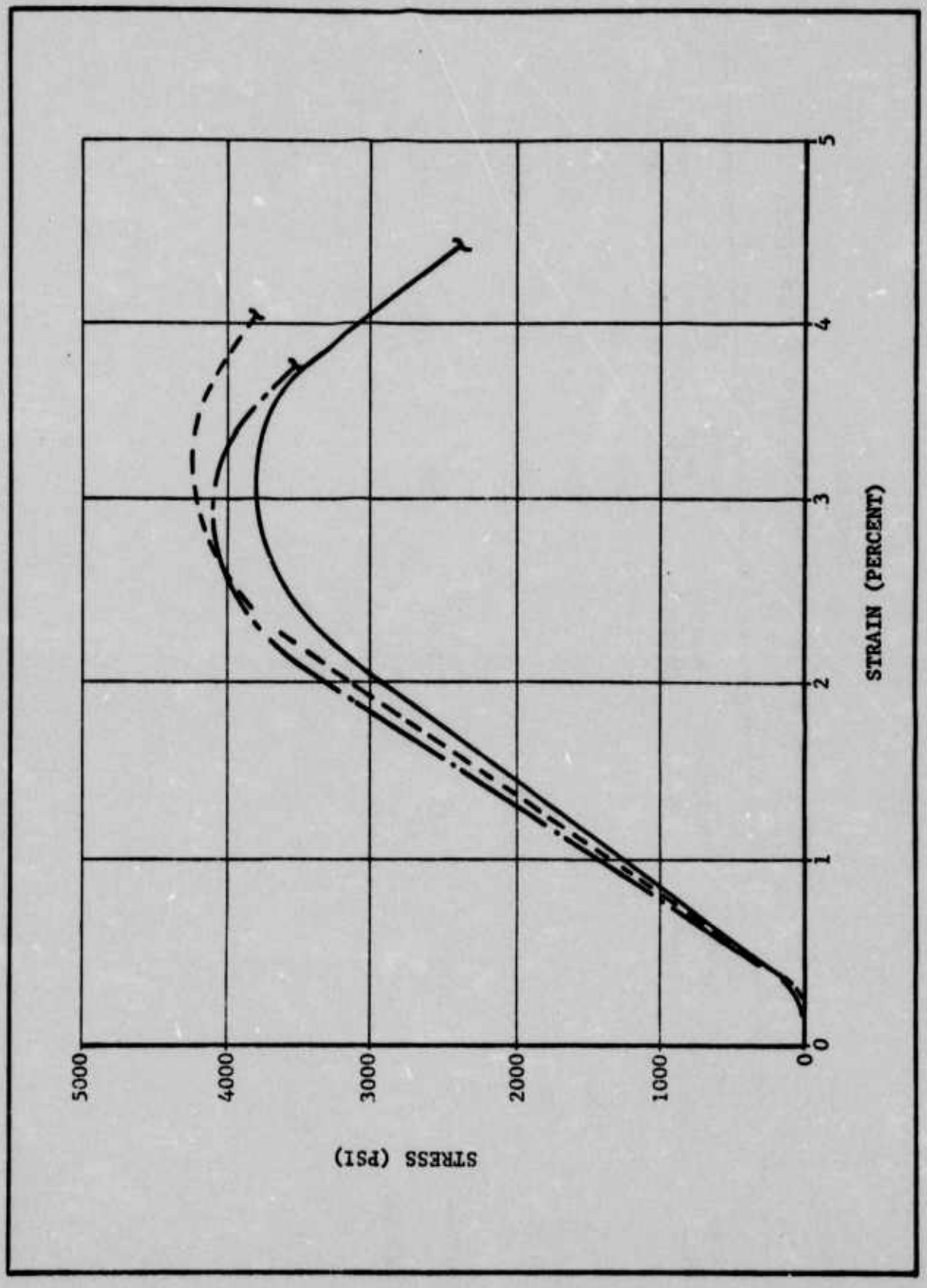

Figure 17. Stress vs strain in compression tests at 0.01 in./min

TABLE XV

COMPRESSION TEST OF INERT SPECIMENS AT 0.01 INCH/MINUTE

Specimen No.	Diameter (inch)	Height (inch)	Weight (gm)	Density (gm/cc)	Maximum Stress (psi)	Strain, % @ Max Stress	Modulus (psi)
1	0.50				3810	3.0	167,500
2	0.50				4230	3.3	165,000
3	0.50				4100	2.8	193,000
Average	--	0.609	4.09	2.09	4050	3.0	175,000
Std. dev.		0.036	0.24	0.013	--	--	--

TABLE XVI

COMPRESSIVE PROPERTIES OF INERT GRAINS

Formulation	Density	Crosshead Speed (inch/min)	Maximum Stress (psi)	Strain, (%) @ max stress	Modulus (psi) X 10^5
90% NaCl/10% Teflon	2.09	0.01	4000 ± 200	3.0 ± 0.3	1.75 (+0.18, -0.10)
90% NaCl/10% Teflon	2.09	1.0	4609 ± 100	1.9 ± 0.15	3.6 (+0.05, -0.05)
95% NaCl/5% Teflon	2.04	0.1	6278 ± 1000	2.2 ± 0.15	3.6 (+0.20, -0.50)
85% NaCl/15% Teflon	2.08	0.1	3867 ± 1000	2.7 ± 0.2	2.0 (+0.6, -0.60)
80% NaCl/20% Teflon	2.12	0.1	2903 ± 50	2.93 ± 0.25	1.38 (+0.10, -0.05)

The accumulated sensitivity data indicate that elemental boron makes formulations containing energetic salts more sensitive to friction. The presence of submicron boron, whether amorphous or crystalline, appears to render such mixtures extremely sensitive. In the case of crystalline boron , the friction sensitivity is apparently directly related to the size distribution of the boron fuel. Submicron particles were eliminated from commercially received -325 mesh boron along with oversized particles, as described in Task 3. Tests showed that substituting this resized material, for the -325 mesh boron used as received, made otherwise equal formulations much less sensitive to friction. For instance, the blend with the resized boron was initiated only by friction forces exceeding 750 lbf at 8 ft/sec (Table XVII) which is much more force than was required to initiate blends using as-received -325 mesh boron.

Direct comparison of formulations with boron and boron carbide in approximately the same particle sizes showed the carbide to be less sensitive. Prior to resizing of the commercially received boron, the use of the carbide appeared promising on the basis of sensitivity.

b. Hydrolytic Stability of Energetic Grains

1) Objective and Scope

The hydrolytic stability of the gas generator formulation is important for two reasons:

(a) Storability

(b) Potential hazards

Storability implies maintaining chemical reactivity and mechanical properties after storage and handling operations. Potential hazards include explosion, fire, and evolution of toxic gases (especially arsenic compounds).

The following specific information is needed:

(a) The minimum level of humidity at which decomposition is detectable.

(b) The effect of humidity level on the rate of decomposition.

(c) Methods of preventing decomposition.

(d) Conditions that represent a fire or explosion hazard.

(e) The amount of arsenic evolved in gaseous form, perhaps as AsF_5, and whether the amount is sufficient to constitute a toxicity hazard.

TABLE XVII

SENSITIVITY DATA

Formulation	Impact (cm)	Friction (lbf @ 8 ft/sec)	Comments
100% $N_2F_4 \cdot AsF_5$	21	> 1000	< 60 mesh
100% NF_4AsF_6	33	> 1000	< 60 mesh
86.5% $N_2F_4 \cdot AsF_5$/8.5% Teflon FEP/5.0% Boron	21	178	< 60 mesh boron (Alfa-Ventron)
85% $N_2F_4 \cdot AsF_5$/11% Teflon FEP/4% Boron	13	> 75	< 325 mesh dry sieved boron (Alfa-Ventron)
85% $N_2F_4 \cdot AsF_5$/11% Teflon FEP/4% Boron	> 17	56	-325 mesh boron, WAD 17.44 micron, US Borax
85% $N_2F_4 \cdot AsF_5$/11% Teflon FEP/4% Boron	6.9	< 10*	WAD 3.60 microns boron (Atlantic Equipment Engineers)
85% $N_2F_4 \cdot AsF_5$/11% Teflon FEP/4% Boron	--	< 10*	-325 mesh boron, US Borax, dry sieved < 400 mesh
87% $N_2F_4 \cdot AsF_5$/10% PPFB[a]/3% Boron	< 11	237	-325 mesh US Borax boron
86% $N_2F_4 \cdot AsF_5$/10% Teflon FEP/4% Boron Carbide	26	237	B_4C -325 mesh, WAD 12.06 microns
80% NF_4AsF_6/20% PPFB[a]	26	> 1000	< 60 mesh NF_4AsF_6
87% $N_2F_4 \cdot AsF_5$/8.5% Teflon FEP/4.5% Boron	< 3.5	< 10*	Submicron amorphous boron
85% $N_2F_4 \cdot AsF_5$/11% Teflon/4% Boron	21	750	-325 mesh boron, wet-sieved and settled. Intermediate sized boron[b]
86% NF_4AsF_6/10% Teflon/4% Boron	26	133	-325 mesh boron (US Borax)

[a] Polyperfluorobutadiene, coarse powder, uncured

[b] 325 mesh US Borax boron treated to remove oversize and submicron particles

* < 10 lb @ 6 ft/sec

Constraints of time and cost allowed only preliminary tests with the objective of broadly defining the problem and indicating areas for further work.

Preliminary tests evaluated the effects of humidity on pressed specimens of the following composition:

N_2F_4 AsF_5	85%
FEP binder	11%
Boron	4%

In view of the difficulty in obtaining quantitative analytical data, the immediate goal was to establish an approximate upper limit of acceptable humidity exposure by qualitative observations.

2) Experimental

Pressed pellets (1/2 in. diameter by 1/10 in. thick, weight 0.8 gm) were exposed to constant relative humidities (RH) of <1 percent, 6 percent, 12 percent, 33 percent, and 53 percent at room temperature for periods up to 20 days. Humidity was maintained by aqueous salt or sulfuric acid solutions in glass containers. The dry extreme of <1 percent RH was maintained by "Drierite" (anhydrous calcium sulfate). Pellets coated with FEP Teflon (total weight of FEP was about 0.4 gm) on two sides in a sandwich configuration were also tested at the lower humidities of <1 percent, 6 percent, and 12 percent. The exposed pellets were evaluated by weight changes, physical and microscopic examinations, and infrared examination of the vapor phase. Infrared spectra of the vapor phase were obtained with a Perkin-Elmer Model 237 Infrared Spectrophotometer using a Teflon sample cell (9.5 cm path length) equipped with BaF_2 windows.

The three components of the present fuel formulation were readily distinguishable under microscope examination in a Halocarbon immersion oil using a combination of transmitted and reflected polarized light.* The boron was easily distinguished from the FEP binder and the $N_2F_4 \cdot AsF_5$ adduct by its relatively small particle size and high reflectivity. The arsenic salt was identified by larger particle size and by its polarization colors. When examined separately, the $N_2F_4 \cdot AsF_5$ adduct was observed to react with the Halocarbon immersion oil, as evidenced by gas bubble formation. This reactivity was also observed with samples from unexposed fuel formulation pellets.

3) Results

The preliminary and qualitative results of the present work are summarized in Table XVIII. Direct chemical evidence concerning the products of hydrolysis of the $N_2F_4 \cdot AsF_5$ adduct was not obtained in this

*The microscopic examinations were carried out by J. A. Kohlbeck.

TABLE XVIII

SUMMARY OF HUMIDITY TEST RESULTS

Designation	Relative Humidity % at 25°C	Infrared Examination of Vapor Phase					Physical Examination		Microscopic Examination		Weight Changes					
		Time (days)	IR Absorption	Pellet Integrity	Time (days)	IR Absorption	Time (days)	Pellet Integrity	Amount As Compound	Reactivity	Time (days)	(gm)	(%)	Time (days)	(gm)	(%)
5210-1-1	<1	1	1030 cm^{-1} (SiF_4) 910 cm^{-1} (NF_3)[8] Both medium	Hard	5	910 cm^{-1} (NF_3)[8]	6	Slightly soft	Small	High	7	-0.101	-13	20	-0.147	-19
5210-1-2	12	1	--	Slightly soft	5	1790/1810 cm^{-1} Doublet Very Weak	6	Pellet dis-integrated	Moderate	Moderate	7	-0.080	-11	20	-0.039	-5
5210-1-3	33	1	--	Soft	5	None	6	Pellet dis-integrated	Large different appearance	Low	7	+0.036	+5	20	+0.056	+8
5210-1-4	33	1	1030 cm^{-1} (SiF_4) 910 cm^{-1} (NF_3)[8] Both medium	Very soft	5	None	6	Pellet dis-integrated	Large different appearance	Low	7	+0.089	+13	20	+0.114	+16
5210-6-1	1				13	None	14	Hard	Large[3]	High	13	-0.091	-12			
5210-6-2	6				13	1030 cm^{-1} (SiF_4) Weak	14	Soft	Large[3]	High	13	-0.001	-12			
5210-6-3	12[1]				13	1030 cm^{-1} (SiF_4) Weak 1610/1640 cm^{-1} Doublet Very weak	14	Very soft	Large[3]	High	13	-0.062	-7			
5210-6-4	12[2]				13	1790/1810 cm^{-1} Doublet Medium 1610/1640 cm^{-1} Doublet Very weak	14	Very soft	Large[3]	High	13	-0.044	-6			
5210-9-I	<1						12	Hard	Small[6]	Low	12	-0.091	-12			
5210-9-II*	<1						12	Hard[4]	Large[7]	High	12	-0.079	--			
5210-9-III	6						12	Soft	Small[6]	Low	12	-0.088	-12			
5210-9-IV*	6						12	Soft[5]	Large[7]	High	12	-0.097	--			
5210-9-V	12						12	Soft	Small[6]	Low	12	-0.076	-10			
5210-9-VI*	12						12	Soft[6]	Large[7]	High	12	-0.065	--			

*Teflon coated on two surfaces; pellet edges remained uncoated.

1. Humidity maintained with 63.1 percent H_2SO_4.
2. Humidity maintained with a saturated LiCl solution.
3. Samples removed from interior of pellets.
4. Teflon coating difficult to remove.
5. Teflon coating readily removed.
6. Samples removed from pellet surface.
7. Samples removed from pellet surface after removal of Teflon coating (i.e., material adjacent to Teflon removed and examined).
8. All NF_3 observed represents <1 percent of gases sampled.

work. The infrared spectra of the vapor phase provided evidence for only small amounts of NF_3 and HF; as noted, this may be due to absorption in the aqueous solutions required for maintaining known levels of RH. Physical observations, however, did provide clear evidence of changes. Weight changes occurred under all humidity conditions, even under the relatively dry environment of <1 percent RH. At this time, the data are too limited to permit a detailed interpretation in terms of the several processes than can conceivably occur, including absorption, diffusion, and the various hydrolysis reaction steps in the FEP/boron matrix. Physical and microscopic examinations proved useful in indicating changes in pellet integrity and in the crystalline form and reactivity of the arsenic salt component of the formulation. These examinations clearly indicated that the changes were greatest at the higher humidities. At the lowest humidity of <1 percent RH, the changes were the least and appeared largely confined to the pellet surface. Also, the observed changes were gradual and did not result in a fire or explosion with the small (0.8 gm) scale pellets used in the present work; ultimately, the effect of charge size must be considered. The observations are discussed in detail below.

The spectra of the vapor phase showed, in general, only small amounts of SiF_4 (indicative of HF formation in the presence of glass) and very weak unidentified absorption doublets at 1610/1640 cm^{-1} and 1790/1810 cm^{-1} (Table XVIII). Very small amounts of NF_3 (910 cm^{-1}) were observed at both high and low humidities after periods of exposure of 5 days or less (Table XVIII). Absorption of gases into the aqueous solutions used to maintain constant humidity level might account for the relatively small amount of gaseous products observed by infrared spectrosopy and, in particular, for the absence of N_2O or NO_2.

Small but significant changes in pellet weights were observed. Small weight increases of 5 to 16 percent after 7 to 20 days were observed at the higher RH of 33 percent and 53 percent, while weight decreases of 5 to 19 percent were observed at the low RH of $\leq$ 12 percent. These weight differences suggest not only that changes had occurred, but also that the kinds of changes varied with the level of RH.

Physical examination of the pellets showed softening of the surfaces after only 1 day at RH of 12 percent or greater, with the softening more pronounced at the higher RH. Further, losses of pellet integrity occurred after 1 to 2 weeks, even at the relatively low RH of 6 percent. These observations indicate that hydrolysis occurs at an appreciable rate even at low ambient humidity conditions. It is encouraging to note, however, that in a dry environment (i.e., <1 percent RH), pellets remained hard and completely intact for up to 2 weeks; only slight surface softening was observed.

Small samples were removed from exposed pellets, immediately immersed in Halocarbon oil, and examined under the microscope. Changes were visible in the crystalline arsenic salt component of those pellets exposed to the higher RH (i.e., 33 percent and 53 percent RH).

These changes were evidenced by changes in the interference colors from a high order white to a low order white. The material after exposure was also less reactive with the immersion oil, as indicated by reduced bubble formation. At the lower RH (i.e., <12 percent), the arsenic salt component of samples removed from interior portions of the pellets remained reactive even after 2 weeks of exposure.

Pellets were pressed with a Teflon FEP coating on the two faces in a sandwich configuration; the edges remained uncoated. The Teflon coatings adhered well to the fuel formulations, and the composite pellets easily survived handling operations. After 12 days exposure at room temperature to less than 1 percent, 6 percent, and 12 percent RH, an area of Teflon coating was mechanically removed and the surface immediately under the coating sampled. Microscopic examination showed relatively large amounts of crystalline material, reactive with the oil and presumed to be the arsenic salt. The surfaces of uncoated pellets exposed to the identical humid environments had relatively small amounts of an unreactive crystalline material. These preliminary observations clearly indicate that a Teflon FEP coating provides protection to the fuel formulation. However, even the sandwich coated pellets underwent a general softening when exposed to RH of 6 percent and 12 percent, presumably via moisture diffusion from the uncoated edges. In the dry environment (i.e., <1 percent RH), the pellets remained hard and the Teflon coating remained strongly adhered to the formulation substrate.

4) Discussion

Previous studies of the hydrolysis of the $N_2F_4 \cdot AsF_5$ adduct have shown that N_2, NO, NF_3, and N_2F_2 are evolved as gaseous products while the arsenic moiety was retained in aqueous solution as the nonvolatile hexafluoroarsenic acid ($HAsF_6$) and its hydrates.[18] These products seem consistent with the ionic structure of $N_2F_3^+$ AsF_6^- assigned by Young and Moy to the adduct.[3] The hexafluoroarsenate ion AsF_6^- is known to be stable to hydrolysis.[19] Consequently, the $N_2F_3^+$ ion is the active species responsible for the observed vigorous reaction with water. Possible products resulting from the hydrolysis of this ion, other than the observed N_2, NO, NF_3, and N_2F_2 cited above, include other nitrogen oxides (i.e., N_2O or NO_2) and hydrogen fluoride (HF). Thus, the hydrolysis of the difluorodiazine-arsenic pentafluoride ($N_2F_2 \cdot AsF_5$) adduct with the suggested ionic constitution ($N_2F^+AsF_6^-$) has been reported to form nitrous oxide (N_2O) and hydrogen fluoride (HF).[20]

The infrared evidence obtained in the present work showed the formation of only small amounts of NF_3 and HF (HF indirectly by the presence of SiF_4). However, the possible formation of other gaseous products must still be considered. Such gases may have been absorbed in the aqueous solutions used to maintain the constant humidity levels. Also, the infrared evidence did not indicate any detectable volatilization of AsF_5 (B.P. = 63° C). Again, absorption by the humidifier solution is an alternative explanation. The correct interpretation needs to be clarified to determine the vapor toxicity. This is particularly important because

recommended upper limit for exposure to arsenic (0.05 mg/m^3 of air for 10 hours/day and 40 hours/week)[21] is undoubtedly below the limit of detection by infrared.

The probable fate of the AsF_6^- ion appears to be formation of hexafluoroarsenic acid ($HAsF_6$), as previously reported for the solution hydrolysis of the $N_2F_4 \cdot AsF_5$ adduct[18] and also postulated for the hydrolysis of the $N_2F_2 \cdot AsF_5$ adduct.[20] This acid has also been identified in aqueous solution as a product of the hydrolysis of dioxygenyl hexafluoroarsenate ($O_2^+AsF_6^-$).[22] A possible product of the present humidity experiments is the hexahydrate of the acid ($HAsF_6 \cdot 6\ H_2O$), which is a known stable, crystalline compound.[19] Both the acid and its hydrate would be expected to remain in the partially decomposed pellets. This interpretation would explain the absence of gaseous AsF_5 evolution and the changes in crystalline structure and reactivity of the arsenic salt observed during microscopic examination.

5) Conclusions

The following conclusions may be drawn from the present preliminary work:

(a) Decomposition at room temperature is gradual and noncatastrophic with small specimens having a relatively large surface area.

(b) The rate of decomposition increases with humidity.

(c) The decomposition threshold appears to be at <1 percent RH at room temperature.

(d) Pressed fuel formulations containing $N_2F_4 \cdot AsF_5$ cannot be exposed to any normally encountered ambient humidity environment for appreciable periods of time without decomposition.

(e) Decomposition in a readily attainable dry atmosphere (< 1 percent RH) appears sufficiently slow at room temperature to offer the possibility of a storable formulation with suitable protection.

(f) The ready adherence under compression of powdered Teflon FEP to the fuel formulation offers a promising lead for encapsulation as a potential protective system. Other potential protective systems should also be considered.

5. Task 5, Chemical Process Data

The objective of this task was to obtain process data in the laboratory for scaling up the synthesis of energetic salts, $N_2F_4 \cdot AsF_5$ or $KClF_4$. This task was predicted on the use of either salt in demonstrating a solid-fueled chemical laser. However, interest in both of these salts for laser testing has subsided. Study showed that decontamination and waste treatment of a laser vacuum system using an arsenic salt, with helium diluent, would be difficult and expensive. $KClF_4$ was not prepared since thermochemical calculations (Task 1) predicted that this salt would not be suitable in a smoke-free laser system. Prior to eventual laser testing, these energetic salts would be replaced with an arsenic-free and smoke-free advanced energetic salt. The existing laboratory synthesis of $N_2F_4 \cdot AsF_5$[3] is sufficient to support the early solid fuel development effort and may be scaled to meet immediate future demands for energetic salt.

Since neither of these energetic salt candidates will be used in a laser demonstration, major efforts were applied to other tasks in this program.

6. Task 6, Delivery of samples

Samples were supplied to the Army Propulsion Directorate according to Table XIX. The selection of samples was agreed to by Dr. O. E. Ayers, of MICOM, and Mr. G. M. Daurelle, of Hercules Incorporated, at Huntsville on 22 and 23 May 1974.[16] The samples were shipped from Hercules Incorporated, Bacchus Works, on 5 July 1974.

Each sample was packaged individually in a Teflon FEP bottle with screw top and placed in a steel pipe nipple (2-in. schedule 40 by 6 in. long) with pipe caps threaded at both ends. The bottle and the pipe were filled with a dry nitrogen atmosphere.[17] The pipe also contained a desiccant, anhydrous calcium sulfate ("Indicator Drierite"). The pipe had been degreased with the solvent 1,1,2-dichlorotrifluoroethane ("Freon TF"). The pipe threads were sealed with Teflon TFE tape. The capped pipes were labeled toxic and were placed in bags filled with lime and overpacked in wooden boxes. The purpose of the packaging precautions was to minimize the risk of moisture enetering the sample or of toxic gases escaping.

C. CONCLUSIONS

1. Task 1, Thermochemical Calculations

Thermochemical calculations predict that a solid formulation consisting of an energetic fluorine salt, a fluorocarbon binder, and the fuel additive, boron (or boron carbide), can supply free fluorine with sufficient energy to keep the net fluorine atomic after the heat loss and dilution of a state-of-the-art laser apparatus. The net fluorine is 6 gm per 100 gm solid if the salt if $N_2F_4 \cdot AsF_5$, or 12 gm per 100 gm solid if an advanced NF_4 salt is used. Further optimization depends on the heat loss and nozzle dimensions of a specific laser apparatus.

TABLE XIX

SOLID FUEL SAMPLES SUPPLIED

Item No.	Quantity (gm)	Description	gm/100 gm		
			Salt	Binder	Fuel Additive
1	2.9516	Teflon FEP (powder)	--	100	--
2	4.0170	Teflon TFE (powder)	--	100	--
3	2.1051	PPFB	--	100	--
4	5.9810	Powdered $N_2F_4 \cdot AsF_5$ < 60 mesh	100	--	--
5	1.7340	Powdered NF_4AsF_6 < 60 mesh	100	--	--
6	2.6601	$N_2F_4 \cdot AsF_5$/Teflon FEP/B	85	11	4
7	2.8217	NF_4AsF_6/PPFB/B	83	15	2
8	3.1140	NF_4AsF_6/Teflon FEP/B	86	10	4

When arsenic is present, cooling causes arsenic trifluoride (AsF_3) to shift to the pentafluoride. Elimination of arsenic will make a solid fuel more tolerant of heat loss.

The combustion product, arsenic trifluoride, is predicted to remain a vapor.

The combustion product, potassium fluoride (KF), is predicted to condense in bulk. Therefore, an energetic potassium salt such as $KClF_4$ is not recommended.

Solid fluorine sources can be screened manually on the basis of the elemental composition and the major products of combustion.

Thermochemically, boron carbide can be substituted for elemental boron almost on a gram-for-gram basis.

2. Task 2, Preparation and Compatibility Studies of Fluorine Compounds

a. $N_2F_4 \cdot AsF_5$

The energetic salt, $N_2F_4 \cdot AsF_5$, was synthesized from N_2F_4 and AsF_5 in batches of 10 gm each. Present methods may be scaled to provide sufficient $N_2F_4 \cdot AsF_5$ for future needs.

b. Subtask 2.1, Insulation Material

A polymer has been developed which may provide a high char yielding insulation for DF laser systems. Initial testing indicates that the polymer is compatible with NF_4AsF_6.

3. Task 3, Combustion and Mechanical Properties

a. General Testing

Combustion specimens were pressed at 7000 to 17,000 psi at room temperature in stainless steel dies without incident. Density was 2.5 gm/cc.

Good combustion required a boron fuel additive. The boron additive should be high-purity elemental crystalline boron, nominally -325 mesh. The oversize particles should be removed by wet wieving and settling.

A pressed solid formulation burns from a regressing surface like a solid propellant. Combustion in a cold nitrogen atmosphere was more efficient at 1000 psi than at 500 or 300 psi. At 1000 psi a burning rate of 1/4 in./sec was typical of different formulations. At 500 psi the burning rate was extremely dependent on the type of boron additive, its particle size, and the gas pressure. The solid-fueled gas generator should be designed to operate at 1000 psi.

Pressed specimens were brittle. Compressive properties of inert specimens were as follows:

Maximum stress, psi	= 3000 - 6300
Modulus, psi	= $1.4 - 3.6 \times 10^5$
Strain at max stress, %	= 1.9 - 3.0

The properties were insensitive to strain rate, suggesting an elastic material. A cartridge-loaded solid grain should be able to withstand ignition pressurization. Binder levels varied from 5 - 20 weight percent.

Three temperature cycles between -196° C and $+110^\circ$ C caused no superficially visible damage. Future specimens should be tested in compression both before and after temperature cycling. As may be expected, the trend appears to be toward improved mechanical properties as increased binder levels.

b. Task 3.1, Precombustor Nozzle Designs

Initial concepts of precombustor nozzle designs were completed by Allegany Ballistics Laboratory (ABL). Cooling the nozzle is necessary and appears feasible with pressurized water. Achievement of nucleate boiling will require development effort.

4. Task 4, Stability and Sensitivity Tests

Specimens were thermally stable to at least the following approximate temperatures:

Salts, $+150^\circ$ C

Powdered formulations, $+100^\circ$ C

The energetic salts and their formulations were considered explosive on the basis of their sensitivity to impact.

Sensitivity to friction depends on concentration of submicron particles of boron, which can be removed from the crystalline boron by wet sieving and settling. Formulations with boron carbide are less sensitive than those with elemental boron of nominally equal particle size. Amorphous boron, which is rich in submicron particles, is extremely sensitive to friction and should be avoided.

Solid formulations with 11 weight percent FEP binder are degraded by humidity. The degradation is nonviolent, and the arsenic is retained. Total encapsulation of the solid grain will apparently be required. Initial data indicates that Teflon FEP is a good encapsulant. Further studies are needed to fully evaluate this task.

5. Task 5, Chemical Process Data

The existing process for making the salt, $N_2F_5 \cdot AsF_5$, appears adequately scalable for preparation of this interim ingredient.

6. Task 6, Delivery of Samples

Samples of energetic salts, fluorocarbon binders in powdered form, and solid formulations were prepared by 30 June 1974 and shipped to MICOM on 5 July 1974. They were enclosed in a dry nitrogen atmosphere.

D. RECOMMENDATIONS

The following future work is recommended:

1. The formulations with the salt NF_4 AsF_6 should be retested with direct substitution of the advanced salt NF_4 BF_4.

2. Mechanical properties should be tested with energetic formulations.

3. Combustion tests should establish the pressure slope of burn rate versus pressure and the particle size distribution of the boron.

4. Combustion tests should be scaled up to 10 gm in the pressurized window bomb and to at least 100 gm in a self-pressurized precombustor.

E. REFERENCES

(1) W. W. Wharton, letter to G. M. Daurelle, 21 March 1974

(2) D. R. Stull and H. Prophet, JANNAF Thermochemical Tables, Second Edition, NSRDS-NBS 37, National Bureau of Standards, Washington D.C., 1971

(3) A. R. Young and D. Moy, "The Reaction of Tetrafluorohydrazine with Arsenic Pentafluoride. Evidence for the Existence of $N_2F_3^+$ Salts, Inorganic Chemistry, Vol. 6, No. 1, pp 178-179 (January 1967)

(4) Quarterly Technical Summary Report No. 3, MRB-2022-93, Contract AF04(611)-8520, Monsanto Research Corp., April 22, 1963

(5) W. E. Tolberg, R. T. Rewick, G. R. Zeilenga, M. P. Dolder, and M. E. Hill, "Synthesis of Energetic Oxidizers (U)", AFRPL-TR-68-47, Contract F04611-67-C-0002, 25 March 1968 (Confidential). Unclassified Excerpt

(6) W. E. Tolberg, R. T. Rewick, R. S. Stringham, and M. E. Hill, "The Synthesis of the Perfluoroammonium Cation, NF_4^+, Inorganic Chemistry, Vol. 6, No. 6, pp 1156-1159 (June 1967)

(7) C. T. Goetschel, U. A. Campanile, R. M. Curtis, K. R. Loos, C. D. Wagner, and J. N. Wilson, Inorganic Chemistry, Vol. 11, p 1696 (1972)

(8) K. O. Christe, R. D. Wilson, and A. E. A. Axworthy, Inorganic Chemistry, Vol. 12, p 2478 (1973)

(9) M. S. Toy, Photochemistry of Macromolecules, edited by R. F. Reinisch, Plenum Publishers, New York, 1970, pp 135-144

(10) J. E. Glanagan, K. O. Christe, D. Pilipovich, "Solid Propellant Laser Fuel Generator", Report AFWL-TR-73-195, Contracts F29601-73-0004, F29601-C-0004, Rocketdyne, Canoga Park, California, November 1973 Confidential, Unclassified excerpt

(11) R. B. Leining and D. T. Sauer, "Energetic Chemicals", Research Progress Report RI-88/5/2-966, work period November 1, 1973 to February 1, 1974, Hercules Incorporated, Magna, Utah, 13 February 1974

(12) Green, G. R., Equilibrium Thermochemistry and Theoretical Specific Impulse Program, Abstract of Program 65005, Bacchus Works, 13 January 1969

(13) Handbook of Chemistry and Physics, 47th Edition, Chemical Rubber Publishing Co., Cleveland, 1966

(14) R. B. Leining and D. T. Sauer, "Energetic Chemicals", Report RI-88/5/2-979, Hercules Incorporated, Magna, Utah, May 2, 1974

(15) J. C. Farber, letter of transmittal to O. E. Ayers (July 3, 1974)

(16) J. C. Farber, "Trip Report MICOM, 22-23 May 1974", memo to D. H. Black, Hercules Incorporated, Magna, Utah, 28 May 1974

(17) J. F. Cross, Hercules Incorporated, letter to R. F. Hardy, Inspector, Bureau of Explosives, June 7, 1974

(18) D. D. Perry, "Advanced Oxidizer Research," Contract NONR-4364(00), Reaction Motors Div., Thiokol Chemical Corp., Denville, New Jersey, December 1965; A. R. Young, S. I. Morrow, and D. Moy, Section II, Task 53, pages 22-24, "Inorganic Oxidizer Synthesis."

(19) H. M. Dess and R. W. Parry, J.Am. Chem. Soc. 79, 1589 (1957), "The Preparation and Properties of Complex Fluoroarsenates."

(20) D. Moy and A. R. Young, J. Am. Chem. Soc. 87, 1889 (1965), "The Preparation of Fluorodiazonium Hexafluoroarsenate (N_2F^+ AsF_6^-) from cis- Difluorodiazine."

(21) "Occupational Exposure to Inorganic Arsenic, Criteria for a Recommended Standard," National Institute for Occupational Safety and Health, U. S. Dept. HEW, 1973 (Bacchus Library BU 74-60253).

(22) A. R. Young, T. Hirata, and S. I. Morrow, J. Am. Chem. Soc. 86, 20 (1964). "The Preparation of Dioxygenyl Salts from Dioxygen Difluoride."

APPENDIX A

STUDY OF COOLED NOZZLE DESIGNS

FOR AN

HF/DF CHEMICAL LASER GAS GENERATOR

SECTION I

SUMMARY AND RECOMMENDATIONS

Three design concepts were developed for the gas generator nozzle and aft chamber closure. Conceptual sketches are provided in the body of the report. One concept, the axial flow-variable velocity configuration, was adopted as a baseline and is recommended for further study. All of these concepts utilize copper as the material of construction, are of simple design, and practical to fabricate. A detailed explanation of the fabrication of the small thin-walled nozzle shell from standard copper tubing is included.

The requirement to provide adequate nozzle cooling at low wall temperatures was found to be the single most critical design parameter. Neither convective nor nucleate boiling heat transfer acting singly was capable of meeting cooling requirements; a combination of the two will most likely be required. A cooling system capable of producing high velocities at low pressures is essential.

Two of the designs were investigated for cooling performance by means of a computerized heat transfer program. Wall temperatures at various locations are presented in Section V of this report. The third design was not analyzed due to the complex flow state present in this concept and time limitations.

A very preliminary structural analysis was carried out to investigate overall design feasibility. The nozzle shell under thermal loading was determined to be the critical area.

The study indicated that a viable design is possible, but that a definitive development effort will be required. Initially, it is recommended that a further analytical study be undertaken which should consider among other things:

(1) Nickel 200 as the basic material of construction. (Some work was done in the current investigation but such areas as availability, formability and structural response need further study.)

(2) Fluids other than water as the coolant. (Low saturation temperature is the most desirable property.)

(3) More in-depth structural analyses.

This effort should be followed by an extensive bench test evaluation of the coolant system. It is emphasized that analytical predictions are subject to a great many assumptions which require verification and that the small size of the nozzle components lend themselves to an inexpensive experimental program. It is suggested that a model be constructed with a solid nozzle shell section to facilitate the measurement of pressures at various locations in the cooling cavity. This is important since the study indicates that cooling is a strong function of pressure and does not necessarily become more efficient as coolant supply pressure is increased.

SECTION II

INTRODUCTION

The work described in this Appendix was performed at Hercules/Allegany Ballistics Laboratory. The objective was to provide a preliminary mechanical design of a gas generator nozzle and chamber featuring concealed water cooling. Conventional ablative materials, graphites, etc. could not be employed for reasons of exhaust gas contamination and corrosion. The scope and some ground rules for the study were described in memo MISC/5/2-987 to E. D. Casseday from J. C. Farber, June 19, 1974. Other ground rules were obtained from References 1 through 5 and are listed in Table I.

The design of the chamber was not considered; all effort was concentrated on the nozzles which is the more difficult design problem. Based on the results of this study, it would appear that standing the chamber in a water pot (assuming a vertical firing attitude is possible) would provide adequate cooling.

The basic challenge is to design a nozzle which can be fabricated to the very small dimensions required and provide sufficient cooling to maintain the throat temperature below the allowable maximum.

TABLE I

GROUND RULES

Chamber Pressure	1000 psia
Mass Flow Rate Discharge Coefficient	10 grams/sec
Calculated Throat Diameter	0.056 in.
Materials Exposed to Gas Stream	Copper or Nickel 200
Maximum Gas Side Material Temperatures	
Copper	440°F
Nickel 200	1340°F
Unit Weight	Unlimited
Water Supply	Unlimited
Water Pressure	Unlimited

SECTION III

COOLANT EFFECTIVENESS

The design of the nozzle is controlled primarily by the requirement to provide effective cooling in the throat region. The maximum allowable temperature, as specified in Table I, is 440°F.

The heat flux which must be absorbed by the coolant was obtained based on the data of Reference 5 and the ratio of throat diameters:

$$h_f = 3000\ (0.15/0.056)^{0.2} = 3651\ \frac{BTU}{hr\text{-}ft^2\text{-}°F}$$

$$q = h\ (T_r - T_w)$$

$$q = 3651\ (5700-440) = 19.18 \times 10^6\ \frac{BTU}{hr\text{-}ft^2}$$

This is an extremely high flux level and cannot be absorbed by conventional cooling alone. It was therefore necessary to consider nucleate boiling. The correlation adopted is due to Rohsenow[6] and is described in Kreith.[7]

$$\frac{C\ \Delta T_x}{H\ P_r^{1.7}} = C_{sf} \left[\frac{q}{\mu\ H} \sqrt{\frac{g_c \sigma}{g\ (\rho_l - \rho_v)}} \right]^{0.33}$$

C = specific heat of liquid, BTU/lb-°F

q = heat flux, BTU/hr-ft^2

H = latent heat of vaporization, BTU/lb

g_c = conversion factor, 4.17×10^8, lb-ft/lb-hr^2

g = gravitational constant, ft/hr^2

ρ_l = density of the saturated liquid, lb/ft^3

ρ_v = density of the saturated vapor, lb/ft^3

σ = surface tension, liquid to vapor interface, lb/ft

P_r = Prandtl number of saturated liquid

μ = viscosity of the liquid, lb/hr-ft

C_{sf} = empirical constant, 0.013^7

ΔT_x = difference in saturated liquid temperature and wall temperature

This equation holds during the nucleate boiling regime in which increasing the temperature differential results in increased heat flux. However, at some point a transition to film boiling occurs which results in a decrease in heat transfer with further increase in temperature differential. This point is commonly referred to as the burnout point for obvious reasons. A correlation(7) for predicting the burnout point is:

$$q_{max} = 14.3\ \rho_v H \left(\frac{\rho_l}{\rho_v} - 1\right)^{0.6}$$

which yields flux values in the range 10^5. Since this value is two orders of magnitude less than the required level, it was concluded that nucleate boiling alone will provide inadequate cooling.

A combination of convective and nucleate boiling will be required. This approach has the additional advantage of making boiling more effective by raising the burnout point. All experimental data indicate that the maximum possible flux level is increased by higher fluid velocities and lower bulk fluid temperatures both of which are associated with convective cooling. Combined heat transfer can be analyzed by simply separating the heat flux into two parts; one a boiling flux and the other a convective flux.

$$q_t = q_b + q_c$$

The convective flux can be evaluated by conventional means such as:

$$\frac{h_c}{C\ G} = 0.023\ R_n^{-0.2}\ P_r^{-0.67}$$

R_n = Reynold's Number

$G = \rho V$, mass velocity, $lb/ft^2\text{-sec}$

where properties are evaluated at the film temperature, the average of the bulk and wall temperature. Several computations indicated that the temperature of the water would not be raised to any extent due to the high flow rate required for effective convection and small area of high heat flux. Therefore, for all subsequent calculations the water bulk temperature was taken as 80°F.

For purposes of computer calculation it was desirable to obtain an overall coefficient which could be input as a function of wall temperature:

$$q_t = q_b + q_c$$

$$h_t\ (T_w - T_b) = K\ \Delta T_x + h_c\ (T_w - T_b)$$

$$h_t = K\ \frac{(T_w - T_s)}{(T_w - T_b)} + h_c$$

Since the liquid bulk temperature was fixed at 80°, the total heat transfer coefficient as a function of wall temperature is known for a given saturation temperature (T_s). Calculations of h_b which is $q_b/(T_w - T_b)$ were made for a variety of saturation temperatures. A useful relation for this work is shown in Figure 1 which relates q_b to T_x as a function of saturation temperature.

Convective heating coefficients are functions of velocity as well as wall temperature; a useful relationship for these calculations is shown in Figure 2.

Three things are necessary to define the heating environment of a given nozzle design, wall temperature, saturation temperature and velocity. The latter quantity is a function of the total initial head and pressure drop through the cooling system. The saturation temperature depends on the local static pressure, increasing as the pressure increases. The two cooling modes require conflicting operating conditions for best performance. Convective cooling is enhanced by higher velocities which require

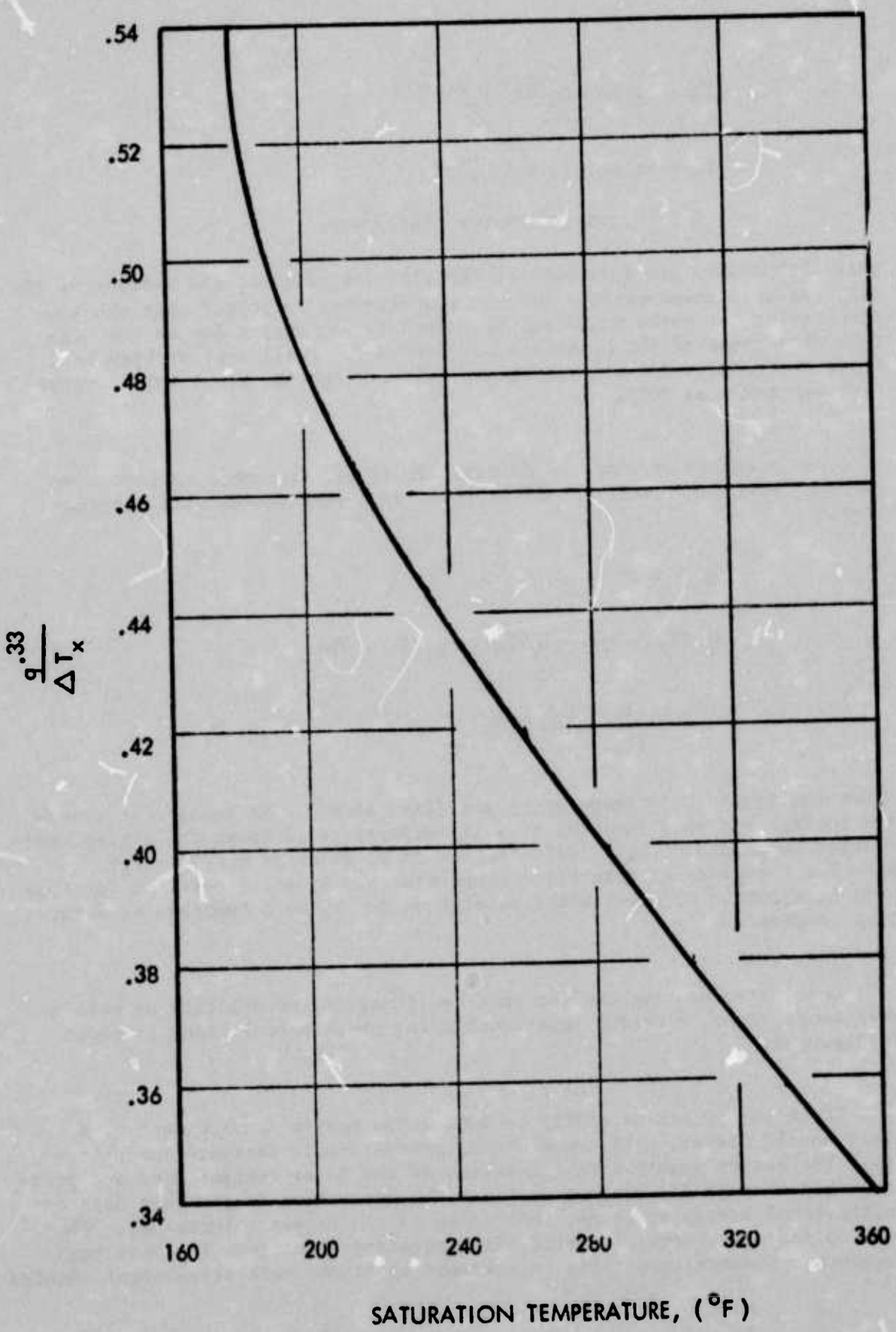

Figure 1. Relationship of Boiling Heat Flux to Temperature Differential as a Function of Liquid Saturation Temperature

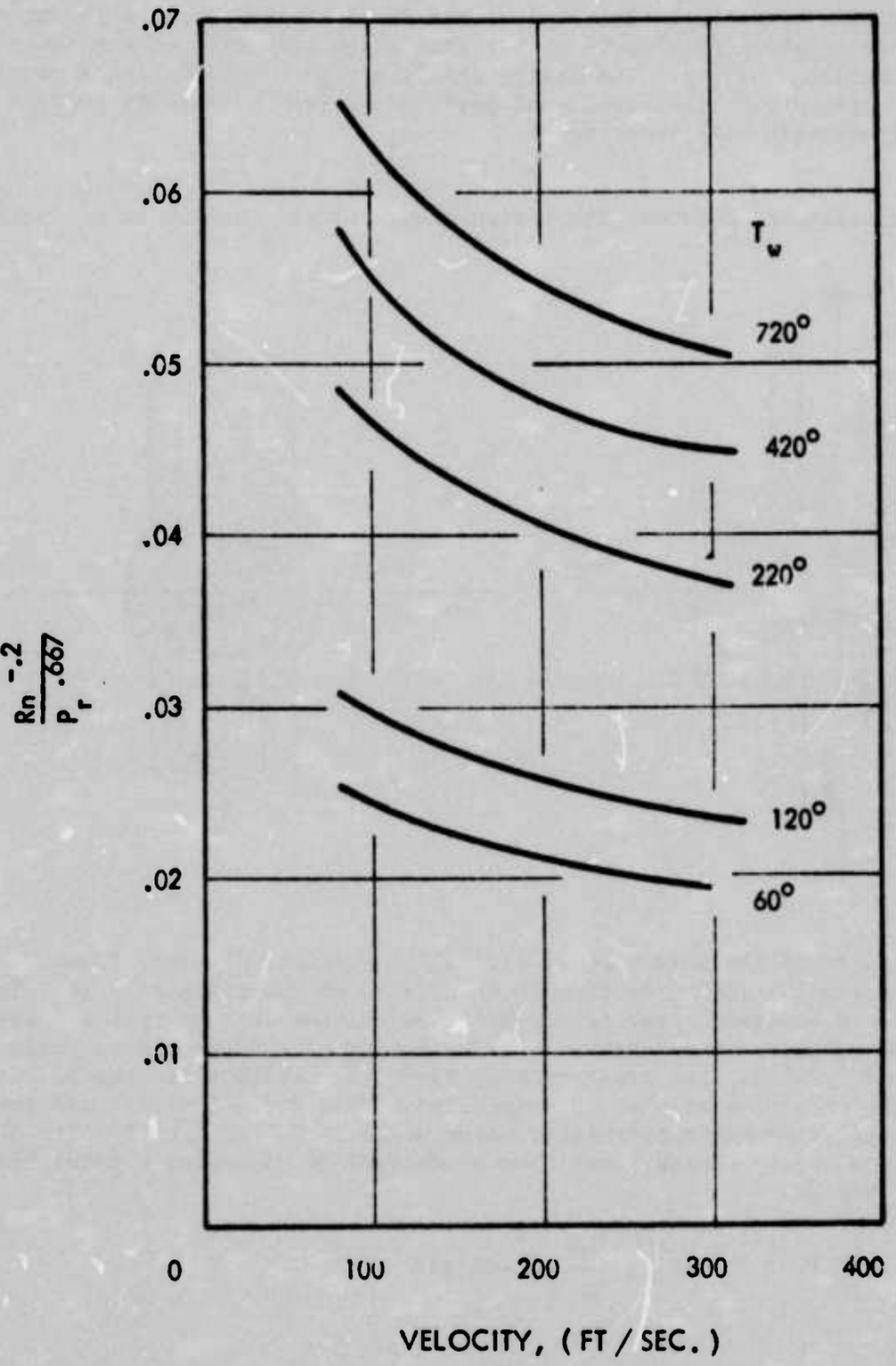

Figure 2. Convective Cooling Parameter as a Function of Coolant Velocity

higher driving pressures. This raises the local static pressure throughout the system which results in higher saturation temperatures and lower nucleate boiling cooling. The design challenge is then to devise a nozzle cooling system which will yield good performance from both modes and produce an acceptable wall temperature.

As an example, consider the design shown below. Cooling water enters

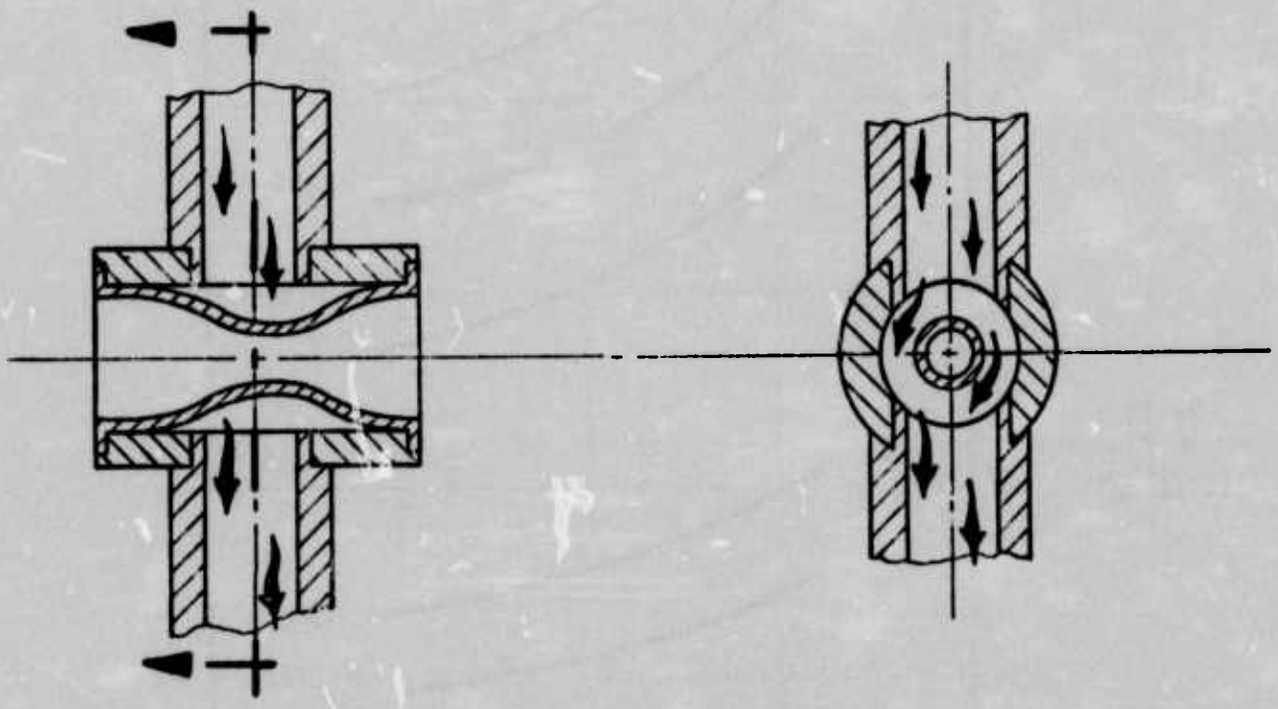

an annulus around the nozzle shell through an orifice, divides, flows around the annulus and exits through an orifice on the opposite side. The annular cross-sectional area is one-half the orifice area so that the average flow velocity is constant. For a velocity of 100 fps and an orifice diameter of 0.25 in., the pressure drop is 60 psi per foot of length. The loss in the annulus must also be considered. Data for 90° elbows and tees[8] indicate that a somewhat optimistic value would be 0.6 of the velocity head. The required supply pressure can then be determined, assuming a total flow length of one foot:

$$P_o = P_L + P_a + \frac{\rho V^2}{2g}(1 + 0.6)$$

$$P_o = 60 + 14.7 + \frac{(62.4)(100)^2(1.6)}{(64.4)(144)}$$

$$P_o = 182.2 \text{ psia}$$

Considering the pressure distribution through the system

Location	P_{total} (psi)	P_s (psi)	V (fps)	T_s (°F)
Tank	182	182	0	
Annulus Entrance	137	70	100	302
Annulus Exit	97	30	100	250
Exhaust	82	14.7	100	

reveals an average saturation temperature in the region to be cooled of 276°F. With this information, the cooling coefficients can be calculated and are shown in Figure 3. To absorb the required heat flux in the throat, a water side wall temperature of 332°F is required:

$q = 3.66 \times 10^4 (332-80)(2.07)$, where 2.07 is an area correction factor

$q = 19.1$ Btu/ft^2-hr

A rough estimate of the gas side wall temperature can be made from:

$$\frac{dT}{dX} = q/K = \frac{14.18 \times 10^6}{2600} = 5450 \frac{°F}{in.}$$

$dT = (5450)\ (0.03) = 163°F$

The gas side wall temperature is therefore expected to be approximately 495°F, which exceeds the allowable of 440°F.

The effect of increasing the flow velocity leads to a similar conclusion. For a source pressure of 1000 psi, a velocity of about 200 fps can be obtained. Considering the pressure distribution

Location	P_o (psi)	P_s (psi)	V (fps)	T_s (°F)
Tank	1000	1000	0	
Annulus Entrance	900	631	200	493
Annulus Exit	318	48	200	278
Exhaust	284	14.7	200	

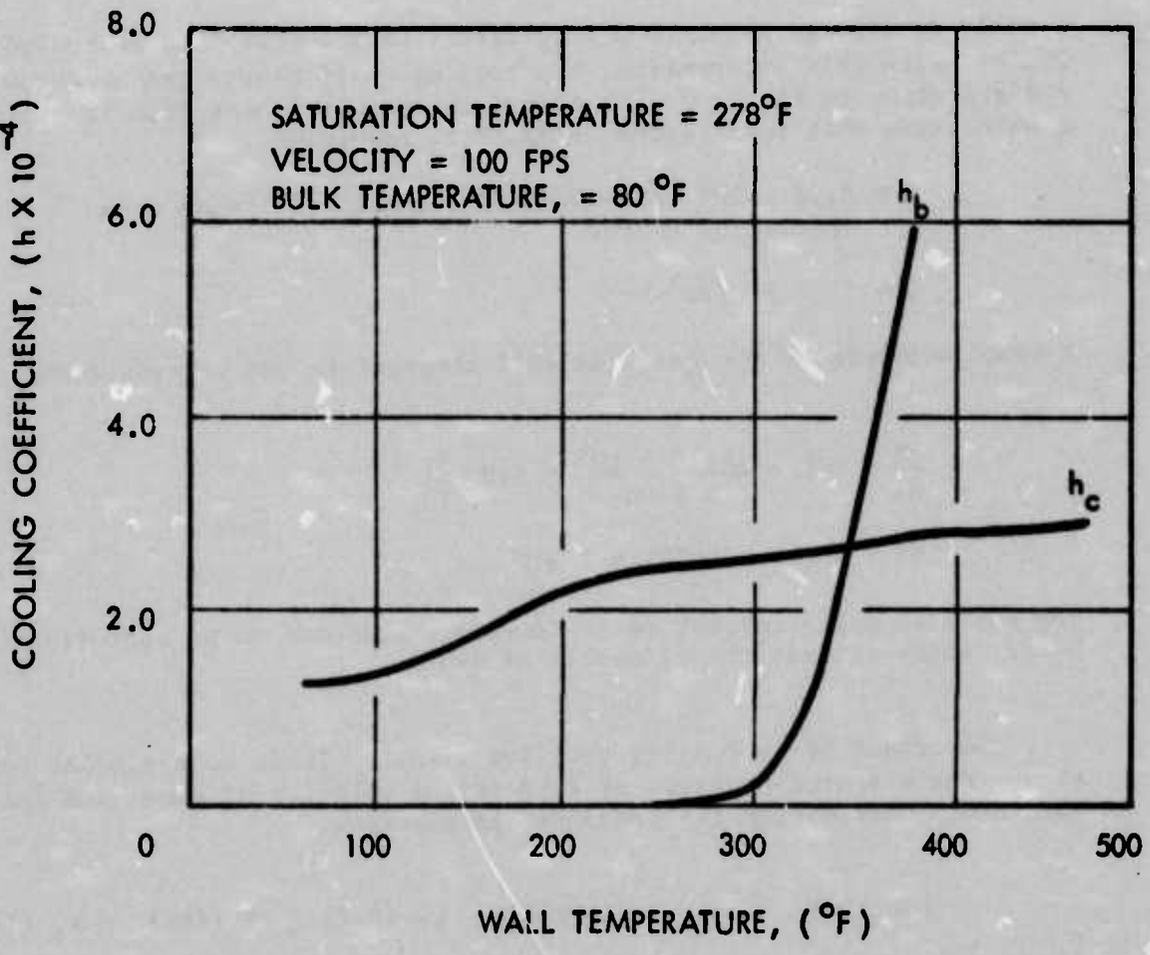

Figure 3. Convective and Nucleate Boiling Cooling Coefficients Versus Wall Temperature

The average saturation temperature is 385°F. In this range the convective coefficient is about 4.4×10^4 which results in water side and gas side wall temperatures of 290° and 453°F, respectively. Since pressure losses vary as the second power of the velocity, to completely convectively cool the nozzle would require a source pressure of approximately 2000 psi which is not practical for a thin wall (0.03 in.) copper nozzle shell.

The solution to the problem lies in obtaining a design which yields high velocities and low static pressures at the critical point. Two designs were developed to meet this criteria; a multi-orifice concept and a variable velocity axial flow configuration. The former produces a complex flow field which could not be analyzed within the study period. From an intuitive standpoint, however, it should produce the desired effect and should be considered for experimental study or more detailed analytical investigation. The axial flow model employs a variable cross-sectional area to increase velocity and reduce pressure in the critical region. The thermal analysis of this concept is similar to that previously discussed and is presented in Section V.

SECTION IV

CONCEPTUAL DESIGNS

Three nozzle design concepts for the HF/DF chemical laser gas generator were evolved. These designs are illustrated in Figures 4 through 6 and are entitled:

A. Variable Velocity Axial Flow Concept

B. Constant Velocity Tangential Flow Concept

C. Multi-Orifice Concept

Each nozzle was designed to the ground rules of Table I. Other design considerations included material corrosivity, simplicity, ease of manufacture, cost, and most important, provision for adequate cooling.

Because of the corrosive environment of the exhaust gas products, namely, atomic fluorine', and the generation of products such as HF, H_2O, etc. which could interfere with proper functioning of the laser, the choice of nozzle materials and their allowable operating temperatures was greatly restricted. Copper was selected as the basic material of construction in preference to nickel because of its known availability and formability. A more detailed study of nickel 200 is desirable prior to final material selection. Wrought copper can be obtained in strength levels from 30 to 60,000 psi depending upon the degree of work. The higher strength level materials tend to be brittle and would be unsuitable for some of the forming operations required in nozzle fabrication. As a compromise between strength and formability, a strength level of 45,000 psi ultimate was selected.

All of the designs employ flat plate type closures with provision for water circulation. The basic nozzle design is also common to the three concepts. It features two-piece construction, consisting of an outer support cylinder and a thin-walled nozzle shell. The insert is a simple low cost and easily assembled component.

The nozzle shell is fabricated from 3/8 in. commercial copper tubing having a 0.03 in. nominal wall thickness. It is formed with a standard tube cutter in which the cutting blade and rollers are replaced with forming dies. The tool is used in the conventional rotation/tighten/rotation manner to incrementally and uniformly form the nozzle shell. The process is aided by inserting a series of diminishing diameter steel back-up rods into the tube during forming. Several nozzles may be processed from a single length of tubing. After cutting the nozzle shells to the required

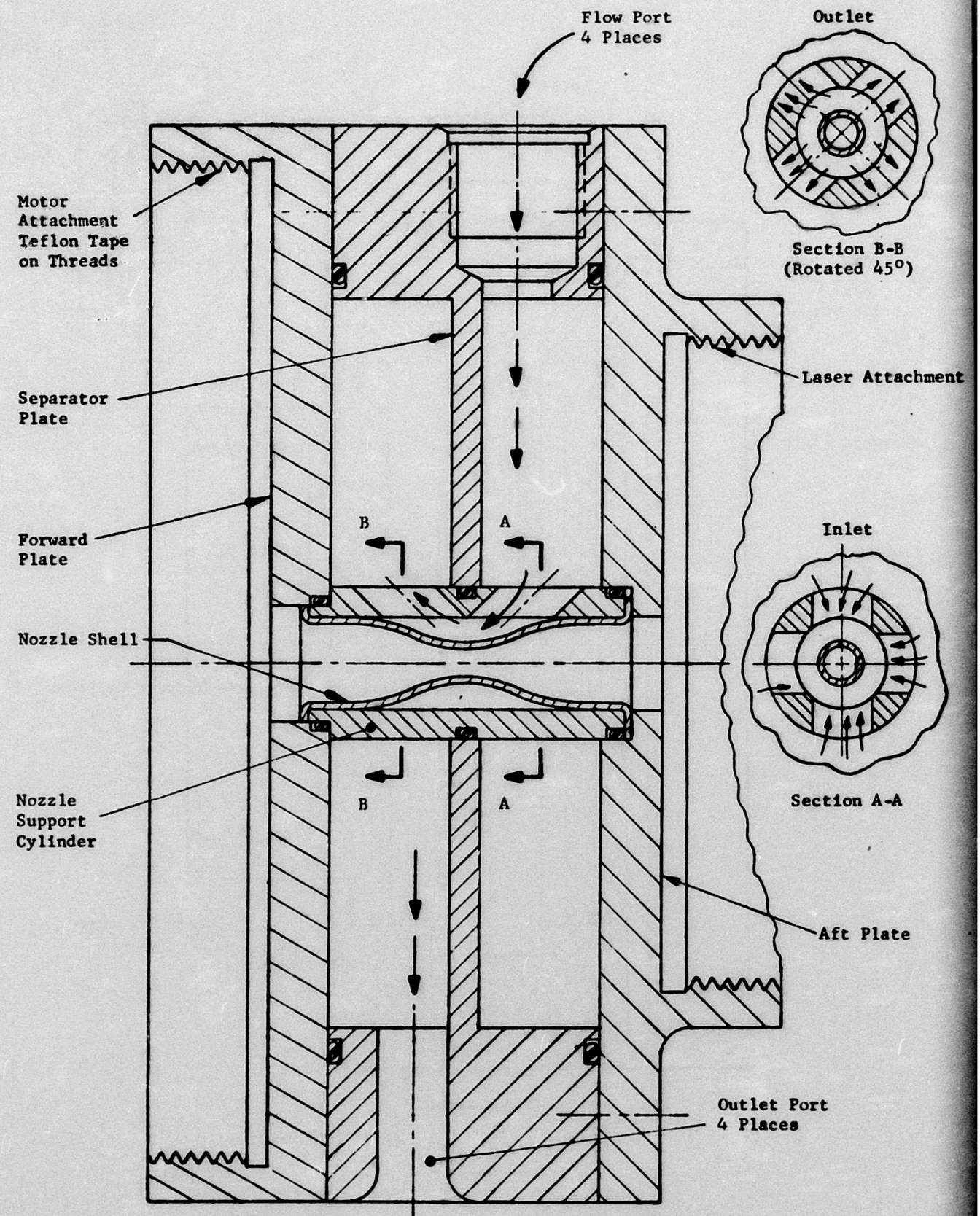

Figure 4. Variable Velocity Axial Flow Concept

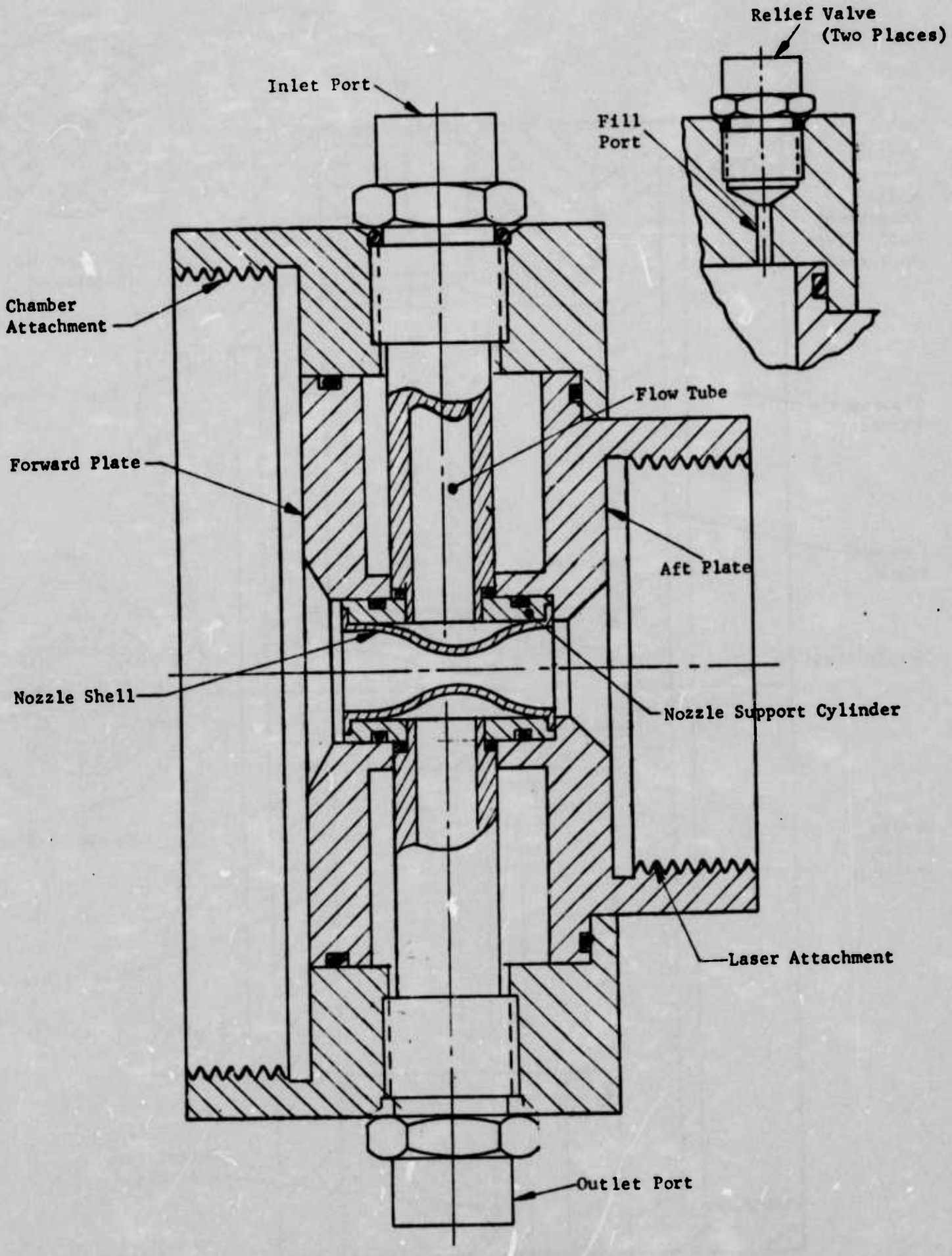

Figure 5. Constant Velocity Tangential Flow Concept

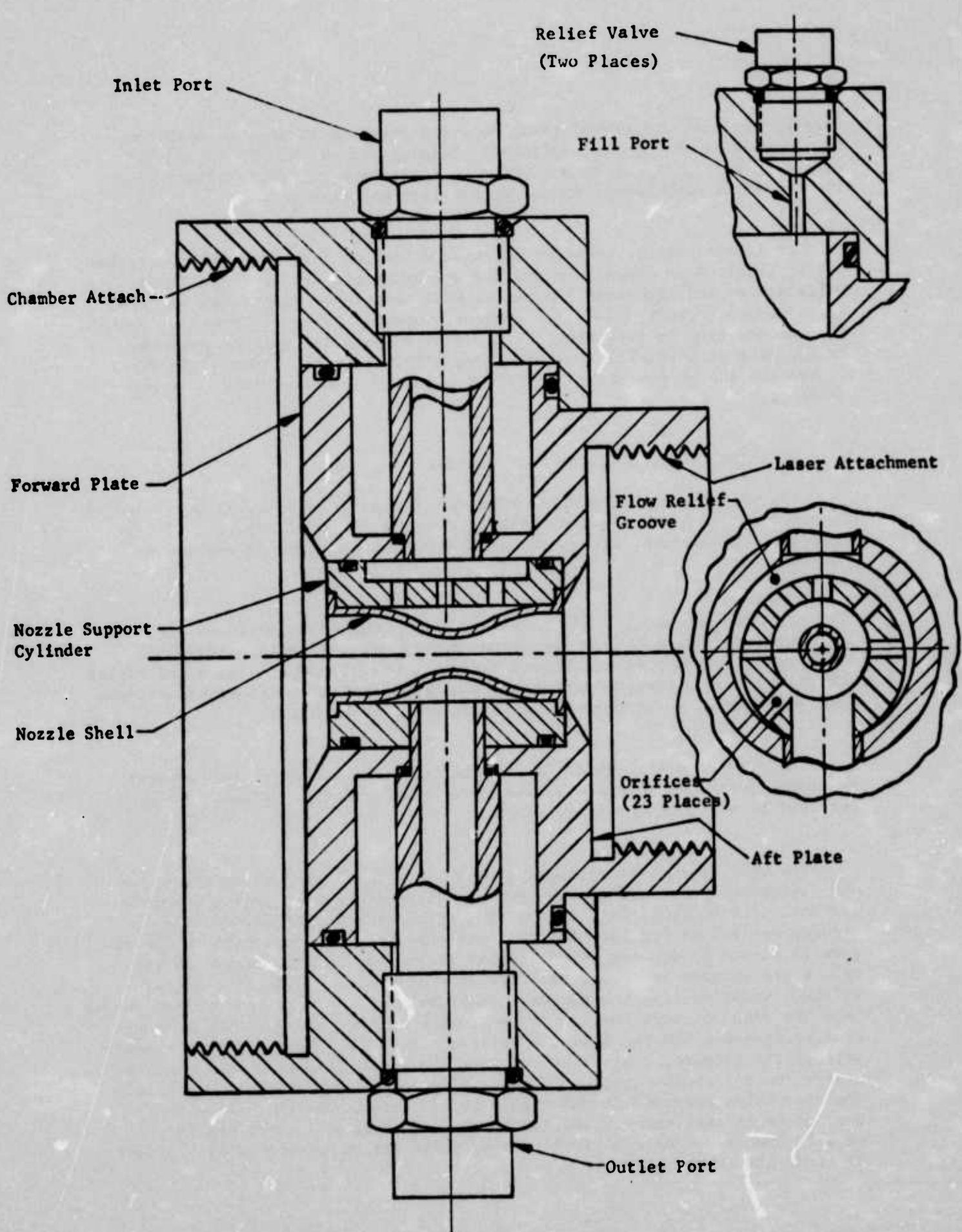

Figure 6. Multi-Orifice Concept

length, the ends are swaged using an arbor press into recesses machined in the ends of the support cylinder. Joining and sealing of the shell to the support cylinder is accomplished by surface soldering of both ends. The throat is then reamed to the proper internal diameter.

An initial throat diameter somewhat different from the 0.056 in. value may be required to compensate for thermal expansion and pressure loads. Calculations indicate that the throat will experience dimetrical shrinkage of approximately 0.004 in. Since the nozzle shell will reach an equilibrium position in less than 0.2 sec (for copper), it will be possible to oversize it initially with almost no effect on performance. The exact dimensions can be determined by finite element analysis and development testing.

A. VARIABLE VELOCITY, AXIAL FLOW CONCEPT

The Variable Velocity Axial Flow (VVAF) concept (Figure 4) was selected as the baseline HF/DF chemical laser gas generator nozzle design. It is felt that this concept offers the most potential in terms of meeting all requirements.

The closure features a three-piece easily assembled sandwich construction consisting of a "T"-shaped spacer bolted between two flat 0.30-in. thick circular end plates. Threaded flanges are provided on both end plates for attachment to the combustion and plenum chambers. An alternate attachment arrangement using only bolts is presented in Figure 7.

The nozzle insert, which is 1.38 in. long and 0.625 in. in diameter, is housed in the closure and is sealed with three Viton O-rings. It is retained by a lip on the aft closure.

The VVAF concept is equipped with an integrated closure/nozzle coolant system which ensures uniform and regulated axial flow over the nozzle surface. The vertical part of the "T"-shaped spacer ring divides the closure coolant cavity into two isolated chambers. As indicated by the arrows in Figure 4, coolant is manifolded to the right-hand closure cavity from a pressurized reservoir via four equally spaced 0.300-in. diameter inlets. After cooling the plenum chamber wall of the closure, coolant passes from the right closure chamber to the nozzle coolant chamber through four equally spaced 0.300-in. diameter inlets. After cooling the plenum chamber wall of the closure, coolant passes from the right closure chamber to the nozzle coolant chamber through four equally spaced, 45° angled, 0.250-in. diameter holes provided in the nozzle throat insert housing. Flow exits the nozzle coolant chamber and enters the left closure cavity via four equally spaced 0.250-in. diameter holes which are circumferentially offset 45° from the inlet holes.

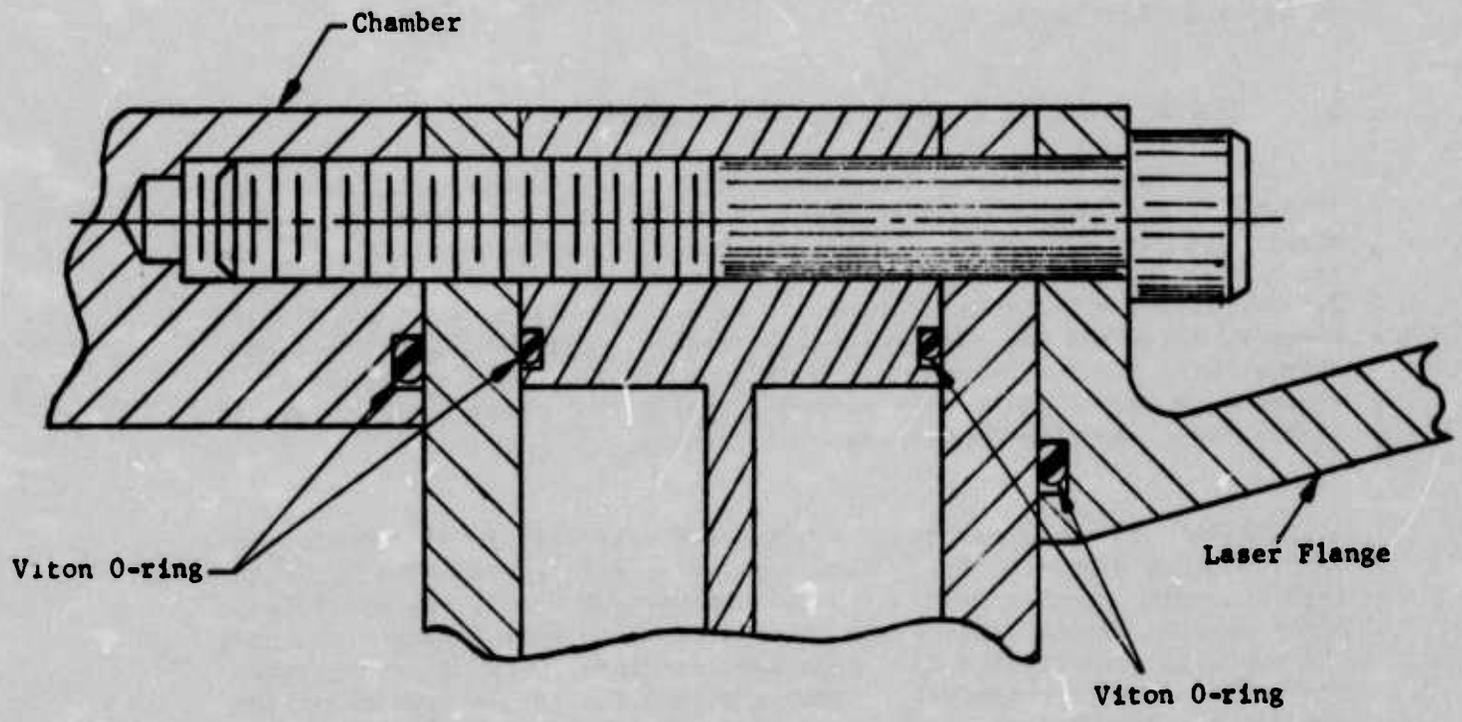

Figure 7. Alternate Attachment Concept

After entering the left-hand closure chamber and providing cooling to this area, the warm coolant exits the system through four equally spaced 0.300-in. diameter vents.

The circumferential offset and the opposing 45° to centerline orientation of the coolant entrance and exit holes provide: (1) a uniform axial coolant flow field over the nozzle shell with minimal head loss, and (2) symmetrical loading of the nozzle tube O.D. by the pressurized coolants. The convergent-divergent nozzle coolant cavity configuration generates a variable velocity flow field with the maximum velocity (minimum flow area) at the throat plane. This fulfills the desired conditions of high velocity and low pressure which maximize both convective and nucleate boiling heat transfer. The maximum wall temperature in the throat region was calculated to be 408°F. The complete temperature distribution is given in Section V.

B. CONSTANT VELOCITY, TANGENTIAL FLOW CONCEPT

The Constant Velocity Tangential Flow (CVTF) nozzle design concept (Figure 5) utilizes a separate closure/nozzle coolant system. Housed within the port of the copper closure, the 1.17-in. long, 0.75-in. diameter nozzle insert is sealed with two Viton O-rings. The 1.31-in. wide, 3.5-in. diameter two-piece closure is easily assembled to form a single-chamber, fixed volume, closure-coolant system. After filling the closure chamber with coolant through the port shown in the upper right corner of Figure 4, a relief valve is inserted in the port to vent steam generated within the chamber during the cooling process.

Coolant is supplied from a pressurized reservoir to the nozzle coolant through a single 0.25-in. diameter sealed delivery tube which is threaded into the outer chamber wall after the chamber and nozzle are assembled. After passing through the nozzle coolant chamber, warm coolant is vented through a tube positioned 180° from and identical to the delivery tube. Since flow area is relatively constant within the nozzle coolant system and the delivery and vent tubes are centered over the nozzle, flow passes tangentially to the nozzle walls at a constant flow rate.

Although the CVTF nozzle concept features simplicity of design and assembly, three major disadvantages compared to the baseline CVTF concept are noted: (1) because of the constant velocity feature, coolant supply and static pressures are high which increase the coolant boiling point and produce high wall temperatures (Section III), (2) some flow separation will occur on the outlet tube side of the nozzle, producing a hot zone in the separated region, and (3) the localized entrance and exit of fluid into the nozzle coolant chamber produces a nonuniform flow field which induces unsymmetrical loading into the thin nozzle shell.

C. MULTI-ORIFICE CONCEPT

The multi-orifice (MO) concept employs the same closure configuration as the constant velocity design (Figure 6). It also features separate closure/nozzle cooling systems and retention, while sealing and bulk size of the nozzle insert are identical to the CVTF nozzle concept.

Coolant passes from the delivery tube into an eccentric groove machined in the nozzle support housing. This cavity distributes pressurized coolant to twenty-three 0.050-in. diameter orifices which are drilled through the nozzle support housing wall in the pattern illustrated in Figure 6. A uniform high velocity spray of coolant is thereby provided to the nozzle shell outer diameter. Warm coolant is vented through a large tube located 180° from the delivery tube.

With the exception of the relatively complex nozzle insert configuration, the MO nozzle design concept features ease of assembly, high heat transfer resulting from the high velocity, low pressure uniform spray of coolant over the nozzle shell outer diameter, and low, symmetrical exterior pressure loading of the thin shell.

Although the coolant flow behavior in the nozzle cooling chamber is complex and could not be analytically investigated within the scope of this study, it would intuitively appear to meet the desired conditions of high velocity and low pressure. Therefore, it is worthy of further consideration and perhaps experimental bench testing.

SECTION V

HEAT TRANSFER STUDIES

Thermal calculations were made primarily to ensure compliance with the maximum gas-side surface temperature limit in the nozzles (440°F with copper and 1340°F with nickel) as influenced by the nozzle shell thickness, geometry, and variation in cooling effectiveness on the water side (different cooling design concepts). These calculations were also required for use in determining structural integrity. Use of a digital computer program was required because of the shape of the nozzles in the concepts studies, the transient period of operation before steady-state heat transfer is achieved, and temperature dependent boundary conditions.

A. MODEL

Because of the general physical similarity of the design concepts and the limited scope and time of this study, one geometry was used for all calculations. The forward and aft sections of the nozzle, with respect to the nozzle throat, are nearly identical, particularly in the thin-wall section. Since the nozzle wall thickness was very small (0.030 in. or less) axial conduction effects were expected to be minimal. Therefore, the model was restricted to the forward half of the nozzle, which is exposed to higher heating rates than the aft section; i.e., the gas side-heat transfer coefficients in the nozzle entry are higher than in the exit section. The section analyzed includes the forward plate section (motor side) of the closure.

Computer program 61004[9] was used for temperature calculations which allowed use of temperature-dependent cooling water heat transfer coefficients and material properties. The model used for the thermal analysis is shown in Figure 8.

B. BOUNDARY CONDITIONS

The nozzle thermal analyses were based on heat transfer coefficients for hot gases on the internal surfaces and cooling water on the external surfaces as indicated in Figure 8. The gas-side (heating) coefficients were calculated based on values in Figure 4 of Reference 3, specifically for the condition of 1000 psia and a circular throat of 0.15-in. diameter. Heat transfer coefficients for the current configuration (1000 psia and 0.056-in. diameter throat) are presented in Figure 9. They were calculated from data in Reference 3 using the conventional $(1/\text{Diameter})^{0.2}$ relationship for the heat transfer coefficient and throat diameter (Section III). The coefficient values for each node in the thermal model were assumed constant.

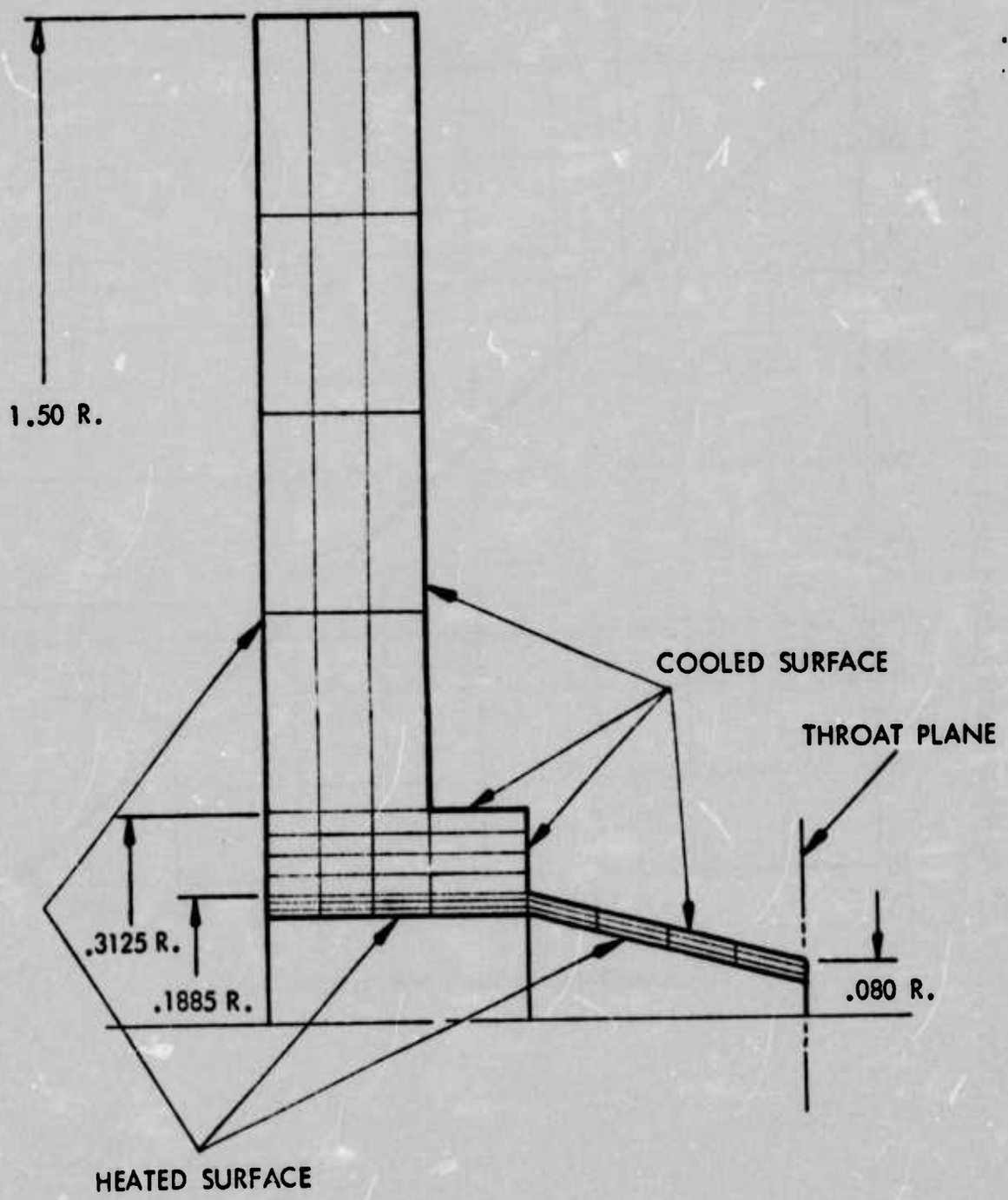

Figure 8. Nozzle Thermal Model

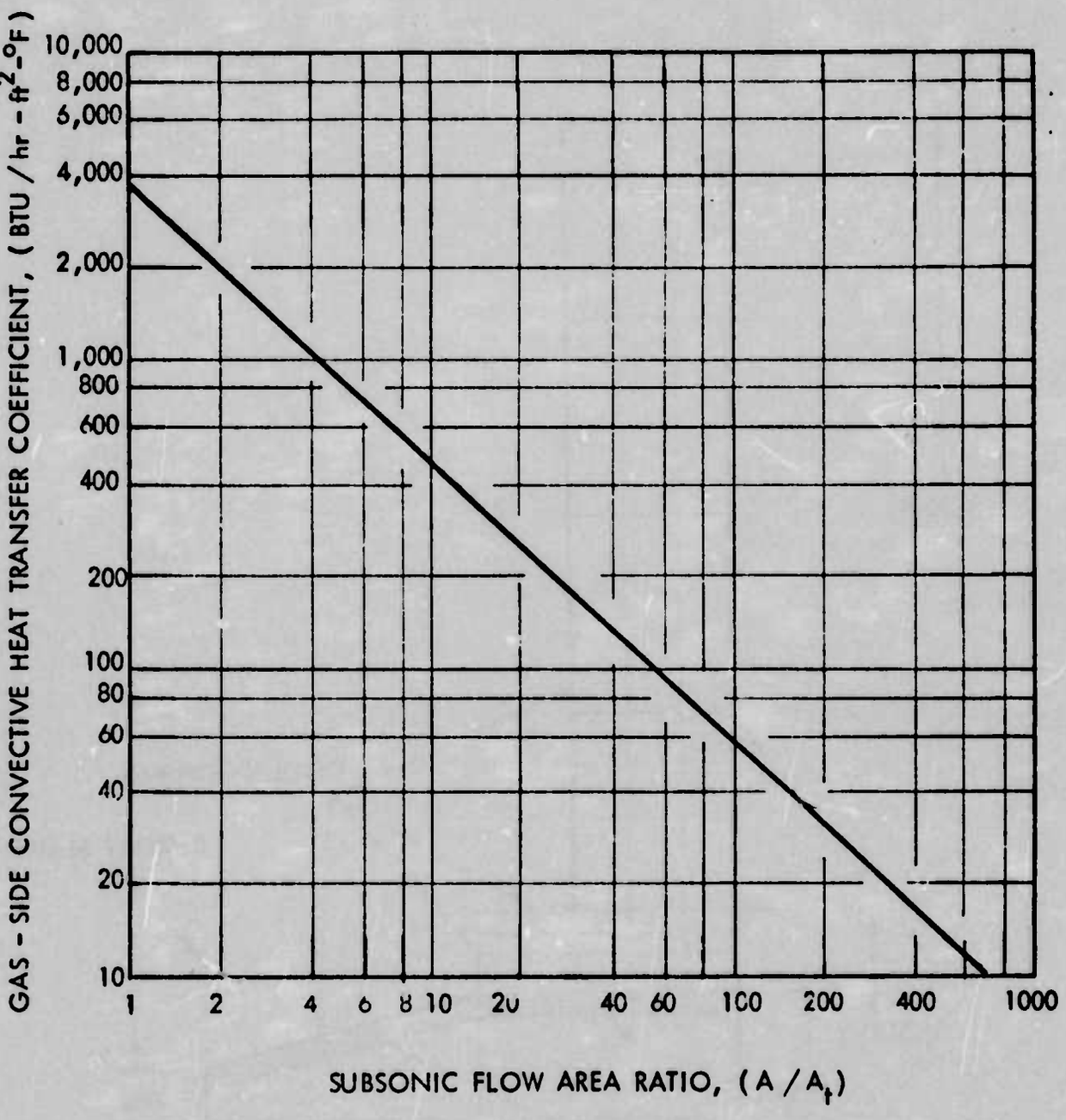

Figure 9. Gas-Side Convection Heat Transfer Coefficient

The heat transfer coefficients on the nozzle surfaces cooled with water were calculated as discussed in Section III. The calculated values, as functions of wall temperature, are summarized in Figures 10 and 11 for the axial flow and tangential flow designs, respectively. The correlation of the curves with position on the nozzle model is identified in Figure 12.

For the axial flow model the required supply pressure was based on the loss incurred in a square elbow[8] and minimal losses in other low velocity areas. For a velocity of 200 ft/sec in the throat region, a supply pressure of 440 psi was found to be required. Velocities in other areas were found by area ratios and the pressure distribution was determined by proportioning pressure losses. The following values were utilized in calculating the coefficients of Figure 10.

Location	P_{tot} (psia)	Area ($in.^2$)	V (fps)	P_s (psia)	T_s (°F)
Tank	440	-	0	440	-
Orifice Entrance	438	0.982	17	436	453
Orifice	398	0.211	81	354	430
Aft Cooling Annulus	330	0.125	135	207	383
Throat	277	0.086	200	8	182
Forward Cooling Annulus	172	0.125	135	50	281
Orifice	118	0.211	81	72	304
Orifice Exit	90	0.982	17	70	303
Outlet	39	0.283	60	15	-

The pressure distribution at a velocity of 100 ft/sec for the tangentional flow concept was discussed in Section III. The film coefficients based on this analysis are shown in Figure 11.

C. MATERIAL PROPERTIES

Temperature-dependent thermal properties were used for the analyses of the copper and nickel nozzles. These properties were obtained from Reference 10. They are presented in Table II.

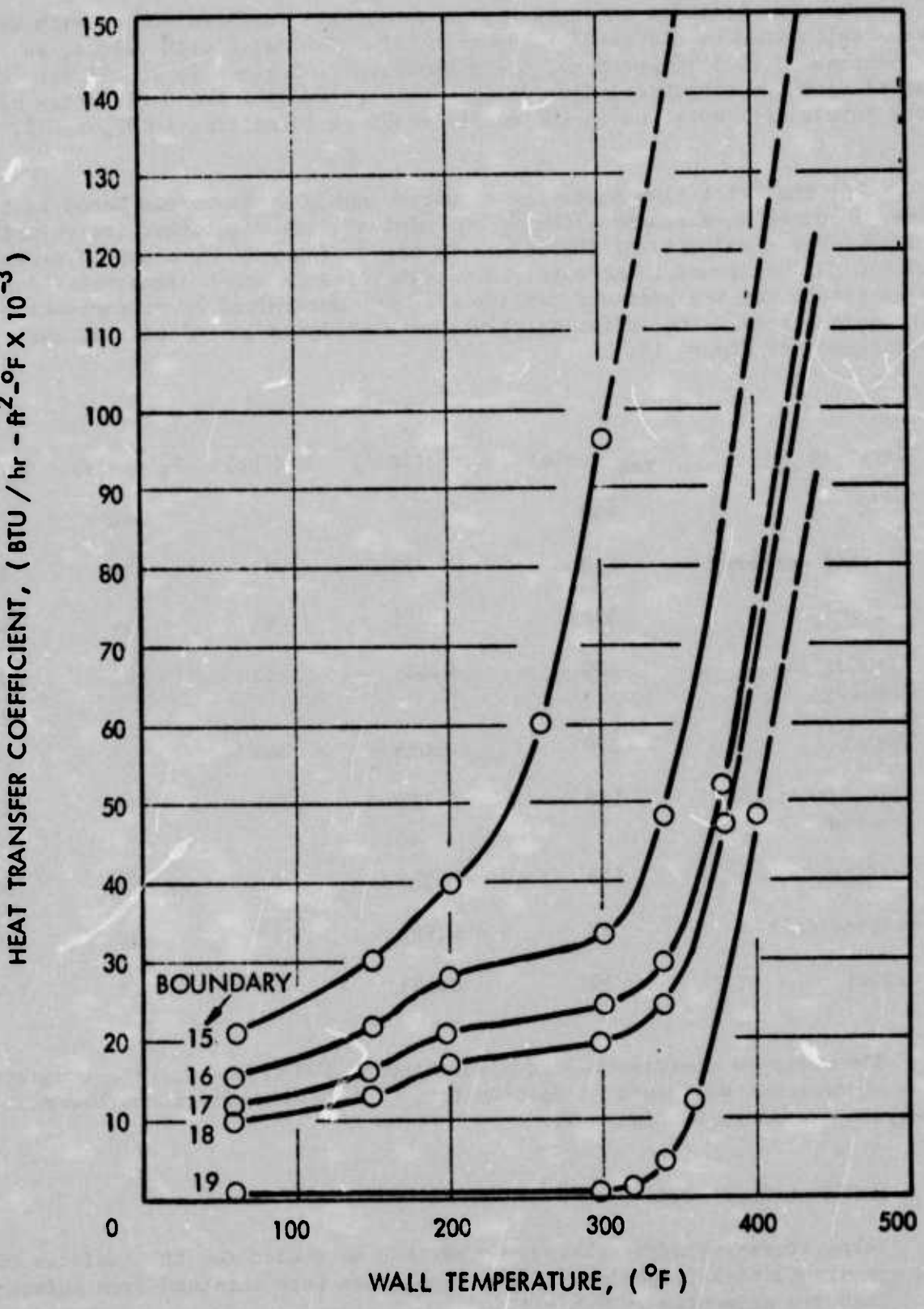

Figure 10. Heat Transfer Coefficients on Nozzle Cooled Surfaces - Axial Flow Concept

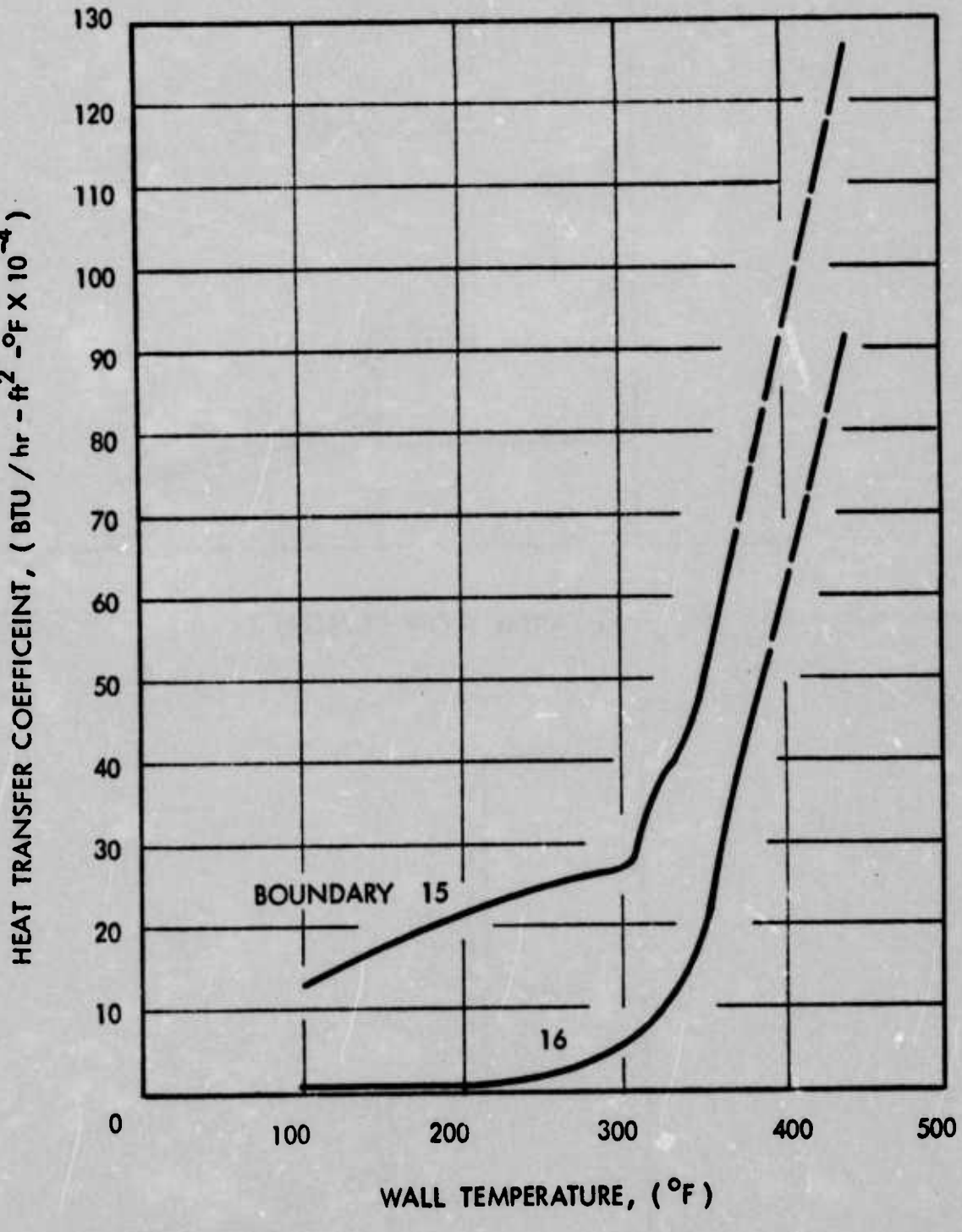

Figure 11. Heat Transfer Coefficients on Nozzle Cooled Surfaces - Tangential Flow Concept

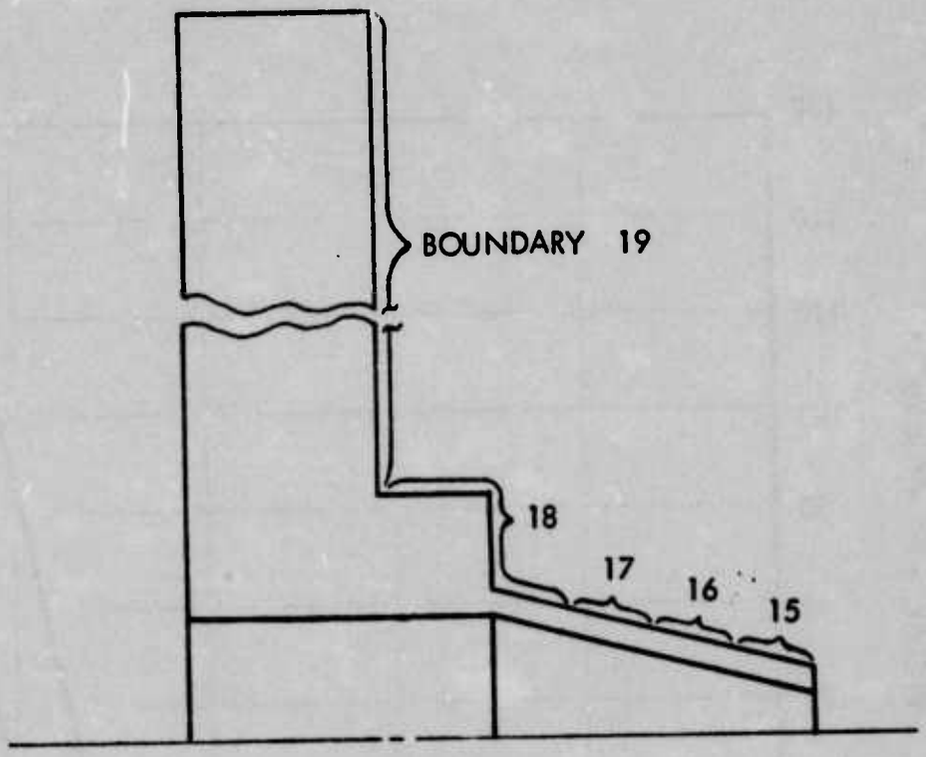

A: AXIAL FLOW CONCEPT

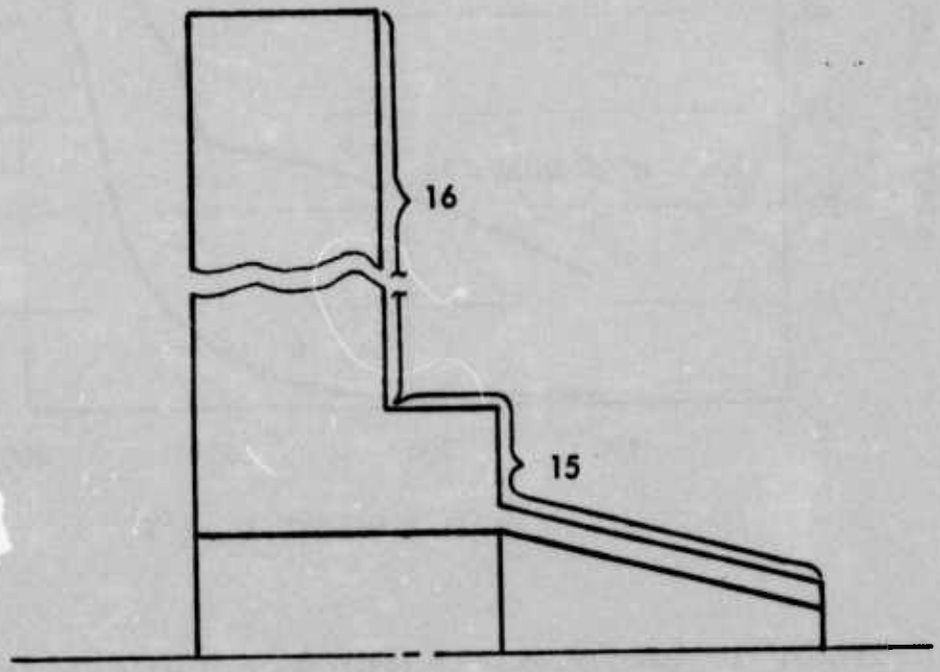

B: TANGENTIAL FLOW CONCEPT

Figure 12. Location of Cooling Water Heat Transfer Coefficients

TABLE II

THERMAL PROPERTIES OF COPPER AND NICKEL

Temperature (°F)	Thermal Conductivity (BTU/hr-ft-°F)	Specific Heat (BTU/lb-°F)
Copper		
0	239.	.090
70	234.	.093
500	217.	.100
1000	201.	.108
1800	186.	.120
Nickel		
0	42.	.100
70	38.	.105
400	30.	.123
700	26.	.160
1000	29.	.124
2500	42.5	.164

Density (lb/ft^3):

Copper - 558.

Nickel - 555.

D. THERMAL RESULTS

Four cases were considered using the computer model and heating/cooling boundary conditions described previously. These were:

Case	Design	Material	Thickness of Nozzle Shell (Inch)
1	Axial Flow	Copper	0.030
2	Tangential Flow	Copper	0.030
3	Axial Flow	Copper	0.015
4	Axial Flow	Nickel	0.030

Results of the temperature calculations for the four cases analyzed are presented in Figures 13 through 16. Shown are isotherms after 10 sec of operation, based on a starting temperature of 77°F. In addition, surface temperature values at selected locations are presented.

Three of the configurations were in compliance with the surface temperature limits (440°F for copper and 1340°F for nickel) in the thin-wall region of the nozzle. The 0.030-inch thick copper nozzle, cooled by the tangential water flow design, had a temperature of 475°F at the throat which is 35° over the limit. However, the tangential flow design would probably be acceptable with a 0.015-in. wall, based on the results of the 0.030 and 0.015-in. axial flow configuration. The entrance corner of all four designs, as analyzed, exhibited temperatures above the limits. However, these are unique to the analysis model and result from the heat concentration at the corner and the increased distance to the cooled back surfaces. This is easily eliminated by rounding or chamfering the inlet corner, as shown in the actual designs. With this feature, all designs will be acceptable in this region.

As expected, the highest temperatures occurred in the nozzle throat region for all designs. These are summarized below:

Water Flow Design	Material	Shell Thickness (in.)	Surface Temperature (°F)	
			Gas-Side	Cooled Side
Axial	Copper	0.030	407	242
Tangential	Copper	0.030	475	313
Axial	Copper	0.015	352	265
Axial	Nickel	0.030	1281	189

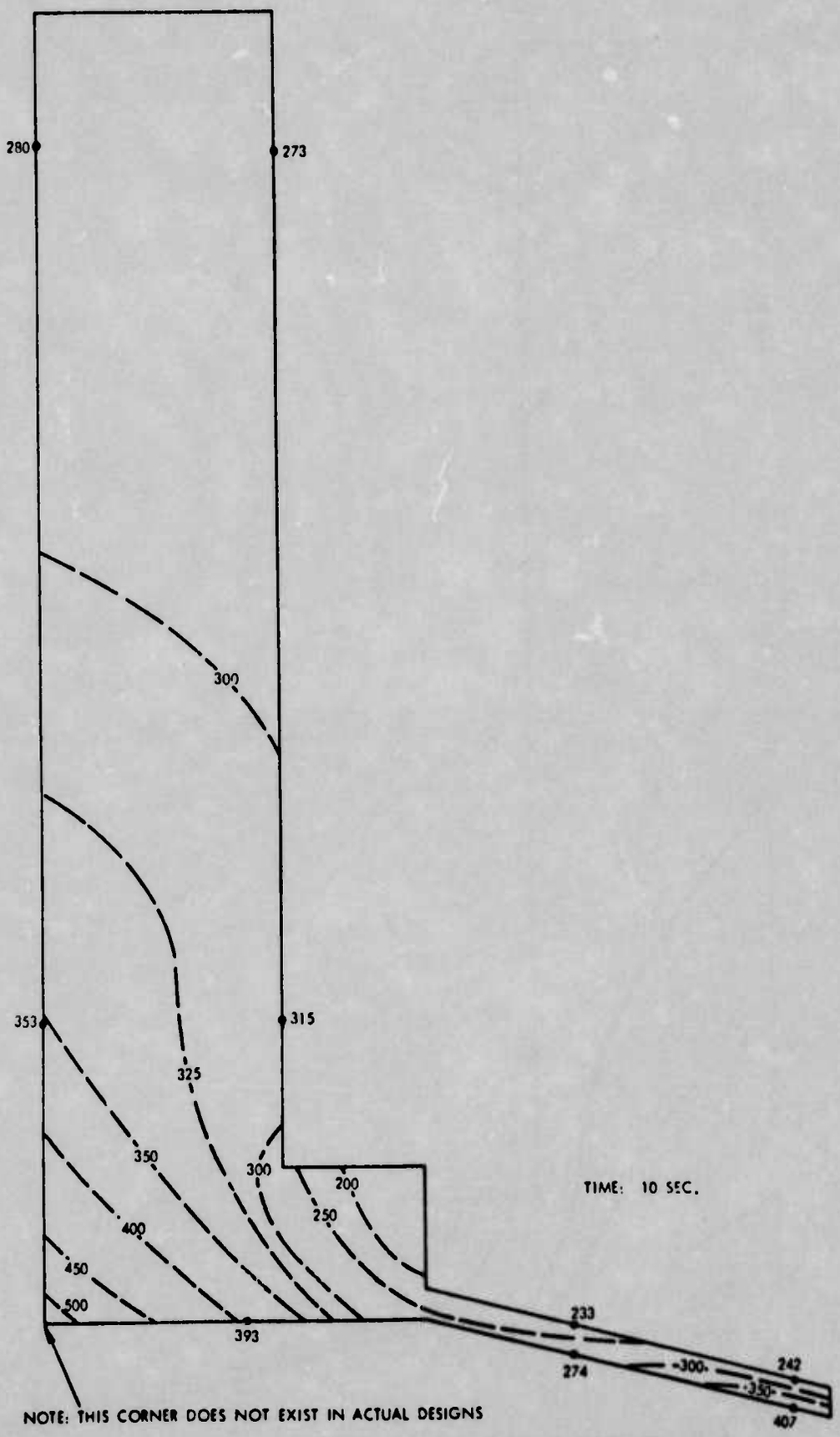

Figure 13. Calculated Temperatures (°F) in 0.030-Inch Wall Axial Flow Copper Nozzle

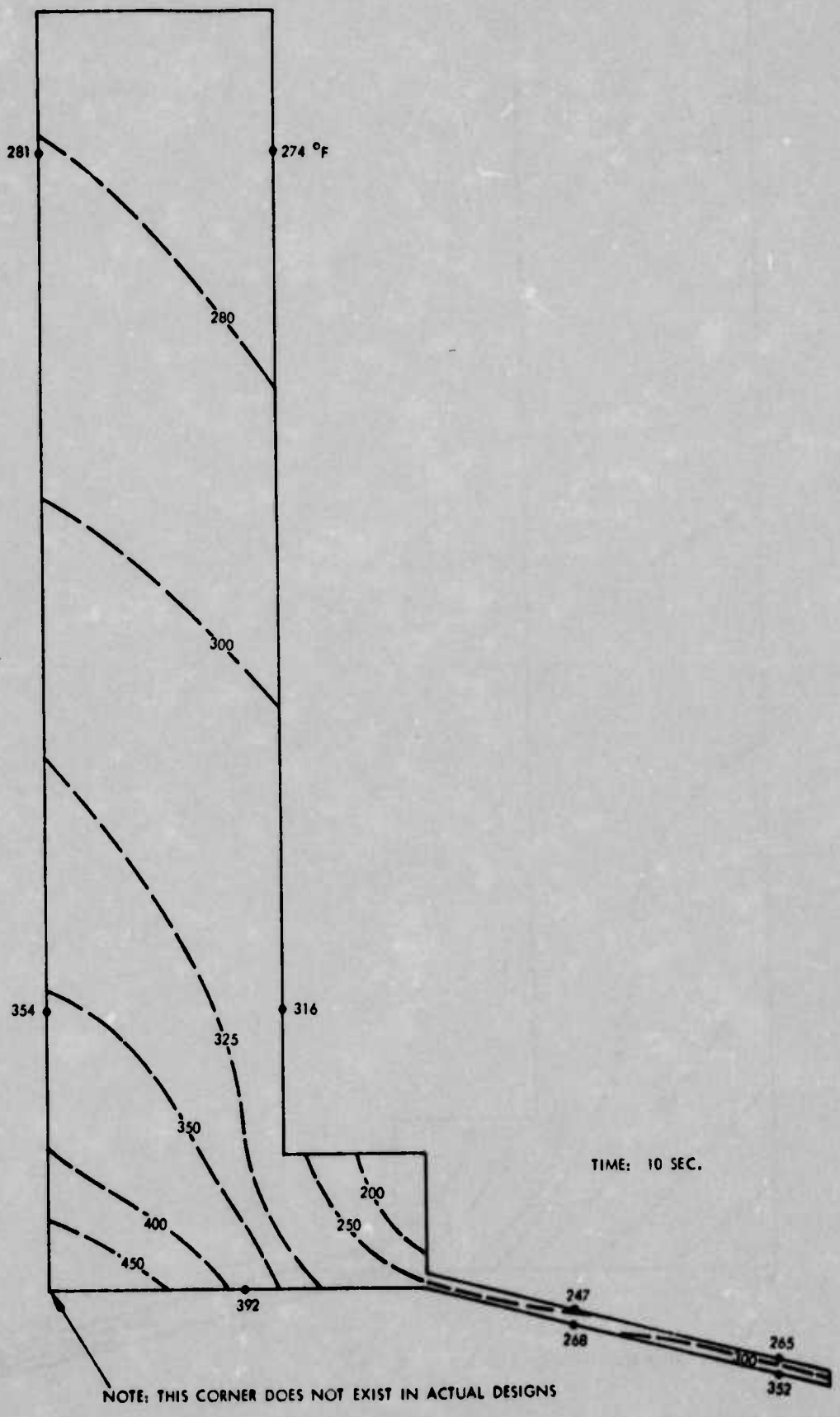

Figure 14. Calculated Temperatures (°F) in 0.015-Inch Wall Axial Flow Copper Nozzle

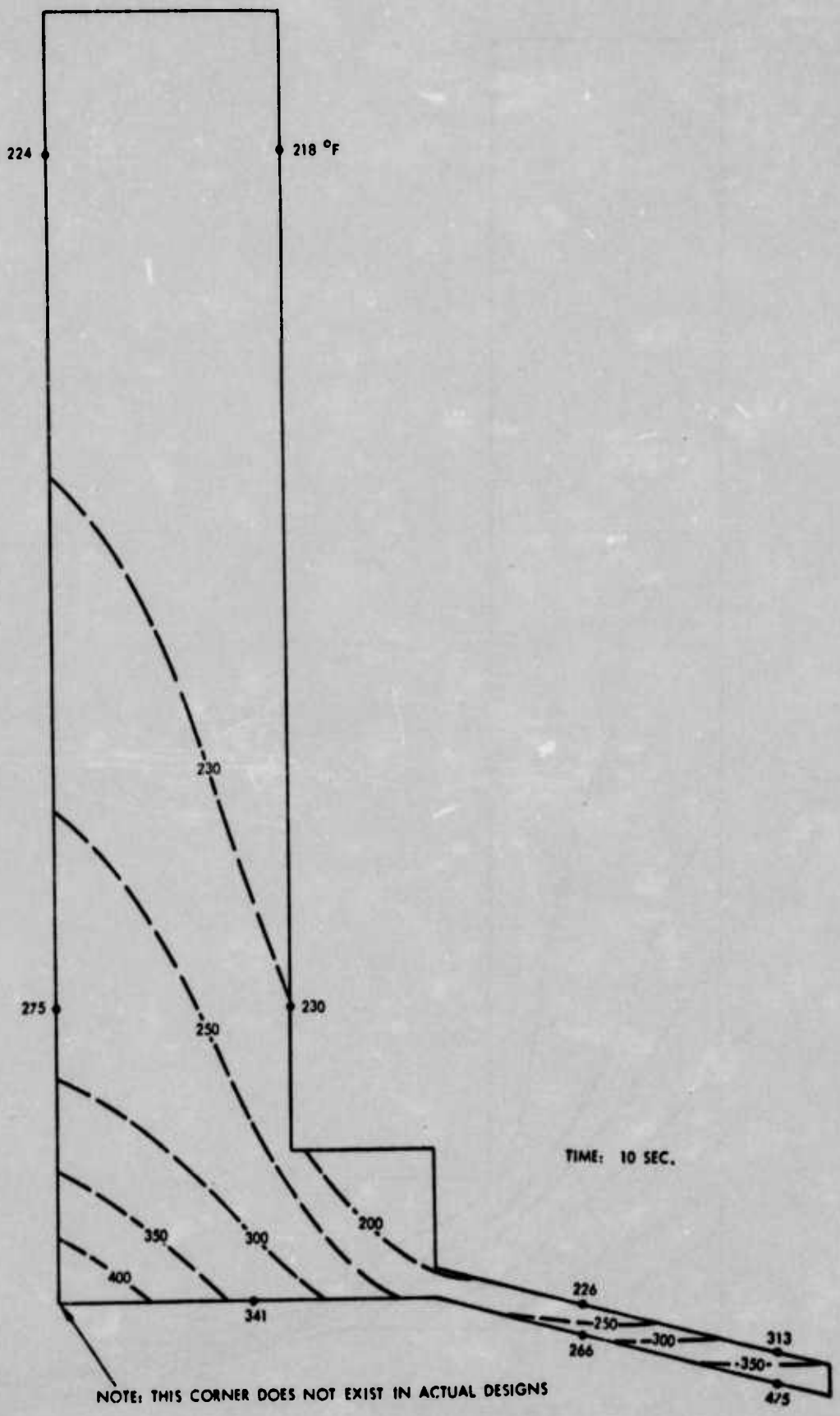

Figure 15. Calculated Temperatures (°F) in 0.030-Inch Wall Tangential Flow Copper Nozzle

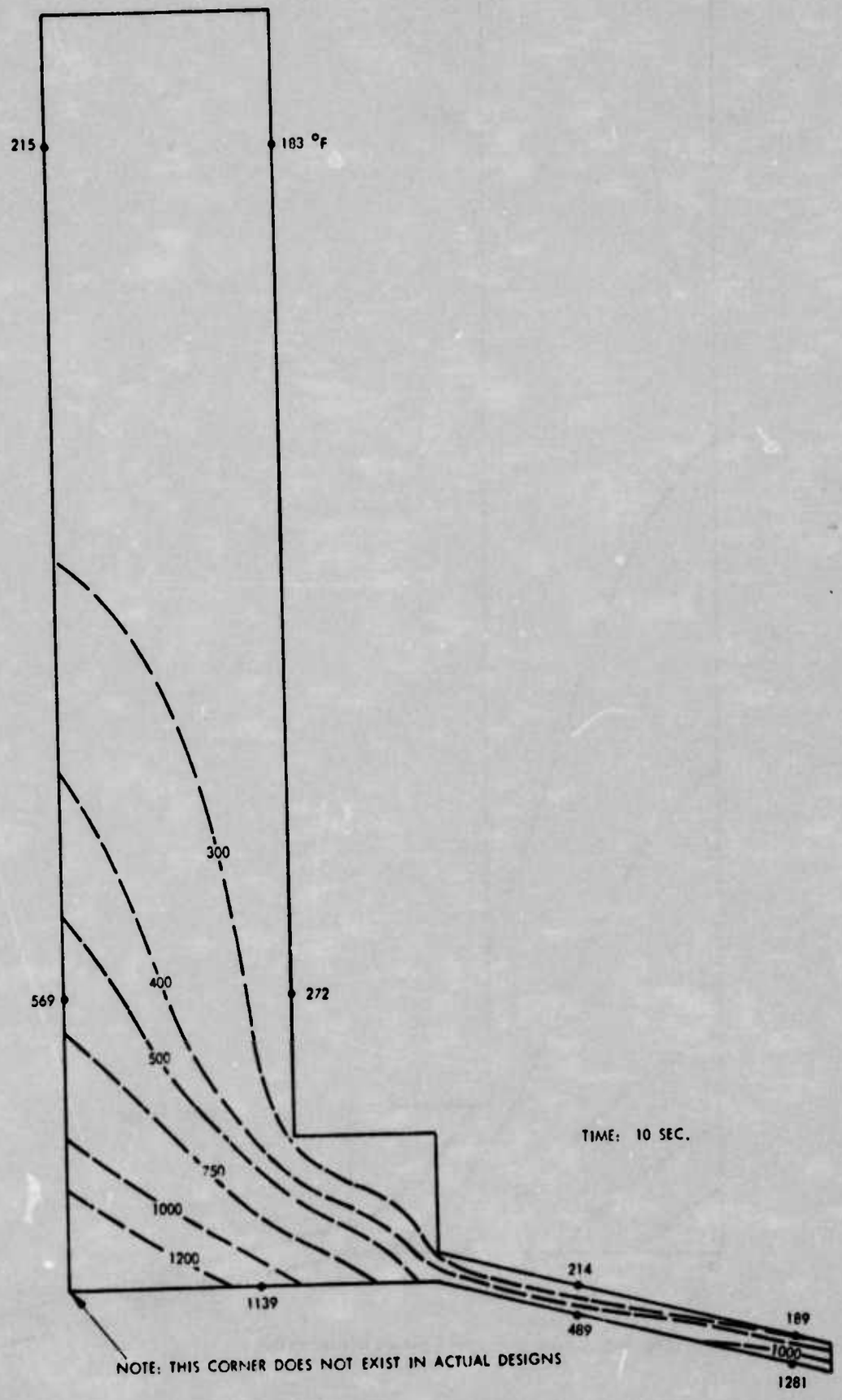

Figure 16. Calculated Temperatures (°F) in 0.030-Inch Wall Axial Flow Nickel Nozzle

The gas-side surface temperature varied significantly due to the variation in thermal resistance produced by differing wall thicknesses or materials. The 0.015-in. thick copper shell operates with a 55°F lower gas-side surface temperature than the 0.030-in. thick shell. The nickel shell is over 800°F hotter than the copper shell in the throat region due to the low conductivity of the former material.

Temperatures in the upper portion of the forward plate of the copper designs are higher than those of the nickel. This apparently results from radial conduction effects related to the very high thermal conductivity of copper.

E. BURNOUT CALCULATIONS

The burnout point for nucleate boiling is much higher in forced convection than in a still liquid. It depends primarily upon the velocity of the flow and the degree of subcooling. The latter term refers to the difference between the saturation and bulk temperatures. Several correlations[11,12] have been proposed to define the burnout point and there is a wide range in the predictions. Several of these were applied to the current cooling requirements and, for the worst case, margins of safety of 0.6 and 1.79 were obtained for the axial and tangentional flow concepts, respectively. The heat flux which must be absorbed by nucleate boiling is well below the burnout point for both designs.

F. COOLANT FLOW REQUIREMENTS

The coolant flow rate is not large for any of the designs. The baseline design will require 7.45 lb/sec and the tangentional flow and multi-orifice about 2.13 lb/sec of water. For a 10 sec test duration plus a 20 sec pretest flow and a small reserve, 300 lb or about 36 gallons of water will be required.

The total heat loss to the water in the axial flow design was calculated to be 34,110 BTU/hr or about 90 BTU during the course of the firing. The temperature rise of the water was found to be:

$$\Delta T = \frac{Q}{C\,\dot{m}}$$

$$\Delta T = \frac{34,110}{(1.0)(7.45)(3600)}$$

$$\Delta T = 1.3°F$$

The rise in the tangentional flow design will be slightly higher but should not be more than the 3° assumed in the heating analysis, i.e., 77° to 80°F.

SECTION VI

STRUCTURAL ANALYSIS

Only a brief preliminary structural analysis was attempted due to time limitations. However, it should be sufficient to verify the overall feasibility of the design concept. Minor design modifications will correct any deficiencies revealed by more sophisticated analyses. In general, the small size and uniform thermal environment of the nozzle tends to maintain stress levels at low values.

A. MATERIAL

Wrought copper can be obtained in various strength levels depending on the degree of work. The throat section should be fairly soft to facilitate the roll forming and swaging operations. As a compromise between workability and strength, a medium soft material having the following properties was chosen:

	77°F	400°F
F_u (psi)	45,000	38,300
F_y (psi)	30,000	25,500
λ (psi)	19,000	16,000
E (psi)	17×10^6	15×10^6
α (in./in-°F)	10×10^{-6}	10×10^{-6}

B. LOADING

The forward closure was considered as a flat plate, inner and outer diameters fixed, loaded by a gas pressure of 1000 psi. The middle separator plate was considered to be loaded by water pressure of 370 psi. The aft closure was considered to be fixed at its outer diameter and loaded by water pressure of 370 psi and a concentrated load of 1992 lb. The latter is one-fourth the pressure area product on the forward closure plus the nozzle shell load (226 lb).

The nozzle support cylinder was considered for compressive loading at the minimum cross section (a plane through the four orifices).

The aft closure lip retaining the nozzle support cylinder was considered for shear.

The nozzle shell was considered for axial stress for combined water and gas pressures. The load will be reacted at both the forward and aft nozzle shell attach points, but since the distribution is unknown it was assumed to react at only one of the attach points (very conservative). The shell was also considered for maximum hoop stress produced by the gas pressure.

The axial stress produced by heating the restrained nozzle shell was calculated.

C. RESULTS

Location	σ	M.S. Ult.	M.S. Yield
Fwd Plate Radial Stress	25,000	0.53	0.02
Center Plate Radial Stress	35,000	0.29	-0.13
Aft Plate Hoop Stress	-41,200	0.095	-0.27
Aft Plate Lip Shear	10,200	0.52	
Nozzle Support Cylinder Axial Compression	-28,000	0.60	0.07
Nozzle Shell			
Axial Stress (Pressure)	-4,120	Large	Large
Hoop Stress (Pressure)	6,250	Large	Large
Axial Stress (Thermal)	-34,500	0.11	-0.26
Axial Stress (Combined)	-38,620	0.0	-0.34

D. DISCUSSION

The results indicate that acceptable margins on ultimate strength exist in all areas except the aft plate and nozzle shell. The aft plate is believed to be adequate since the major loading is transferred from the forward plate which can absorb more load than assumed without fracturing. In addition, the formulas used are normally conservative; redistribution of load generally occurs with deflection.

The nozzle shell is believed to be the critical point. While the temperature rise is not large, the assumption of complete axial restraint produces very high stress levels. Some relief will be provided by the rise in temperature of the ends of the nozzle support cylinder, but this will be minimal. The average temperature (298°F) assumed may be too high since it was not calculated on a volume basis. It is recommended that a detailed finite element analysis of the nozzle shall be conducted to ascertain the actual stress state. This could not be done in the current study due to time limitations. If the stresses prove to be excessive, relief of some sort must be provided. A recommended approach would be to retain the nozzle support cylinder from the forward closure

(strengthened for this purpose) and section the cylinder near the aft plate. The pressure loads acting on the nozzle shell would then be supported directly by the shell but it should be adequate for this purpose.

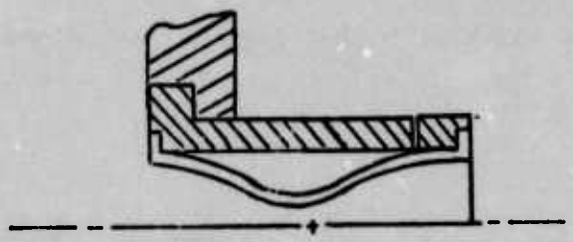

Yielding of material will occur in several local areas but this should not prevent disassembly and reuse.

It is concluded that the nozzle concepts, as presently conceived, are feasible and that only minor modifications in design would be required to make them completely acceptable from a structural standpoint.

REFERENCES

(1) Leining, R. B., and Sauer, D. T., "Solid Fuel for Chemical Laser," Monthly Progress Report, A.O. 0633/5/2- , March 1974.

(2) Leining, R. B., and Sauer, D. T., "Solid Fuel for Chemical Laser," Monthly Progress Report, A.O. 0633/5/2-974, April 17, 1974.

(3) Leining, R. B., and Sauer, D. T., "RI-88 Energetic Chemicals," Research Progress Report, RI-88/5/2-975, April 17, 1974.

(4) Leining, R. B., and Sauer, D. T., "Solid Fuel for Chemical Laser," Monthly Progress Report, A.O. 0633/5/2-980, May 13, 1974.

(5) Memo, P. E. Christensen to J. W. Kordig, RI-88/6/AO-4308, April 4, 1974.

(6) Rohsenow, W. M., "A Method of Correlating Heat Transfer Data for Surface Boiling Liquids," Trans. ASME, Vol. 74 (1952), pp. 969-975.

(7) Kreith, F., Principles of Heat Transfer, International Textbook Co., (1960), pp. 406-409.

(8) Mark's Mechanical Engineer's Handbook, Theodore Barrmeister, Editor, McGraw Hill Book Co., (1958), pp. 3-78.

(9) Mayberry, J. L., "HETRAN II Program - Revised," Hercules Incorporated, Bacchus Plant, 16 August 1971.

(10) Goldsmith, A., et al., "Handbook of Thermophysical Properties of Solid Materials," Vol. I: Elements, Revised Edition, 1961.

(11) McAdams, W. H., Heat Transmission, 3rd ed., McGraw Hill Book Co., 1954.

(12) Gunther, F. C., "Photographic Study of Surface Boiling Heat Transfer with Forced Convection," Trans. ASME, Vol. 73 (1951), pp. 115-123.

APPENDIX B

THERMOCHEMICAL PROPERTIES

Ingredients	State	Heat of Formation ΔHF°_{298} Kcal/g mole	Source	Density grams/cc	Source
$N_2F_4 \cdot AsF_5$	Cryst	-332.9	Est	2.6	Calculated from a pressed formulation
Teflon $-C_2F_4-$	Cryst	-196		2.2	
Boron, B	Cryst	0.0		2.32	
Boron Carbide, B_4C	Cryst	-12.7		2.51	
Boron Nitride, BN	Cryst	-60.7			
NF_4AsF_6	Cryst	-338.9	(?)	2.71	AFRPL-TR-68-47
NF_4BF_4	Cryst	-338	AFWL-TR-73-195	2.36	AFRPL-TR-68-47
PPFB-C_4F_6		-95.6	Est by TRW		
$KClF_4$	Cryst	-178	(?)		

Products	State	Heat of Formation Kcal/g mole	Source	Heat Capacity (cal/g mole)	Source
AsF_3	Ideal gas	-248.1 (-219.06)	(a) (b)	$C_p = 19.04 + 0.52 \times 10^{-3} T - 3.12 \times 10^{5} T^{-2}$	
AsF_5	Ideal gas	-320.18	(a,b)	T ($^{\circ}$K) / C_p / $H^{\circ}-H^{\circ}_{298}$: 298 / 22.988 / 0; 500 / 27.656 / 5.188; 1000 / 30.605 / 19.968; 1200 / 30.956 / 26.127; 1500 / 31.251 / 35.462; 2000 / 31.486 / 51.155	(a,b)

(a) O'Hare, P. A. G., "The Thermodynamic Properties of As, AsF_3, and Some Arsenic Fluorides," ANL-7456, November 1968

(b) Kelly, K. K., "Contributions to the Data on Theoretical Metallurgy XIII," Bulletin 584, Bureau of Mines, 1960

(U) DISTRIBUTION LIST

Addressees

1. Huntsville Defense Contract Office (1)
   Rohm & Haas Company
   Attn: Dr. H. M. Shuey
   HIC Building NR 2
   1312 Meridian Street
   Huntsville, Alabama 35801

2. Commander
   U. S. Army Missile Command
   Attn: AMSMI-RK (6)
   AMSMI-RB (5)
   AMSMI-R (1)
   AMSMI-ON (1)
   Redstone Arsenal, Alabama 35809

3. Defense Documentation Center (2)
   Cameron Station
   Alexandria, Virginia 22314

4. Commander (1)
   White Sands Missile Range
   Attn: STEWS-TE-E, Mr. R. C. Strom
   White Sands Missile Range
   New Mexico 88002

5. Commander (1)
   Watervliet Arsenal
   Attn: Librarian
   Watervliet, New York 12189

6. Commander (1)
   U. S. Army Engr. Res. and Dev. Laboratory
   Attn: Librarian
   Fort Belvoir, Virginia 22060

7. Office, Chief of Res. & Dev. (1)
   Missiles and Space Division
   Attn: LTC Hastings
   Washington, D. C. 20301

8. Office, Chief of Res. and Dev. (1)
   Director of Development
   Washington, D. C. 20301

9. U. S. Army Research Office (1)
   Energy Conversion Br.
   3045 Columbia Pike
   Arlington, Virginia 22209

10. U. S. Army Foreign Science & Technology Center (1)
    Munitions Building
    Washington, D. C. 20315

11. Office, Dr. of Def. Res. and Engr. (1)
    Weapons Systems Evaluation Group
    The Pentagon
    Washington, D. C. 20201

12. Commander (2)
    U. S. Army Materiel Command
    Attn: AMCRD-MT, Mr. Matos
    Washington, D. C. 20315

13. Commander
    U. S. Army Ballistic Research Laboratories
    Attn: Mr. C. Odum (1)
    Librarian (1)
    AMXRD-BID (2)
    Aberdeen Proving Ground
    Maryland 21005

14. Commander
    Picatinny Arsenal
    Attn: SMUPA-VG (2)
    SMUPA-RT-S (1)
    Dover, New Jersey 07801

15. Commander (1)
    U. S. Army Munitions Command
    Attn: AMSMU-RU-R, Dr. John Erway
    Dover, New Jersey 07801

16. Commander (1)
    U. S. Army Weapons Command
    Attn: Librarian
    Rock Island, Illinois 61202

17. Commander (1)
    U. S. Army Research Office
    Attn: Librarian
    Box CM, Duke Station
    Durham, North Carolina 27706

(U) Addressees

18. Commander (1)
U. S. Army Research Office
Attn: Librarian
Box CM, Duke Station
Durham, North Carolina 27706

19. AF Office of Scientific Res. (1)
Attn: SREP, Mr. Wolfson
1400 Wilson Blvd.
Arlington, Virginia 22209

20. AF Res. & Technology Div. (1)
Bolling AFB
Attn: Maj. T. P. Mott-Smith
Washington, D. C. 20332

21. AF Systems Command (1)
Attn: SCPSL
Andrews AFB
Washington, D. C. 20331

22. Naval Air Systems Command
Attn: AIR-330, (1)
-5367, (1)
-53672, (1)
-604 (1)

23. NASA
Lewis Res. Center
Attn: Mr. D. L. Nored (1)
Ch.,Liq. Rkt. Tech. Br.
Tech. Library (1)
21000 Brookpark Road
Cleveland, Ohio 44134

24. NASA
Attn: PD-RV, Mr. Chandler (1)
PM-AA-MGR, Mr. L. Belew
Marshall Space Flight Center
Alabama 35812

25. California Inst. of Technology (1)
Jet Propulsion Laboratory
Attn: Library, TDS
4800 Oak Grove Drive
Pasadena, California 91103

26. Office, Dir.of Def. Res. & Eng. (1)
Assistant Director, Engineering
Technology
Mr. G. R. Makepeace
The Pentagon
Washington, D. C. 20301

27. Naval Weapons Center
Attn: Mr. Couch, 4522 (1)
Mr. Dettling, 4505 (1)
Dr. Thelen,4505 (1)
China Lake, California 93555

28. AF Rocket Prop. Laboratory
Attn: MKPC (1)
MKPA (1)
LKCP (1)
RTCS (1)
MKMA (1)
MKC (1)
Edwards, California 93523

29. NASA Headquarters (1)
Attn: Code RPS, Dr. R. Levine
Washington, D.C. 20546

30. NASA Scientific & Tech Info Facility
Attn: SAF/DL, ACQ Div. (1)
P. O. Box 33
College Park, Maryland 20740

31. Central Intelligence Agency (1)
Attn: CRS/ADD
Washington, D. C. 20505

32. CPIA (1)
Johns Hopkins University
Applied Physics Laboratory
8621 Georgia Avenue
Silver Spring, Maryland 20910

33. AF Aero Propulsion Laboratory
Attn: APR (1)
Wright-Patterson AFB, Ohio 45433

(U) Addressees

34. Institute for Defense Analyses (1)
Science & Technology Div.
Attn: Dr. Oliver
400 Army-Navy Drive
Arlington, Virginia 22202

35. Space & Missile System Division (SAMSO) (2)
Technology Support Division (SMTN)
Attn: Maj. Warren K. Stobaugh
Norton AFB, California 92409

36. Advanced Materiel Concepts Agency (1)
Attn: Firepower Division
2461 Eisenhower Avenue
Alexandria, Virginia 22314

37. Naval Ordnance Systems Command (1)
Attn: ORD-0331
National Center, Bldg. 2
Washington, D. C. 20360